Application of Isoleucine Epimerization to Assess Terrestrial Contamination and Constrain the Duration and Effects of Aqueous Alteration of Carbonaceous Chondrite Meteorites

by

Adam Alexander Monroe

A Dissertation Presented in Partial Fulfillment
of the Requirements for the Degree
Doctor of Philosophy

Approved November 2014 by the
Graduate Supervisory Committee:

Sandra Pizzarello, Co-Chair
Peter Williams, Co-Chair
Ariel D. Anbar
Everett L. Shock

ARIZONA STATE UNIVERSITY

December 2014

ABSTRACT

Carbonaceous chondrites (CCs) present a unique opportunity for learning about the earliest organic chemistry that took place in our Solar System. The complex and diverse suite of meteoritic organic material is the result of multiple settings and physicochemical processes, including aqueous and thermal alteration. Though meteorites often inform origin-of-life discussions because they could have seeded early Earth with significant amounts of water and pre-biotic, organic material, their record of abiotic, aqueous, and organic geochemistry is of interest as well.

CC materials previously resided on asteroidal parent bodies, relic planetesimals of Solar System formation which never accreted enough material to develop long-lived, large-scale geological processes. These bodies were large enough, however, to experience some degree of heating due to the decay of radiogenic isotopes, and the meteorite record suggests the existence of 100-150 parent bodies which experienced varying degrees of thermal and aqueous alteration for the first several 10 Myr of Solar System history.

The first chapter of this dissertation reviews literature addressing aqueous alteration as an essential participant in parent body geochemistry, organic synthesis, or both (though papers which address both are rare). The second chapter is a published organic analysis of the soluble organic material of Bells, an unclassified type 2 chondrite. Analytical approaches to assess terrestrial contamination of meteorite samples are also reviewed in the first chapter to allow introduction in chapter 3 of kinetic modeling which rules out certain cases of contamination and constrains the timing of thermal and aqueous alteration. This is the first known application of isoleucine epimerization for either of

these purposes. Chapter 4 is a kinetic study of D-*allo*-isoleucine epimerization to establish its behavior in systems with large, relative abundances of *allo*isoleucine to isoleucine. Previous epimerization studies for paleontological or geological purposes began with L-isoleucine, the only protein amino acid of the four isoleucine stereoisomers.

Kinetic model calculations using isoleucine stereoisomer abundances from 7 CR chondrites constrain the total duration of the amino acids' residence in the aqueous phase. The comparatively short timescales produced by the presented modeling elicit hypotheses for protection or transport of the amino acids within the CR parent body.

ACKNOWLEDGMENTS

Before acknowledging the people whose insight, experience, patience, and guidance were essential to my research and program at Arizona State University, I would first like to express how grateful I am for the many exceptionally talented and dedicated teachers and professors who instructed me before graduate school. I also would like to thank Lynn Rothschild and Richard Zare, co-advisors for my M.S. thesis in chemistry at Stanford, for introducing me to the fields of astrobiology and cosmochemistry.

The interdisciplinary nature of this dissertation would not have been possible without the diverse expertise of my committee members and the faculty, staff, and other graduate students at Arizona State University. I am eternally indebted to: Sandra Pizzarello for her mentorship and instruction in meteoritic organic analysis, Peter Williams for his mentorship, instruction in grant writing, and insightful discussions, especially about instrument design and chemical physics, Ariel Anbar for being the welcoming director of the NASA Astrobiology Institute at ASU and helping with scientific writing and communication, and Everett Shock for engaging and encouraging me in the laboratory and in field work of the wilds of Yellowstone.

I acknowledge Phil Christensen, George Cody, Steve Desch, Laurence Garvie, Ian Gould, Ron Greeley, Hilairy Hartnett, Pierre Herckes, Meenakshi Wadhwa, Maitrayee Bose, Klaus Franzreb, Christopher Glein, Aurelie Marcotte, Marc Neveu, Kirtland Robinson, Ian Pahk, and Brian Woodrum for consultations practical, theoretical, and everywhere in between. Finally, I must thank the ASU librarians for their incredible powers in finding obscure meteorite papers and conference proceedings.

This work was made possible by financial support from the Department of Chemistry and Biochemistry, the ASU NASA Astrobiology Institute, the NASA Cosmochemistry and Origins programs, and the ASU Graduate and Professional Student Association.

TABLE OF CONTENTS

Page

CHAPTER Page

APPENDIX Page

LIST OF TABLES

Table Page

LIST OF FIGURES

Figure Page

Figure Page

I. AQUEOUS ALTERATION AND SOLUBLE ORGANIC MATERIAL IN METEORITES

Aqueous alteration of asteroidal parent bodies is the process of extraterrestrial, chemical weathering by water which may occur before or after their accretion. In this chapter, meteorites, their classification, and aqueous alteration are introduced, a summary of the asteroidal parent body processing vs. pre-accretionary or "nebular" processing debate is included, and literature regarding aqueous alteration and amino acid synthesis on carbonaceous chondrite is reviewed. The chapter concludes with a review of analytical approaches to distinguishing terrestrial contamination from meteoritic organic compounds.

1.1 Aqueous Alteration

Aqueous alteration occurred in varying extents aboard the 100-150 suspected asteroidal parent bodies (Burbine, McCoy, Meibom, Gladman, & Keil, 2002) in existence before impactors disintegrated the parent bodies into smaller fragments, some of which landed on Earth to be discovered and identified as meteorites. The total number of named iron, stony iron, and stony meteorites at the time of this writing according to the Meteoritical Bulletin Database of the Meteoritical Society was just over 50,000. This growing collection of materials, the most primitive samples of the history of the Solar System, contains evidence of the extent of heating, melting, and exposure to liquid water which these materials endured.

The decay of short-lived, radioactive isotopes such as ^{26}Al and ^{60}Fe (Urey, 1955; McSween, Ghosh, Grimm, Wilson, & Young, 2002; Dyl et al., 2012) was responsible for the majority of heat generated on the parent bodies. Gravitational potential energy from

accretion and collisional energy from impactors added some heat to these systems, but the enduring source of energy was radioactive decay. This post-accretional heating led to varying degrees of melting of the primitive bodies and, in the presence of water, chemically weathered Mg,Fe-silicate rock into phyllosilicates (clays), and formed secondary minerals such as carbonates, magnetite, ferrous olivine ($Fa_{40\text{-}100}$), salite-hedenbergite pyroxenes ($Fs_{10\text{-}50}Wo_{45\text{-}50}$), wollastonite, andradite, and nepheline (Zolensky, Krot, & Benedix, 2008).

The current, two-dimensional method for classification of chondritic meteorites includes group and petrologic type and has remained fundamentally unchanged for nearly 50 years. Group, designated by letter, is determined by chemical composition in the form of elemental and Fe or MgO to SiO_2 ratios and Fe^0/Fe and other indicators of iron oxidation. The actual letter corresponds to the first, major representative meteorite of that group, and some examples include Ivuna (CI), Mighei (CM), Renazzo (CR), Ornans (CO), and Vigarano (CV). Oxygen isotopes were later shown to effectively distinguish members of meteorite groups according to fractionation lines on a $\delta^{17}O$ vs. $\delta^{18}O$ plot (Clayton, 1993). Petrologic type, designated by a number 1-7, is determined by "mineralogical and textural differences that appear to reflect the degree of equilibration experienced." The effective center of the scale, reserved for unaltered meteorites, is assigned to petrologic type 3. Type 1 indicates the most extensive aqueous alteration, and 7 the most extensive thermal alteration (Van Schmus & Wood, 1967; Weisberg, McCoy, & Krot, 2006).

Organized into four major models, explanations of the presence of alteration phases vary in hypothesized timing or setting:

> "(1) reaction of anhydrous, high-temperature condensate phases with water vapor as the solar nebula cooled to temperatures below ~375K, (2) hydration of anhydrous dust in icy regions of the nebula during the passage of shock waves, (3) alteration within small (tens of meters), ephemeral parent bodies that were subsequently disrupted and their altered components accreted with unaltered materials into the final asteroidal parent bodies (pre-accretionary alteration), and (4) alteration within asteroidal parent bodies" (Brearley, 2005).

The literature does not seem to strictly exclude nebular (1) or parent body (4) processing and suggests that reality is inevitably the combination of multiple settings for aqueous alteration. Detailed, isotopic studies remain the most promising approach to distinguish the effects of each kind of processing. Though models 1–3 provide plausible aqueous settings for meteoritic organic synthesis, the remainder of the dissertation will refer to aqueous alteration as it relates to organic geochemistry of the asteroidal parent bodies.

1.2 Constraining the Temperature, Age, and Duration of Aqueous Alteration

Direct characterization of asteroidal parent body fluids is made difficult due to the scarcity of samples: most fluid material has been incorporated into hydrous minerals or outgassed into the vacuum of space at the surface of the parent body, but some inclusions remain. Even if such an inclusion is found, analysis is difficult because of small sample size, the risk of contamination by terrestrial water during sample preparation, and the inevitable, localized heating form thin section preparation or ion-beam analyses (Zolensky, et al., 2004).

In the absence of the fluid itself, analyses are directed to the last materials the fluid affected: matrix or fine-grained chondrule rims. One thermometric method uses carbonates in 'clumped-isotope' thermometry by exploiting the thermodynamically-

driven preference of heavier isotopes ^{13}C and ^{18}O to form the same carbonate ion (Guo & Eiler, 2007). Other approaches measure relative mineral abundances, varying enrichments of heavy O-isotopes, and the oxidation state of iron to determine geochemical conditions such as temperature (Table 1) or composition such as water/rock ratio or the fugacity of molecular oxygen.

Table 1. Temperatures ranges from geochemical, mineralogical, and isotopic studies (and references therein) to generalize alteration of asteroidal parent bodies (Zolensky, Barrett, & Browning, 1993; Zolensky, Krot, & Benedix, 2008; Schrader, et al., 2011; Krot, et al., 1998; Guo & Eiler, 2007).

	CO	**CR**	**CM**	**CV**	**CI**
temperature range (°C)	≤ 50	≤ 150	20 - 75	< 300	50 - 150

Absolute and relative dating of aqueous alteration phases are difficult because multiple, distinct phases have altered some meteorites. Mineralogical analyses have been applied to arrange distinct phases in an alteration sequence (Palmer & Lauretta, 2011), but absolute dates require measurement of long-lived isotope systems which are usually "anchored" to an early-forming mineral phase such as a Calcium-Aluminum-Rich Inclusion (CAI). Relative to CV CAIs with an absolute Pb-Pb age of 4567.2 ± 0.6 Ma (Amelin, Krot, Hutcheon, & Ulyanov, 2002), short lived isotope chronology using ^{26}Al-^{26}Mg, ^{53}Mn-^{53}Cr, and ^{129}I-^{129}Xe in secondary minerals indicates that aqueous alteration may have occurred in a window which began 1.5 ± 0.5 Myr after the CAIs and lasted up to 15 Myr (Krot, et al., 2006; Zolensky, Krot, & Benedix, 2008).

The system most widely used for dating aqueous alteration episodes is the ^{53}Mn-^{53}Cr (half-life of ^{53}Mn is 3.7 Myr), for its isotopes are sufficiently abundant, have half-lives of suitable duration to precisely date ~Myrs processes, and fractionate readily into the carbonates which are deposited during aqueous alteration. A number of studies have been newly tabulated here (Table 2).

It is not the purpose of this dissertation to review isotope systematics applied to the dating of Solar System bodies and processes, but reviews regarding the timescales of alteration of chondritic meteorites and planetesimal differentiation (Krot, et al., 2006; Wadhwa, Srinivasan, & Carlson, 2006) and references therein would serve the interested reader.

It should also be mentioned that absolute age determinations before 2010 assumed constant $^{238}\mathrm{U}/^{235}\mathrm{U} = 137.88$, and later recognition of $^{238}\mathrm{U}/^{235}\mathrm{U}$ variations in meteorites led to the conclusion that absolute ages had been overestimated (i.e., formation was closer to the present than previously thought), and in the case of CAIs, overestimated by up to 5 Ma (Brennecka, et al., 2010).

Table 2. Aqueous alteration ages and durations organized by meteorite, analytical approach, and investigators. Any conclusion, age, or study which falls below the meteorite in the table applies to it, and some conclusions, ages, and investigators include multiple meteorites. Isotope chronometry is used to date carbonate deposition in carbonaceous chondrites. Allende CAIs (Pb-Pb, re-calculated after Brennecka et al., 2010) fall within 4567.0 ± 0.5 Ma (Bouvier and Wadhwa, 2010), angrites 4563.37 ± 0.25 Ma (Brennecka and Wadhwa, 2012).

approach	**Short-lived radionuclide systematics of ^{53}Mn-^{53}Cr in secondary carbonates**										**carbonate compositions**	**phyllosilicate & magnetite abundance, pyrrhotite & pentlandite corrosion**		
group and petrologic type	CR2	CR1	CR2-like (incl. CI, CM fragments)		CM2.1		CM2	CM1		ungrouped C2 (CI-, CM-like)	CI1			
meteorite	Renazzo	GRO 95577	Kaidun		QUE 93005	ALH 83001	Y791198	ALH 84034	ALH 84049	ALH 84051	Tagish Lake	Orgueil	Ivuna	Tonk & Alais
relative or absolute age	with CM, CI, CV, and CO		began ≤ 4 Myr after CAIs		began ≤ 3.93 ± 0.23 Myr after CAIs	with or shortly after CAIs	with CAIs	~ 6 Myr before angrite differen-tiation		~ 11 Myr before angrite differen-tiation	> 1 Myr after QUE 93005, ALH 83001, and Kaidun carbonates	16.5 ± 1.7 Myr after CAIs		
duration of alteration		> Renazzo		> 8 Myr		> 4 Myr	~ 15 Myr	< 5 Myr			4562.8 ± 0.94 Ma		multiple episodes	> Tonk & Alais	< Orgueil & Ivuna
investigators	Jilly et al., 2013		Petitat et al., 2011	Hutcheon et al., 1999	Lee et al., 2012	de Leuw et al., 2009	Brearley et al., 2001	Tyra et al., 2009; Tyra et al. 2010			Blinova et al., 2011; Blinova et al., 2012	Endreβ and Bischoff, 1996	Bullock et al., 2003	

1.3 Aqueous Alteration and Meteoritic Organics

"Can any relationship be observed between organic constituents and degree of metamorphism in the unequilibrated and related chondrites? If so, to what may the observed trend be attributed? To alteration or destruction of indigenous organic materials? To differing initial distributions and concentrations?"

-- J. M. Hayes (1967)

The Strecker-cyanohydrin amino acid synthesis is included in most hypotheses regarding the role of aqueous alteration in the synthesis, catalysis, or racemization of meteoritic organics, and the apparent scientific majority opinion is that it was at least a major synthetic route for the meteoritic α-amino acids (the α-carbon is the carbon nearest to the carboxyl group). The reaction takes place in the presence of HCN, NH_3, an aldehyde or ketone precursor, and H_2O. One characteristic feature of the Strecker synthesis is the reaction pathway after the consumption of ammonia. Abundant H_2O reacts instead of ammonia in the final step to produce hydroxy- rather than amino- acids

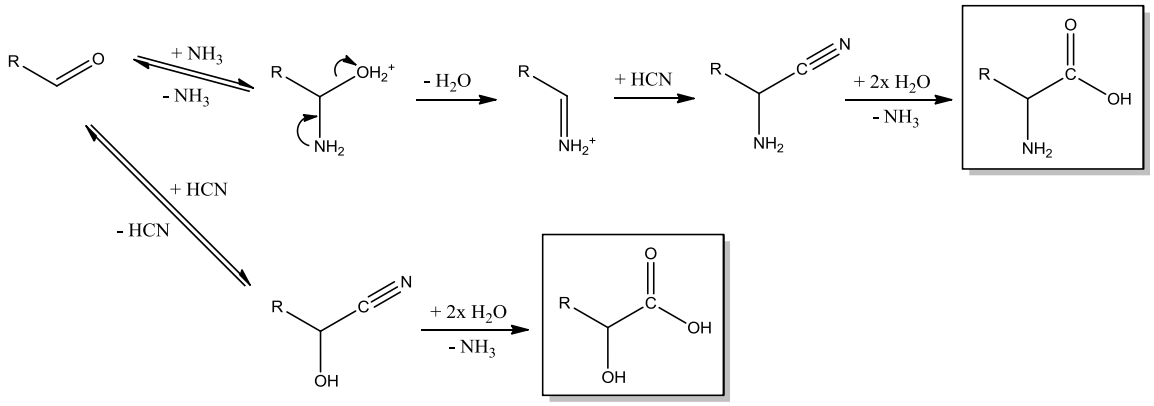

Figure 1. Adapted figure of the Strecker-cynanohydrin synthesis (Peltzer, Bada, Schlesinger, & Miller, 1984; Pizzarello, Wang, & Chaban, 2010). Protonation and deprotonation are not depicted.

which share the same R-group and are said to be "corresponding" between the molecular groups, and the presence of corresponding amino- and hydroxy- acids has been used to strengthen the case for the Strecker synthesis on asteroidal parent bodies (Peltzer, Bada, Schlesinger, & Miller, 1984). This evidence was later enhanced by studies which again detected the similar distributions of L and D amino acid enantiomers (chapter 3 contains an extended introduction to chirality) between corresponding amino- and hydroxy-acid groups and found similar isotopic enrichment between the corresponding groups (Pizzarello, Wang, & Chaban, 2010). That the amino- and hydroxy-acids share a common precursor seems clear, but questions regarding the timing of the formation of amino acids and any role of water remain if a Strecker synthesis is responsible. The first of these is the relatively short lifetime of HCN ($<10^4$ yr at 0°C), and the second is the finding of abundant amino acids in aqueously unaltered meteorites (Peltzer, Bada, Schlesinger, & Miller, 1984; Pizzarello, Schrader, Monroe, & Lauretta, 2012).

Correlative studies of amino acids and other organics in meteorites of known petrologic type have measured trends in relative ratios of amino acids (Botta, Glavin, Gerhard, & Bada, 2002; Glavin, Callahan, Dworkin, & Elsila, 2011). The increase in β-alanine and decrease of α-aminoisobutyric acid relative to glycine with aqueous alteration (Fig. 2) led to the suggestion that these β-alanine/glycine ratio could gauge the extent of aqueous alteration. Glycine is an abundant protein amino acid, however, so it is used in diagnostic ratios with attention to possible contamination.

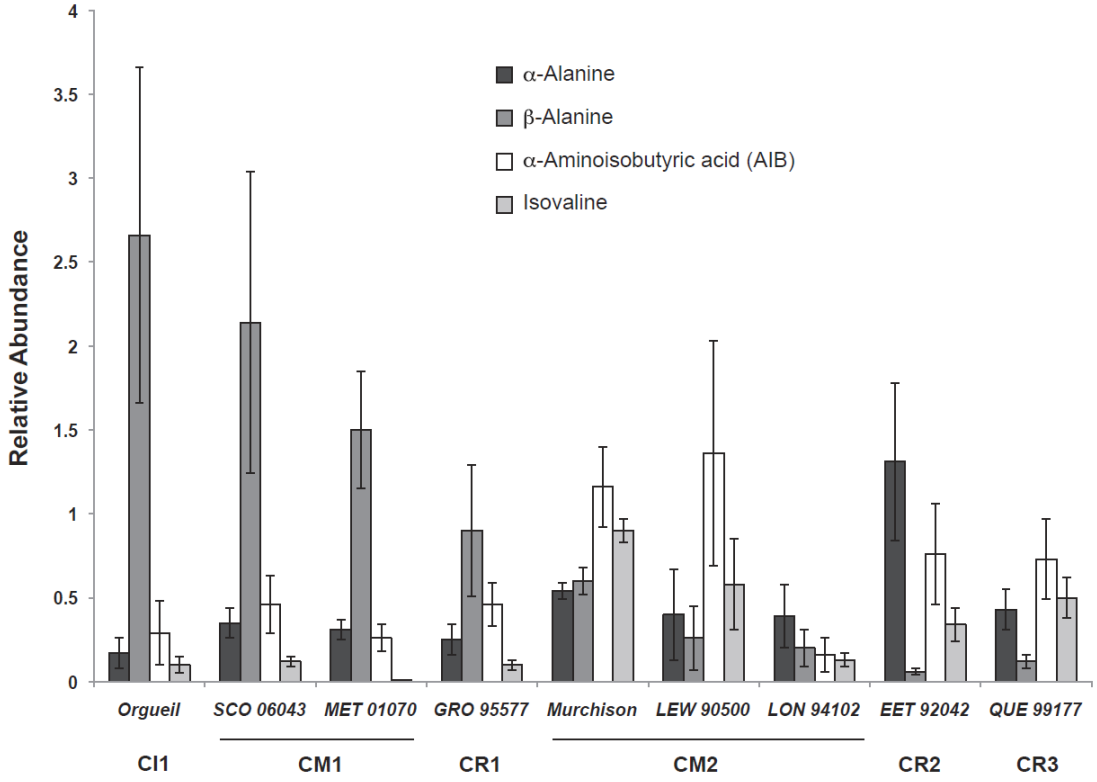

Figure 2 (reprinted with permission). Comparison of relative amino acid abundances by meteorite and ordered left to right according to petrologic type 1-3 (Glavin, Callahan, Dworkin, & Elsila, 2011).

A recent study of the Tagish Lake meteorite provided an opportunity to study fragments with various degrees of aqueous alteration from the same meteorite (Herd, et al., 2011). The same increase in β-alanine/glycine was observed with increasing aqueous alteration, and the availability of isotopic data allowed several other conclusions about the effects of aqueous alteration by linking increased hydrothermal alteration to: (1) decreases in aliphatic character (H/C), (2) depletion of deuterium by fluid exchange, and (3) increases of $\delta^{13}C$ in monocarboxylic acids by exchange with ^{13}C-enriched fluid carbonates. Enantiomeric ratios (D/L) of the amino acid isovaline (Fig. 3) negatively

Figure 3. 5-carbon amino acids L-isovaline (left) and D-isovaline (right).

correlated with abundances of hydrous minerals in Murchison (Pizzarello, Zolensky, & Turk, 2003) but did not correlate in Tagish Lake. In fact, only one of the four analyzed fragments showed an excess of L-isovaline (molecular asymmetry, chirality, and enantiomeric excess are introduced in greater detail in chapter 3).

The majority of these studies employ bulk, wet chemical analyses of powdered, extracted meteorites, and though this approach is extremely well-suited for separating the complex mixtures of organics in meteorites, a disadvantage of these analyses is their homogenization of potentially illuminating differences within a heterogeneous sample.

In situ studies cannot separate individual compounds but can associate organic assemblages with mineralogy: to name a few studies, (unspecified) organics reacted with OsO_4 were detectable *via* scanning electron microscopy (SEM) and found almost exclusively among phyllosilicates (Pearson, Kearsley, Sephton, & Gilmour, 2007), near-field infrared microspectroscopy demonstrated the correlation between phyllosilicates and regions rich in C-H bonds (Kebukawa, et al., 2010), and NanoSIMS analyses of high D/H and $^{12}C/^{28}Si$ ratios coupled with SEM images illustrated that organic-rich regions were surrounded by hydrous minerals (Remusat, Guan, Wang, & Eiler, 2010). Since phyllosilicates are products of hydrothermal alteration of olivines—minerals commonly found in unweathered portions of both iron-rich meteorites and terrestrial mafic and

ultramafic igneous rocks—the collocation of organics with these minerals indicates that aqueous alteration played at least some role in their formation or deposition.

It is possible that these studies detected only insoluble organic material (IOM), the aromatic, kerogen-like component which contains most of the organic carbon in carbonaceous chondrites. IOM is insoluble in water or organic solvents such as dichloromethane or methanol. Soluble organic material is comprised of smaller molecules such as amino acids, carboxylic acids, sugars, etc. which are easily extracted from meteorites powders with water or organic solvents.

1.4 Assessing Terrestrial Contamination

The commonalities between organic materials in meteorites and the biosphere provide motivation for their study but at the same time complicate it with the possibility of contamination. Whenever meteoritic material reaches Earth, it first comes into contact with something other than a sterile sample container. Even if meteorite fragments are recovered quickly, local weather may heat or wet the sample and change its contents before collection occurs. These meteorites are called “falls” on account of their falling’s being observed and, especially if radar or other telemetry data are available, an estimated trajectory is used to assist in locating any surviving fragments. On the other hand, meteorites which arrived unnoticed and are later found are called “finds.” Deserts and the Antarctic are convenient, natural curatorial environments for finds because of their low relative humidities and, in the case of the Antarctic, cold temperatures which discourage terrestrial chemical modification. Another benefit of Antarctic curation is the encasement and concentration of meteorites in ice flows. These flows are eventually forced upward by transarctic mountain ridges to expose the encased meteorites (Cassidy, 2012).

If organic analyses of meteorites are to be helpful in understanding asteroidal parent body organic chemistry, the indigenous components of a meteorite sample must be distinguished analytically from the terrestrial contaminants. Contamination can be identified using three major approaches, each with a different underlying set of assumptions and analytical instrumentation. For the purposes of this dissertation, these approaches are referred to as holistic, isotopic, and thermodynamic/kinetic. The thermodynamic/kinetic approach applied to L-isoleucine contamination is newly presented in chapter 3, section 3.2., but the other two approaches have been used extensively.

Before the addition of isotope ratio mass spectrometry (IRMS) to chromatographic techniques, individual amino acids could only be separated by ion or gas chromatography following chemical derivatization of meteorite extracts, and contamination was ruled out by (1) the presence of non-protein amino acids or (2) racemic mixtures of amino acid enantiomers (Kvenvolden, et al., 1970). Several amino acids themselves were also identified as likely contaminants. The low thermal stability of serine, abundance of tyrosine, phenylalanine, and methionine in the biosphere, and presence of serine, citrulline, and ornithine in bodily fluids made their detections cause for suspicion (Vallentyne, 1964; Hamilton, 1965; Engel & Nagy, 1982).

The scientific consensus of the time was that parent body environments were a-biotic and a-chiral in chemical synthesis and catalysis, so detections of non-protein amino acids and racemic mixtures of amino acid enantiomers would be expected for uncontaminated, extraterrestrial samples. While amino acid identification and quantification contribute to every modern assessment of organic, terrestrial contamination of meteorites, it should be mentioned that isoprenoids were used for this purpose until improvements in the separation and quantification of amino acids allowed the use of amino acids as well.

Isoprenoids (also known as terpenoids) are hydrocarbons with multiples of 5 carbons based on the isoprene molecule (Figure 4). In the biosphere at large, isoprenoids are generally synthesized and employed by plants as common sources of scent, flavor, or color (Mangal, 2007), and these compounds also happen to be found in meteorites. The association of low n-alkane/isoprenoid ratios with meteorite contamination is thoroughly

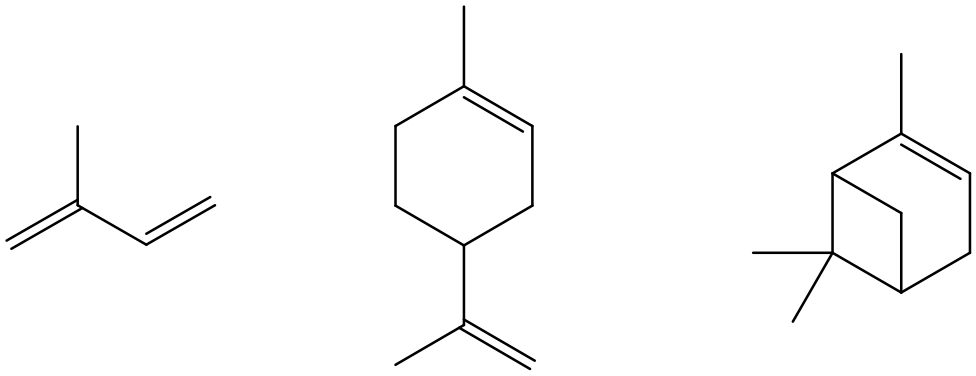

isoprene limonene (±)-α-pinene

Figure 4. Isoprene (C_5H_8) and monoterpenes ($C_{10}H_{16}$) limonene and (±)-α-pinene. Limonene is a major constituent of citrus fruit peels, and α-pinene, the most abundant terpene in nature, is a major constituent of pine resin (Başer & Buchbauer, 2010).

reviewed elsewhere (Hayes, 1967), but the basic approach is essentially the same as for amino acids: there exist abundant molecules in the biosphere which also are found in meteorites, and "contaminated" samples will exhibit characteristically high or low values in ratios involving molecules that are pervasive in the biosphere. This "holistic" approach is effective so long as the expectations for contamination (and quantitative expectations for ratios) are established over many samples and with careful attention to any other possible contaminants.

The combination of IRMS with a chromatographic separation technique enabled measurement of compound-specific isotopic enrichment, a boon to meteoriticists, specifically for identifying and quantifying amino acid contamination (Engel & Macko, 1997), characterizing precursor environments (Epstein, Krishnamurthy, Cronin, Pizzarello, & Yuen, 1987; Pizzarello & Huang, 2005), or identifying pathways of amino acid synthesis by searching for characteristic isotopic enrichments (Elsila, Charnley, Burton, Glavin, & Dworkin, 2012). As a result, gas chromatography (GC)-C-IRMS is now the most commonly used technique for isotopic analysis of soluble organic material extracted from meteorites. Though GC-C-IRMS is considered to have ample detection and quantitation limits for the environmental sciences, space samples are often too scarce to meet these limits, especially when there are other competing analyses required to maximize characterization of the meteorite's diverse, extractable contents. As a side note, nanoliquid chromatography-high-resolution MS is a promising, relatively new technique which reduces sample requirements for chiral separation and quantification of amino acid enantiomers (Callahan, Martin, Burton, Glavin, & Dworkin, 2014). If sufficient sample for GC-C-IRMS exists, contamination may be ruled out by measurement of relative

isotopic enrichments of an enantiomeric pair. This is made possible by the virtually exclusive contamination of L-enantiomers with isotopically light, terrestrial material.

One analysis of Murchison contained D-glutamic and L-glutamic acid with $\delta^{13}C$ of +32.2 ±1.7 ‰ and +14.6 ± 0.4‰, respectively, indicating that some L-glutamic acid was contaminated by isotopically light, terrestrial L-glutamic acid (Pizzarello & Cooper, 2001). Conversely, the isotopic enrichment of L-aspartic vs. D-aspartic acid (+29 ± 4‰ and +24 ± 4‰) has been used to exclude contamination in an extract of the Tagish Lake meteorite (Glavin, et al., 2012). Both conclusions follow from the assumption that the meteorite's indigenous L- and D- enantiomers contain roughly equal isotopic enrichments. In the case of Murchison, the isotopically lighter L-glutamic acid indicates contamination, and in Tagish Lake, the isotopically heavier L-aspartic could not have been substantially contaminated. Sample and instrumentation permitting, these approaches distinguish heavier, extraterrestrial materials from their isotopically lighter versions on Earth and improve confidence in assessments of contamination.

II. SOLUBLE ORGANIC MATERIAL IN A PRISTINE FRAGMENT OF BELLS, AN ANOMALOUS CARBONACEOUS CHONDRITE

This chapter consists of a manuscript slightly updated and modified since its publication in Geochimica et Cosmochimica Acta (Monroe & Pizzarello, The soluble organic compounds of the Bells meteorite: Not a unique or unusual composition, 2011).

The Bells meteorite is an ungrouped chondrite that has long been considered anomalous for having mineralogical and isotopic differences from CMs together with an overall affinity to CIs in its matrix. The only unweathered Bells stone was extracted with water and solvents and studied for its soluble organic composition. Bells contains abundant organic compounds, which are predominantly O-containing such as hydroxy- and di-carboxylic acids, and a scarcity of amino acids and other N-containing compounds. Amines were not detected, and ammonia is less abundant than in both the Murchison and Ivuna meteorites. Overall, Bells' soluble organic composition is more similar to Ivuna's than Murchison's. The observation that Bells' amino acid suite shares a distinct distribution of characteristic molecular species with other stones that are thought to have experienced extensive parent body aqueous alteration (Orgueil, Ivuna and recently analyzed GRO 95577 CR1 meteorites) seems to allow the suggestion that such a composition is secondary to prolonged aqueous alteration processes that superseded some of the initial compositional distinctions determined by the asteroidal environments.

2.1 Introduction

Several carbonaceous chondrites have the unique compositional attribute of containing soluble organic compounds. So far, these have been described in CI, CM, CR,

the CV3 Allende and unclassified Tagish Lake meteorites (Pizzarello, Cooper, & Flynn, 2006) (and references therein for a review); for references after 2006; (Glavin & Dworkin, 2009; Glavin, Callahan, Dworkin, & Elsila, 2011; Pizzarello & Holmes, 2009; Pizzarello, Huang, & Alexandre, 2008; Martins, Alexander, Orzechowska, Fogel, & Ehrenfreund, 2007; Pizzarello, Wang, & Chaban, 2010). Because several of the meteoritic compounds are also found in the biosphere, their finding has acquired a unique exobiological significance and their study may offer insights into both the exogenous organic inventory available for the development of early life on the Earth and the prior cosmochemical evolution of biogenic molecules.

CC organic compositions were found to be highly heterogeneous in the abundance and distribution of their individual components. As a general characterization, referring to comprehensively studied meteorites and allowing for significant compositional differences often observed within individual meteorite fragments (Pizzarello, Zolensky, & Turk, 2003), we may describe the CC soluble organic suites as follows.

CM chondrites contain a large variety of molecular species and CM2s, in particular, often show complete series of isomeric and homologues compounds to the limit of their solubility; a recent study estimates the total number of Murchison compounds to exceed five thousand (Schmitt-Kopplin, et al., 2010). Amino acids, undoubtedly the compounds of the most direct prebiotic appeal, are present mainly as alkyl species, with all possible distributions of the amino group along the alkyl chain and with abundances that decline with chain lengthening. These suites appear to have

followed stochastic trends in their build up; hydrocarbons and carboxylic acids are their most abundant constituents.

The CI suites, although more challenging to define because the known meteorites of this family have been exposed to long terrestrial residence and possible contamination (Pizzarello & Huang, 2002; Sephton, Pillinger, & Gilmour, 2001), appear to contain fewer compounds and lower abundance of the ones that are present. Distributions within compound groups differ from those in CMs, *e.g.*, β-alanine appears to be CI's most abundant indigenous amino acid (Ehrenfreund, Glavin, Botta, Cooper, & Bada, 2001). Other non-α-amino acids have also been seen in Orgueil and Ivuna with higher relative abundance than in CM2s.

CR chondrites (CR2s in particular) were analyzed only recently with pristine finds from Antarctica and found to be so far unique in containing predominant water-soluble compounds and abundant N-species in particular. In these meteorites, ammonia and amino acids are the most abundant single molecule and compound group, respectively, while hydrocarbons and O-containing molecular species such as carboxylic acids are less abundant than in CIs and CMs by orders of magnitude (Pizzarello, Huang, & Alexandre, 2008).

Isotopic analyses have shown most meteoritic organic compounds to be enriched, to various degrees, in D, ^{13}C and ^{15}N, demonstrating their indigeneity and allowing the general hypothesis that these molecules' synthetic lineage, or that of their direct precursors, can be traced back to cold cosmic regimes (Sandford, Bernstein, & Dworkin, 2001; Pizzarello, 2006). CR2s contain the largest deuterium enrichment of presently analyzed CCs by far (Pizzarello & Huang, 2005; Pizzarello & Holmes, 2009).

The diversity observed in the molecular and isotopic distribution of organic compounds in various meteorite types raises several questions about their formative histories. One is whether the observed differences are primary, *i.e.*, relate to different pre-solar molecular environment, or are the effect of solar processes. This question could be answered, if partially and in general terms, on the basis of elemental composition; *e.g*, the slightly larger nitrogen elemental content of CR2s (Kerridge, 1985), were it to include reactive molecules such as ammonia (Pizzarello, Williams, Lehman, Holland, & Yarger, 2011; Pizzarello & Williams, 2012), would seem to allow the hypothesis that their amino acid abundances related to that original compositional difference.

By contrast, when the cases in question are the specific distribution and abundance of molecular species in various meteorites, many variables related to solar processes become relevant and answers are not readily apparent. The comparison of a meteorite's organic composition *vis-à-vis* its geochemical and mineralogical make-up has allowed to estimate the feasibility and range of organic reactions. For example, the observation of an aqueous record in several of Murchison mineral phases (Bunch & Chang, 1980) gave insights on how these reactions might have proceeded after asteroidal accretion. Unexpectedly, a recent comparison of the chiral and abundance distributions of Murchison amino- and hydroxy acid diastereomers' suggested that certain water-requiring synthetic pathways for amino acids' formation may have proceeded even before asteroidal accretion when abundant ammonia was present (Pizzarello, Wang, & Chaban, 2010).

However, the overall understanding of these processes is still limited by the absence of similar comparative studies between meteorites, the inherent difficulty in

correlating specific geological features with organic distributions and our still profound lack of knowledge about how many of the meteoritic compounds were indeed formed (Pizzarello, et al., 2001). The Bells meteorite appears to offer a unique opportunity to analyze the soluble organic composition of a meteorite that, within the classification of CM2, shows several geochemical differentiations with CM as well as CI meteorites (Brearley, 1995) whose organic compositions are already well known. We report here on a comprehensive analysis of the water- and solvent-soluble organic compounds extracted from the Bells meteorite, evaluate their distributions relative to those of the Murchison (MN), a CM2, and Ivuna (IV), a CI, chondrites and attempt an explanation of the differences/commonalities observed between them.

2.2 Materials and Methods

2.2.1 Sample Preparation

The Bells and Ivuna samples employed in this study were obtained from the Center for Meteorite Studies at Arizona State University. The Bells fragment weighed 925 mg and was taken from the unweathered stone collected at the meteorite's fall (Grady, 2000), and the Ivuna sample consisted of several small fragments for a total weight of 530mg. Both Bells and Ivuna were powdered in an agate mortar and the powders subdivided for individual compounds' analyses as follows. Bells: a) 395 mg were used for peptide/unhydrolyzed amino acid analyses and extracted with 2ml of water, in evacuated vial, at 25^{o}C, for 24h; after decanting of the extract, the powders were again extracted as above at 100^{o}C. Both extracts were desalted through a cation-exchange resin (BioRad AG-50, 200-400 mesh) and the eluates of water and ammonium hydroxide (NH_4OH) collected. The water eluates were further fractionated on an anion exchange

resin (Bio-Rad AG-4, 100-200 mesh) and the water, acetic acid, and HCl eluates from this resin collected (Pizzarello, Wang, & Chaban, 2010); b) 250 mg were extracted at 100^{o}C and the extract was decanted, dried, hydrolyzed with 6N HCl at 100^{o}C for a day, dried and separated as above for the analyses of hydrolysable water soluble compounds; c) 200mg were used for the search of aldehydes and ketone and d) 150 mg were extracted for the separation of amines and carboxylic acids. Ivuna powders were also divided in for the analyses of aldehydes, amino-, hydroxy and di-acids and, respectively, amines and carboxylic acids: a) 280mg were extracted with water and the extract used for the analyses of aldehydes, carboxylic, amino-, and hydroxy acids by the same methods as above; b) 250 mg were also extracted with water and the extract analyzed for amines, as above; the residue from the cryogenic transfer was hydrolyzed for the analyses of amino-, hydroxy and di-acids. All water extracted powders were subsequently combined, dried and extracted with a 9:1 (v:v) dichloromethane DCM: methanol (MeOH) solution for 24h, at 100^{o}C in an evacuated vial.

2.2.2 Molecular Analyses

All samples were analyzed by gas chromatography-mass spectroscopy (GC-MS) after derivatization to acquire the desired volatility of the compounds of interest; analyses were performed employing an Agilent 6890N GC system and 5973N*etwork* Mass Selective Detector. Estimation of compound abundances was based on comparison of their total and/or single ion peak areas with yields obtained from commercial standards. When compounds had poor resolution in the chromatograms, such as in the case of the numerous branched-chain linear hydrocarbons, their combined area was assessed based on the unit area value of a compound of similar m/z in a standard calibration curve. A

similar approach was used for unknown peaks if standards were not available and the general type of the compound was known from its mass spectrum and/or retention time. In the case of amino acids, all compounds found in the meteorites had reference standards. Additional information, when needed, is given in the table legends. A separate fragment of the same unweathered Bells stone from the CMS used in this study had been analyzed previously for amino acids by liquid chromatography with fluorescence detection (Cronin, Pizzarello, & Gandy, 1979); the data obtained were examined against our new GC-MS data and found comparable.

Amino Acids and Peptides

Amino acids and peptides were searched for in the NH_4OH eluates from cation exchange separation of the extracts. The eluates were dried and derivatized with isopropanol HCl (~3N) at 25^{o}C for one day for the room T extract and at 100^{o}C, for one hour, for the 100^{o}C extracts. Following evaporation of the alcohol, the isopropyl esters were reacted with trifluoroacetic anhydride (TFAA) in dichloromethane (DCM; 1:4, v:v) at room T for 30 min. The resulting N-TFA-O-isopropyl amino acid derivatives were concentrated by evaporation under He at room temperature and re-dissolved in dichloromethane. GC-MS analyses employed a Chirasil-Dex-CB column of 25 m x 0.25 mm and 0.25 μm film thickness by Varian, used a helium flow of 0.6 ml min^{-1}, and oven temperature program of 65^{o}C initial, for 7 min, 2^{o} min^{-1} to 85^{o}, 4^{o} min^{-1} to 200^{o}.

Amines and Ammonia

Amines and ammonia were found by making their solutions basic with NaOH (semiconductor grade, Aldrich Chem. Co.) and cryogenic transfer (Pizzarello & Holmes,

2009). The collected solutions were made acidic with HCl, dried on rotary evaporator, derivatized with TFAA (as above) and analyzed by GC-MS on the Chrompak column, also described above, with the T program: 34^{o}C in. T, to 43^{o} at 3^{o} min^{-1}, 10 min hold, to 200^{o}C at 4^{o} min^{-1}.

Monocarboxylic Acids

Monocarboxylic acids were also obtained by cryogenic transfer of the unhydrolyzed extract, which was made acidic with phosphoric acid (> 99.9999% pure, Aldrich Chem. Co.) (Pizzarello, Huang, & Alexandre, 2008); the transferred solution, plus a drop of phosphoric acid, was extracted with DCM and the DCM extract concentrated under helium at room temperature for analysis by GC-MS, with conditions as for amines.

Neutral Compounds

Neutral compounds were searched for in the water eluate of the anion exchange after drying and derivatization as for amino acids.

Hydroxy- and Dicarboxylic Acids

Hydroxy- and dicarboxylic acids were analyzed from the acetic acid eluate of the anion exchange. The sample was treated as for those containing 100^{o}C-extracted amino acids, with the only change of substituting acidified isobutanol for isopropanol in the esterification step.

Aldehydes and Ketones

Aldehydes and ketones were obtained by their direct derivatization in the water extracts, adding a 1:1 (v:v) 2.5mM solution of 2,3,4,5,6-pentafluorobenzyl

hydroxylamine (PFBHA), and subsequent extraction in hexane (Pizzarello & Holmes, 2009). A deuterated acetone (D_3CCOCH_3) standard was refluxed in water at 100 ^oC for two weeks, an aliquot of the sample taken at 24h (the extraction time) did not show any deuterium exchange. Isotopic analyses were performed by GC-Combustion-Isotope Ratio Mass Spectrometer using the same general chromatographic conditions established for molecular analyses, a combustion reactor of 1/4" OD, 1/16" ID, 600mm length, containing a chromium filling kept at 1050^oC and a Micromass IsoPrime IRMS (Pizzarello, Wang, & Chaban, 2010).

Hydrocarbons

Hydrocarbons were analyzed from the DCM:methanol extract after concentration at room T. GC-MS used a 60m x 0.25mm (0.25 μm film thickness) DB-17MS column (J&W Scientific) and the T program: 70^oC to 100 @ 2 min^{-1}, to 300 @ 5 min^{-1} with 40 min. hold.

2.2.3 Materials

Water and 6N HCl were triple and double distilled, respectively; DCM (VWR, 99.5%) was distilled once. Derivative isobutanol and isopropanol (J.T. Baker) were double distilled, acetyl chloride and TFA were from Sigma-Aldrich (derivatization kit); ammonium hydroxide was double distilled (Sigma-Aldrich, PPB/Teflon grade); sodium hydroxide (99.99% pure, semiconductor grade) and phosphoric acid (85+% in water, 99.9999% pure) were from Sigma-Aldrich. The reference standards for δ-hydroxyvaleric and ε-hydroxycaproic acids were obtained by hydrolysis of the corresponding lactones (Sigma-Aldrich).

2.3 Results

Results from the analyses of individual compound groups in the Bells and IV meteorites are summarized in Table 3, where they are also compared to data from previous studies of Murchison (Pizzarello, Cooper, & Flynn, 2006). Several differences can be observed between the compositions of the three meteorites. As the following tables of individual compounds show in more detail, these establish some recognizable affinity between the soluble organic distributions of Bells and Ivuna and a contrast with those of Murchison, such as for amino-, and hydroxy-acid relative and total abundances. Bells' depletion of extractable ammonia also demonstrates a more significant divergence from Ivuna than Murchison.

Table 3. Molecular abundances of the main groups of organic compounds found in the Murchison, Bells and Ivuna meteorites.

	Murchison[1]		**Bells**		**Ivuna**	
compound(s)	**nmol/g**[2]	**n**[3]	**nmol/g**	**n**	**nmol/g**	**n**
ammonia	1100		280		5300	
amines	130	20	nf[4]		38	5
amino acids	600	>85	93	13	156[5]	12
aldehydes/ketones	200[6]	18	134	14	1369	23
hydroxy acids	455[7]	17	1231	11	2136	10
di-carboxylic acids	300	26	43	15	857	15
carboxylic acids	3000	48	495	11	937	14
hydrocarbons	1850	237	265	82	221	30
alkanes	350	140	32	32	221	30
aromatic	300	87	250	27	489[8]	34
polar	1200	10	ne[9]		ne	

[1]nanomoles/gram meteorite, indicates total weight of compounds identified with reference standards; [2]Pizzarello et al. 2006 and references therein unless otherwise noted; [3]number of species in the group; [4]not found; (Ehrenfreund, Glavin, Botta, Cooper, & Bada, 2001)[5], also reported on Ivuna amino acids, amounts in the table are new to relate all quantitative data to the same meteorite fragment; [6]Pizzarello and Holmes, 2009; [7]Pizzarello et al., 2010; [8]phenanthrene-subtracted;[9]not estimated.

2.3.1 Amino Acids

Bells amino acid suite appears limited in both number of molecular species and their abundance compared to those of other type 2 such as Murchison and Murray; peptides were not detected. Four 2C-5C long n-alkyl, two branched and one N-methylated α-amino acids were found (Table 3 and Fig. 7), together with seven additional compounds having the amino group in position at C_3-C_6 (examples in Fig. 5); β-alanine is the most abundant among the non-α-amino acids with 16 nanomole•g^{-1} of meteorite and an adjusted ratio to glycine of ~0.75. Ivuna's suite is similar to Bells' in having terminal amino acids up to six-carbon, but some of these have different abundances than in Bells: the β-4C amino acids are less abundant while γ-aminobutyric acid approaches 50% of the abundance of β-alanine (although this latter increment may be due to decarboxylation of contaminant glutamic acid, see below) and N-methyl alanine was detected only in trace amounts. β-alanine and glycine are more abundant than in Bells and their abundance ratio is ~1.2. No non-protein amino acids in the two meteorites showed *ee*.

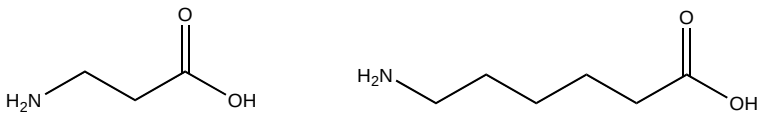

β–alanine **ε-aminocaproic acid**

Figure 5. Examples of n-ω- amino acids.

Bells amino acids were not eluted equally during the stepwise extractions: the β-compounds are released almost in their entirety at 25°C, while the α-amino acids are released at 25°C and 100°C (the proportion is ~2:1); γ-, δ-, and ε-amino acids were found only in the hydrolyzed extracts. Both Bells and Ivuna extracts showed terrestrial

contamination in ~33% L-alanine's enantiomer excess (*ee*) as well as the presence of nanomoles of L-valine, L-isoleucine, L-leucine L-threonine, L-serine and L-glutamic acid; L-glutamic acid was particularly abundant in Ivuna (~7 nanomole•g^{-1}). Glycine abundances should be estimated for both meteorites by reducing its analytically determined amount by the % of the contaminant L-alanine's ee; indigenous DL alanine abundances should be similarly projected at two times that of D-alanine.

Table 4. Amino acids detected in Bells hydrolyzed water extracts. Abundances are reported in nanomoles/gram of meteorite.

amino acid	nmol/g
L-aspartic	14.1
L-serine	10
D-glutamic	23.9
L-glutamic	
glycine*	42.1
D-alanine	6.1
L-alanine	12.1
N-methyl alanine	0.9
α-aminoisobutyric	1.7
α-aminobutyric	2.2
valine	2.5
isovaline	0.6
norvaline	1
L-isoleucine	2
L-leucine	2.7
β-alanine	2.5
N-methyl β-alanine‡	0.3
β-aminobutyric	2.5
β-aminoisobutyric	2.1
γ-aminobutyric	6.8
δ-aminopentanoic	1.8
ε-aminohexanoic	7.4

*≈30% should be considered contaminant based on L-excesses of other proteinogenic amino acids (see text), ‡identified with mass spectral library only.

2.3.2 Ammonia and Amines

As Table 3 shows, the abundance of ammonia in Bells is about one fourth of that found in Murchison (Pizzarello, Feng, Epstein, & Cronin, 1994) and well over an order of magnitude less than in Ivuna. Ivuna also contains picomoles of methyl, ethyl, isopropyl, propyl and butyl amines, *i.e.*, a variety of small molecules that resembles the distribution of other meteoritic compounds, albeit in lower amounts and smaller number of species; Bells, on the other hand, showed only a fairly large (~50 nmol) butyl amine peak that, by being the single amine detection and for its amount, had to be considered a contaminant.

2.3.3 Hydroxyacids

Hydroxyacids are the most abundant group of compounds in Bells as well as Ivuna and contain comparable molecular species in both meteorites; their overall amount is over 40% higher in Ivuna than Bells (Table 5). Comparable to distributions within amino acids, Bells and Ivuna hydroxyacid suites contain fewer molecular species than found in Murchison and include a larger presence of non-α compounds such as γ-hydroxybutyric, δ-hydroxyvaleric, and ε-hydroxycaproic acids not previously found in Murchison. A search of the records of previous analyses of Murchison extracts for these acids showed that they may be present in some samples but not others, which would be consistent with the previously observed heterogeneity of organic content in different fragments of the meteorite (Pizzarello, Zolensky, & Turk, 2003). As seen in all CC analyzed so far, lactic acids displayed L-*ee* of 24% in Bells and 20% in IV. Unlike the amino acids but consistent with some procedural losses seen previously for glycolic and lactic acids during the analytical work-up (Pizzarello, Wang, & Chaban, 2010), the

largest yield of hydroxyacids reported in Table 5 was observed before and not after hydrolysis of the extracts.

Table 5. Hydroxyacids identified in the Murchison, Bells, and Ivuna meteorites; in nanomoles/g meteorite. [1]Pizzarello et al., 2010; [2]seen in some samples, see text.

Hydroxy Acid	**Murchison[1]**	**Bells**	**Ivuna**
Linear α-hydroxy acids R-CH(OH)-COOH			
glycolic	65.0	473.2	993.6
DL-lactic	84.2	509.5	735.5
DL-2-hydroxybutyric	19.0	39.0	49.8
DL-2-hydroxyvaleric	4.5	18.2	32.6
DL-2-hydroxycaproic	65.0	15.0	37.0
Branched α-hydroxy acids R-C(CH_3)(OH)-COOH			
2-hydroxyisobutyric	30.0	90.1	31.4
DL-2-hydroxy-2-methylbutyric	12.4	1.7	nf
DL-2-hydroxy-3-methylbutyric	36.5	nf	nf
DL-2-hydroxy-2-methylvaleric	3.0	nf	nf
DL-2- hydroxy-3-methylvaleric	≤1	nf	nf
DL-2- *allo* " "	≤1	nf	nf
DL 2-hydroxyisocaproic	≤1	nf	nf
β, γ, δ, and ε-hydroxy acids R-CH(OH)-R-COOH			
β-lactic	33.5	63.8	146.5
DL[b] 3-hydroxybutyric	10.5	8.1	70.9
DL[b] 3-hydroxyisobutyric	6.1	2.0	3.5
4-hydroxybutyric	nf	10.2	32.2
5-hydroxyvaleric	nf	6.8	19.1
6-hydroxycaproic	nf	7.1	87.0
Dicarboxylic hydroxy acids HOOC-R-CH(OH)-COOH			
DL malic	7.6	nf	nf
DL 2-hydroxyglutaric	7.7	nf	nf
DL citramalic	≤1	nf	nf
Total	**387.0**	**1260.7**	**2239.1**

2.3.4 Aldehydes and Ketones

Bells contains a suite of aldehydes and ketones that compares in abundance with that of Murchison, a rather surprising finding because these are reactive compounds and their presence in the meteorite is hard to reconcile with either a direct presolar or solar origin in view of the predicted oxidative conditions of the aqueous phase within the parent body (Brearley, 1995). The high abundances of formaldehyde and acetone found in Ivuna could be the result of terrestrial contamination; were this the case, Bells, Murchison, and Ivuna carbonyl compounds would have approximately similar abundances. As seen in Table 6, Bells displays a larger ketones/aldehydes concentration ratio than Murchison (1.7 *versus* 0.7). The deuterium enrichment of a few of Bells' aldehydes and ketones confirms their indigeneity (Table 6). How extensively these values were modified during the parent body aqueous phase is difficult to estimate, however, for H-exchange between these compounds and solvent water is significant due to stabilization by enolate. To gauge the rate of exchange, we prepared a 6-D (totally deuterated) acetone standard that we extracted at 100^{o}C. Though our standards showed no detectable D/H exchange within the extraction time (see Methods, *2.2.6.*), after two weeks at 100^{o}C, all detectable deuteron enrichment had been lost to the solvent.

Table 6. δD values (‰) of selected aldehydes and ketones of the Bells meteorite.

Compound	δD‰
formaldehyde	+324
acetaldehyde	+429
propionaldehyde + acetone	+326
hexanal	+145
3-hexanone	+241
hexanone	+37

Table 7. Carbonyl compounds in the Murchison, Bells and Ivuna meteorites; in nanomoles/g meteorite. [1]Pizzarello and Holmes, 2009; [2]not found.

	Murchison[1]	Bells	Ivuna
Aldehydes			
formaldehyde	10.0	32.0	303.1
acetaldehyde	24.0	70.7	41.6
propionaldehyde	23.5	30.8	30.6
butyraldehyde	32.2	47.2	22.2
isobutyraldehyde	3.2	nf[2]	≤1
valeraldehyde	1.3	5.3	21.3
2-methylbutyraldehyde	6.0	≤1	≤1
hexanal	10.8	41.0	77.6
benzaldehyde	7.6	26.3	113.0
Total aldehydes	119	254	610
Ketones			
acetone	47.3	86.8	649
2-butanone	6.9	40.3	8.6
2-pentanone	1.5	6.2	3.5
3-pentanone	2.0	≤1	≤1
3-methyl-2-butanone	1.5	1.7	≤1
2-hexanone	25.0	146.5	77.0
3-hexanone	2.0	60.0	18.6
3-methyl-2-pentanone	≤1	nf	nf
2-heptanone	nf	nf	26.5
2-octanone	nf	nf	27.0
2-nonanone	nf	nf	25.0
2-decanone	nf	nf	22.5
Total ketones	87	342	859
Total (ketones and aldehydes)	**206**	**596**	**1469**

2.3.5 Carboxylic and Dicarboxylic Acids

Carboxylic acids have been found in all carbonaceous chondrites analyzed so far, from the ungrouped, Tagish Lake stones which saw an oxidizing environment (Pizzarello et al., 2001) to the nitrogen- and amino acids-rich GRA 95229 CR2 (Pizzarello, Huang, & Alexandre, 2008). Bells and Ivuna are therefore no exception in containing these acidic compounds, which were found with chain lengths from 1C-10C. However, Bells and Ivuna contain less overall amounts of the acids than in Murchison, and their general distribution also differs in having fewer and less of branched molecular species. Moreover, both meteorites' preparations showed signs of possible terrestrial contamination. Bells' carboxylic acid extract was the most likely exposed, for it contained an overabundant formic acid peak (~ 30% of the total amount reported in Table 2) plus a series of chlorinated hydrocarbons known to be atmospheric contaminants (Muir, Norstrom, & Simon, 1988). The Ivuna extract showed several alcohols, ketones, and small phenols which could be indigenous, but there was also a concentration maximum at the linear 6C acid (hexanoic acid) and unusually abundant peaks for 7C-9C linear acids.

Dicarboxylic acids, also ubiquitous in CC to date, were found to be abundant in Bells and Ivuna. They are present with linear alkyl chain lengths of 4C to 14C and as several branched species up to 8C; 4C-6C unsaturated species were also detected. Overall the dicarboxylic acids' distributions in both Bells and Ivuna appear to correspond closely to that described for MN (Pizzarello & Huang, 2002). No tricarboxylic acids (Cooper et al., 2011) were found.

2.3.6 Hydrocarbons

Both alkanes and polycyclic aromatic hydrocarbons (PAHs) were detected in the Bells and Ivuna meteorites, and of these, Bells' alkanes appear to have a distribution most similar to those described for other CM2s such as Murchison and Murray in having linear species of increasing chain-length accompanied by several branched chain forms; their abundance maximum is at 15C (Fig. 9). Cyclic hydrocarbons that are also typical of Murchison were not found. Bells hydrocarbons are not completely free of terrestrial contaminants: we searched for isoprenoid alkanes, which could be decomposition products of phytol and phytol esters and likely contaminants (Cronin & Pizzarello, 1990), and detected a few. Ivuna extracts showed larger overall amounts of alkanes, more isoprenoids, and a bimodal n-alkane distribution with modes at 14C and 21C. Exclusively linear alkanes up to 28C are likely due to contamination (Fig. 9).

The PAHs found in both Bells and Ivuna extracts make up complex mixtures that appear to have been heavily compromised by contamination. The largest peak in the Bells GC-MS chromatogram is dibutylphthalate, and other phthalates and large peaks of compounds of likely atmospheric provenance were also seen (Simoneit, 2002). The PAHs listed in Table 7 are compounds that show typical meteoritic distributions, *i.e.*, of being present in several homologous and isomeric forms. Amounts still have to be considered approximate, *e.g.*, the larger amount of phenanthrene relative to anthracene seen in Ivuna is typical of atmospheric contamination. Its amount was subtracted from the PAHs total in Table 2, and total amounts for polar hydrocarbons were not estimated.

Table 8. Hydrocarbons detected in the Bells and Ivuna solvent extracts.

	Bells		**Ivuna**	
PAHs	nmol/g[1]	n[2]	nmol/g	n
naphthalene	39 ± 4		14 ± 1	
C_1-naphthalenes	41 ± 4	2	11.3 ± 0.5	2
C_2-naphthalenes	46 ± 5	7	5.3 ± 0.5	4
C_3-naphthalenes	21 ± 3	10	11 ± 1	6
C_5-naphthalenes	nf[3]		38 ± 4	1
biphenyl	61 ± 7		nf	
C_1-biphenyl	7 ± 1	1	nf	
C_2-biphenyl	nf		15.1 ± 1.5	4
phenanthrene	14 ± 2		1230 ± 110	
anthracene	2.9 ± 0.5		5.1 ± 0.5	
C_1-phenanthrene/anthracenes	nf		251 ± 24	4
C_2-phenanthrene/anthracenes	nf		10.8 ± 1	11
fluoranthene	6 ± 1		98 ± 10	
pyrene	3.8 ± 0.5		8 ± 1	
1-phenylnaphthalene	nf		15.2 ± 1.5	
o-terphenyl	nf		6 ± 1	
Heteroatom-containing PAHs				
acetophenone	10 ± 1		nf	
anthracenedione	1.0 ± 0.2		nf	
benzothiazole	3.3 ± 0.5		nf	
benzothiophene	0.7 ± 0.1		nf	
dibenzothiophene	1.1 ± 0.1		46 ± 4	

[1]nanomoles/g meteorite; [2]number of molecular species; [3]not found.

2.4 Discussion

The highly brecciated and aqueously altered mineral composition of the Bells meteorite and the alteration stages this composition implies indicate that the original organic inventory of the meteorite's asteroidal parent body could have been altered or destroyed as well. This anomalous nature poses difficulties in interpreting the above results and deciphering which of the analytical traits we determined for Bells' soluble organic compounds could be related to those of other meteorites or their precursor environments.

The most readily apparent similarities observed between the results of this study are the equivalent distributions of amino and hydroxyacids in the Bells and Ivuna meteorites. These include a correspondence of both compound groups' relative abundances as well as the type of molecular species detected in each group; examples include the absence in Bells and Ivuna of dicarboxylic amino-, and hydroxyacids and the higher relative abundance of molecular species carrying the OH/amino functional group at the terminal carbon. This latter distinction might be in part a result of terrestrial exposure because recent analyses of a pristine Orgueil stone (Glavin & Dworkin, 2009) showed an amino acid distribution more comparable to that of Murchison that contains a sizeable amount of isovaline seen previously in low or no abundance in stones with a different curatorial history. These findings would seem to indicate that CI composition could have been severely reduced and/or altered by these meteorites' long terrestrial residence. Nevertheless, both pristine and contaminated samples of the Ivuna, Bells, and Orgueil meteorites that we analyzed during this study were all found to contain the

characteristic non-α-amino acids' predominance that seems to distinguish the meteorites together with a larger abundance of hydroxyacids over amino acids.

According to the evaluation of how ammonia abundances would control the relative abundances of amino- and OH-acids during a Strecker-type synthesis (Peltzer, Bada, Schlesinger, & Miller, 1984), the above results in Bells could be interpreted as showing that the meteorite's low ammonia determined its higher OH-acid/amino acid abundant ratio. On the other hand, the unambiguous difference found between Bells and CIs is Bells' lower amount of ammonia and CIs still display a high hydroxy- to amino acids ratio (Pizzarello et al. 2011) in spite of having an ammonia content that, although not quite as high as in CR2 (Pizzarello & Holmes, 2009), is much larger than in Bells or Murchison. What's more, recent analyses of a CR1 showed that this meteorite also displays an amino acid distribution (Glavin, Callahan, Dworkin, & Elsila, 2011), and a CR2 contained high hydroxy-/amino acids ratio similar to Bells and CIs even with an abundant 8.2 μmol/g of amino acids (Pizzarello, Williams, Lehman, Holland, & Yarger, 2011).

These similarities and differences would seem to point to both a cosmochemical distinction between CI and Bells formative environments as well as to the fact that the aqueous phase of their respective parent bodies must have had the common effect of destroying their most reactive water-soluble compounds. This would seem especially likely for α-amino acids, compounds that are particularly reactive molecules and whose breakdown/reprocessing is possible due to the interactive proximity of their two functional groups as well as the mild acidity of their α -carbon. A Strecker decomposition could be an example involving enolization under oxidative conditions, imine formation

and decarboxylation. The amino acids with an amino group not adjacent to the carboxyl such as the terminal carbon-amino acids are more stable compounds that do not enolize; some could have been protected further by their intramolecular amide bond formation and cyclization into lactams. Though the pHs of the parent bodies' aqueous phases are likely diverse and not precisely known, it is worth noting that lactams are stable at the pHs of carbonaceous chondrite meteorite extracts (8.5, 7.5, and 6.8 for MN, Bells and IV, respectively).

Lactams (Fig. 6) have a thermal and hydrolytic stability highest for γ- and lowest for β-cyclic forms (γ > ε > δ >> β) (Wan, Modro, & Yates, 1980; Cooper & Cronin, 1995), and their presence would explain the extraction behavior observed for Bells' terminal-amino acids at different T. According to these speculations, therefore, it could be possible that CI and Bells starting amino acid suites were more similar to those of CRs and CMs, respectively, than they appear after alteration.

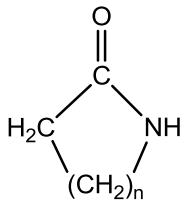

Figure 6. 3- through 6-carbon lactams. n = 1, β-lactam; n = 2, γ-lactam; n = 3, δ-lactam; n = 4, ε-lactam.

From a mechanistic point of view, it is interesting to note the new finding in Bells of β, γ, δ, and ε-hydroxy acids along with their corresponding non-α amino- acid forms in both Bells and IV. This similarity between the two groups of compound had been generally assumed to be limited to α-forms and due to their common origin from aldehydes and ketones, however, the consistent observations of non- α amino-, and

hydroxy acids in various water altered meteorites must lead to the suggestion of another common formative pathway, albeit not easy to propose. The first study of terminal ketoacids in Murchison and other meteorites included the suggestion that precursor nitriles, HCN, and ketene might have led to terminally functionalized keto-compounds by the addition of ketene to the radical of the nitriles' last carbon in the chain (Cooper, Reed, Nguyen, Carter, & Wang, 2011). On this idea, it would seem possible to envision that an extended water and mildly oxidizing phase of the parent body could have led from the keto-compounds to the non-α hydroxy- and amino-acids *via* substitution of the carbonyl with hydroxyl- and, in the presence of ammonia, amino functions.

The commonality of amino acids' distribution in meteorites exposed to extensive aqueous alteration also leads to the realistic suggestion of possible interactions between organic compounds during their syntheses and the clay phases known to form during this stage. In Bells the dominant phyllosilicate phases saponite, tochilinite, and cronstedtite appear in two types of fine-grained aggregates: one type is fine-grained, rarely greater than 200nm on the major grain axis, and the other type even finer with grain sizes < 1nm (Brearley, Aqueous alteration and brecciation in Bells, an unusual, saponite-bearing CM chondrite, 1995). Such sizes allow facile access of the aqueous phase to matrix constituents and, of immediate interest here, improved mineral surficial exposure for any aqueous phase containing organics or synthetic precursors therein. Additionally, organics previously deposited in the matrix by an early alteration phase could be later revisited and efficiently altered by repeat alteration phases.

Interactions between organic and mineralogical processes are likely to have taken place at different stages of the cosmochemical evolution of organic compounds and are to

be expected during the asteroidal aqueous phase; however, these possibilities have been little explored. Pearson et al., 2002 stained organic matter with osmium tetroxide (OsO_4) on a cut surface of Murchison to determine associations with inorganic components. Although not distinguishing between soluble and insoluble components, the authors were able to demonstrate that organic materials in Murchison are associated with phyllosilicates and aggregate in chondrules' water-altered surroundings. Of the few model experiments conducted so far, one followed the decarboxylation of the amino acid isovaline in the presence of Murchison powders (previously freed of organic materials) and showed an effect of the powders in the chiral retention of the amino acid's starting ee. The result was explained with the hypothesis of an intervention by metal catalysts in binding and stabilizing the decarboxylated carbanion (Pizzarello, 2003). Also, Murchison mineral phases were found to influence a Fisher Tropsch type synthesis of amino acids from CO, H_2, and NH_3 toward a larger production of α-aminoisobutyric acid than glycine, as often observed in Murchison extracts (Pizzarello, 2012).

Previous studies of amino acid behavior during exposure to higher temperatures while imbedded in their meteoritic matrixes (Cronin & Pizzarello, Amino acids in meteorites, 1983) is relevant considering that Bells and Ivuna experienced 50-150^{o}C alteration compared to Murchison's lower 0-50^{o}C (Brearley, 1995). One plot from this exposure study is reprinted here as Fig. 10 and shows the survival and/or production of β-alanine *versus* the decrease of other amino acids in Murchison; α-aminobutyric acid seems to have an intermediate fate, decreasing in concentration at first and remaining stable afterwards. The abundance increase or absence of reduction for some amino acids

was interpreted as deriving from destruction of non-hydrolysable derivatives or insoluble material.

Although not exactly related to meteorites, there is also the vast literature on clays, their binding of organic molecules and participation in organic reactions (Yariv & Cross, 2002). All these references, however, do not appear to offer direct information on the processes that might have led to Bells, CI and CR1 amino acid characteristic compositions. A finding of particular interest in this regard could come from analyses which showed that three CM1 meteorites from Antarctica (Botta, Martins, & Ehrenfreund, Amino acids in Antarctic CM1 meteorites and their relationship to other carbonaceous chondrites, 2007) do not share Bells' amino acids composition despite their petrological classification for water alteration. A detailed petrographic comparison of a variety of Type 1 meteorites of different grouping would be most welcomed, as it may be able to reveal relevant compositional differences of the mineral phases, their potential for possible interactions in organic processes and, through target model experiments, would offer some promise of analytical evidence.

2.5 Conclusions

The Bells meteorite contains abundant organic compounds with the total abundance of 2.3 μmole g^{-1}. These are predominantly hydroxy- and carboxylic acids, carbonyl-containing compounds and hydrocarbons. Amino acids are scarce, lower amines are absent and ammonia has the lowest abundance compared to any CC in which it has been measured so far.

The relative distributions of O-, and N-containing compounds as well as the makeup of the amino acids' suites are analogous among Bells, Ivuna and a CR1 but differ

between these meteorites and CM2 or CM1 chondrites. These comparative results show that Bells organic composition is not unique or unusual.

In the absence of favorable fall and curatorial environments, meteorites are known to acquire terrestrial contamination after their falls. Bells and Ivuna are no exceptions, however, and their likely contaminants were detailed within each group of compounds and their presence does not appear to infringe upon the main conclusions derived from this study. Also, the δD values for a set of Bells' aldehydes and ketones were determined, found to be all in the positive range (+39 to +429‰) and this enrichment confirmed the compounds' indigeneity.

That Bells' extant organic compounds may have derived from a CM2 type composition as the effect of long aqueous processes and interactions with mineral phases remains a logical explanation of the data and a possibility, but evidence will have to be pursued with comparative mineralogical analyses of other meteorites of interest and model experiments.

Acknowledgments

We thank the Center for Meteorite Studies at Arizona State University for the Bells and Ivuna samples used in this study and ZymaX Forensic Laboratory for performing the isotopic analyses of aldehydes and ketones. We gratefully acknowledge George Cooper, Laurence Garvie, Pierre Herckes, Edward Skibo for helpful discussions as well as two anonymous referees and Associate Editor Christian Koeberl for their reviews and comments. This study was supported by NASA Astrobiology Institute at Arizona State University (AAM) and NASA Cosmochemistry, Exobiology and Origins of the Solar System programs (SP).

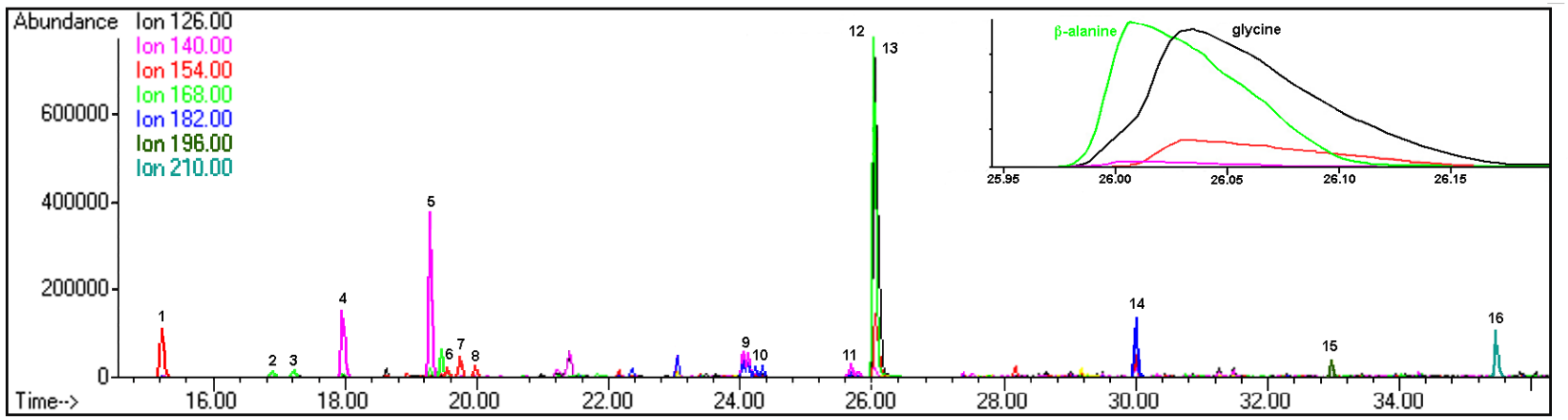

Figure 7. Amino acids identified in water extracts of the Bells meteorite. (1) α-aminoisobutyric acid (a); (2) L-isovaline; (3) D-isovaline; (4) D-alanine; (5) L-alanine; (6) D-N-methyl alanine; (7) L-N-methyl alanine +D-α-aminobutyric acid; (8) L-α-aminobutyric acid; (9) DL-β-aminobutyric acid; (10) DL-β-aminoisobutyric acid; (11) N-methyl β-alanine; (12) β-alanine; (13) glycine; (14) γ-aminobutyric acid; (15) γ-aminovaleric acid; ε-aminocaproic acid.

Insert (top right): expanded view of (12) and (13) partial coelutions.

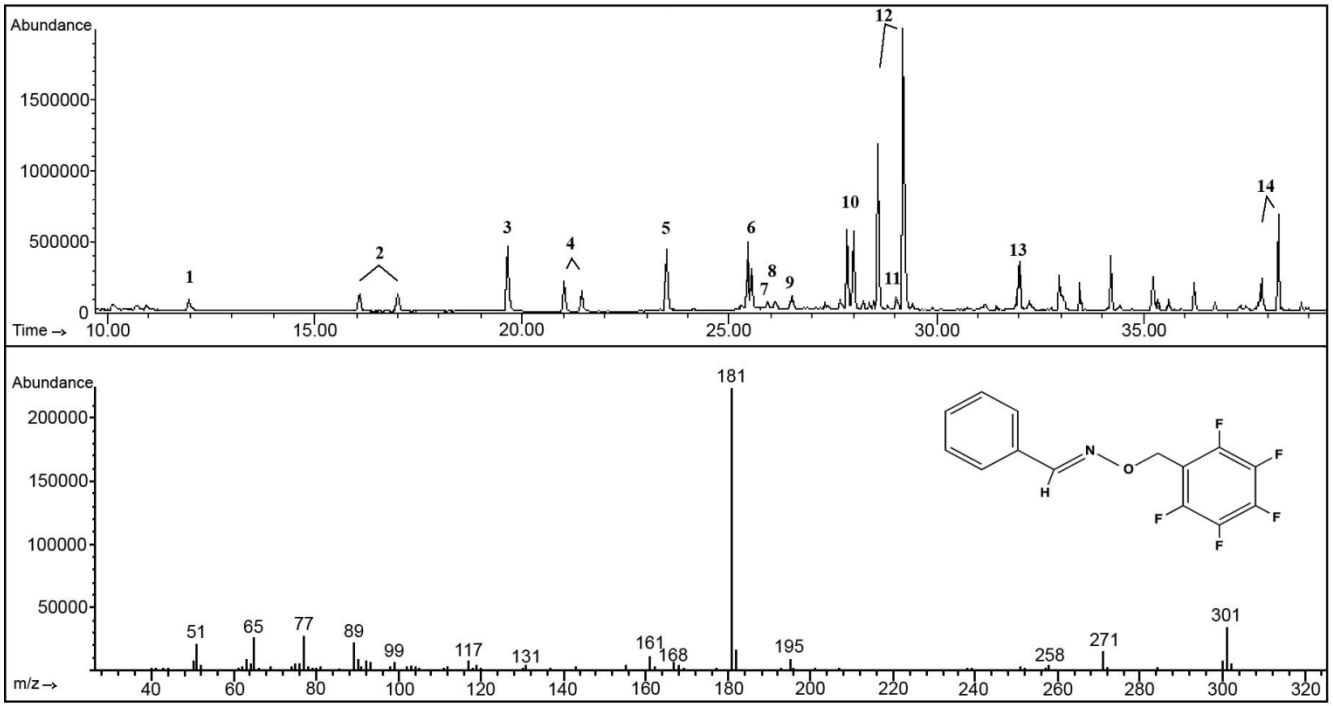

Figure 8. Top: chromatographic resolution of Bells aldehydes' and ketones' pentafluorobenzyl oxime (PFBO) derivatives. (1) formaldehyde; (2) ethanal; (3) acetone; (4) propanal; (5) butanone; (6) butanal; (7) 2-methyl-butan-3-one; (8) pentan-3-one; (9) pentan-2-one; (10) hexan-3-one; (11) pentanal; (12) hexan-2-one; (13) hexanal; (14) benzaldehyde. The double peaks seen for some compounds represent their *syn* and *anti* PFBO derivative isomers.

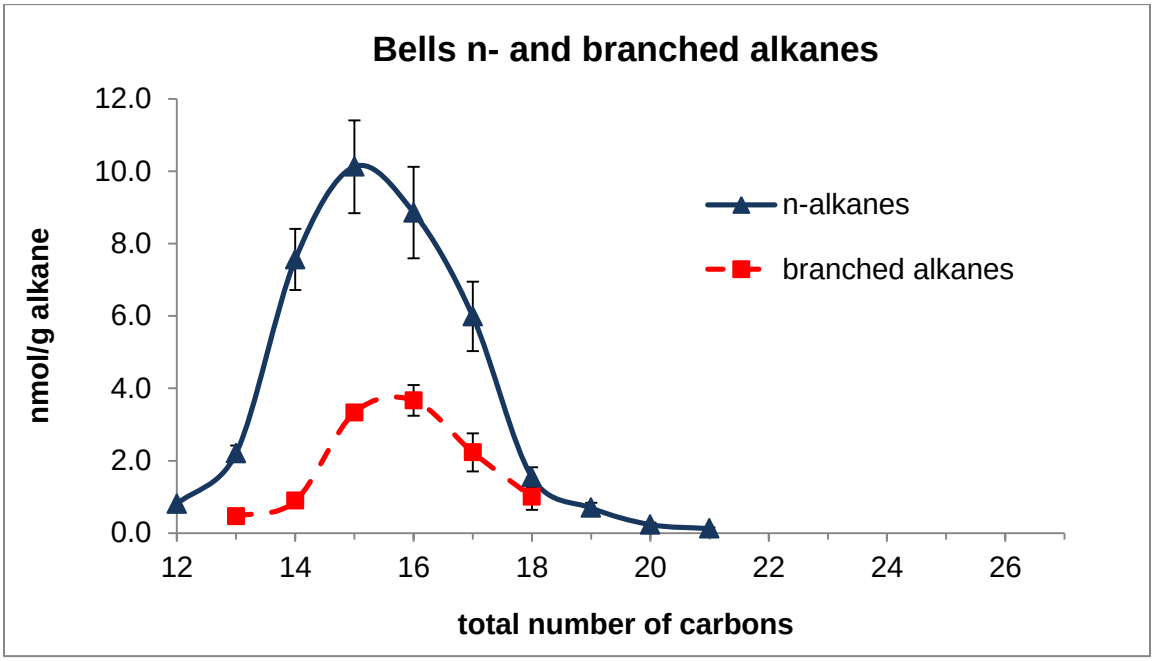

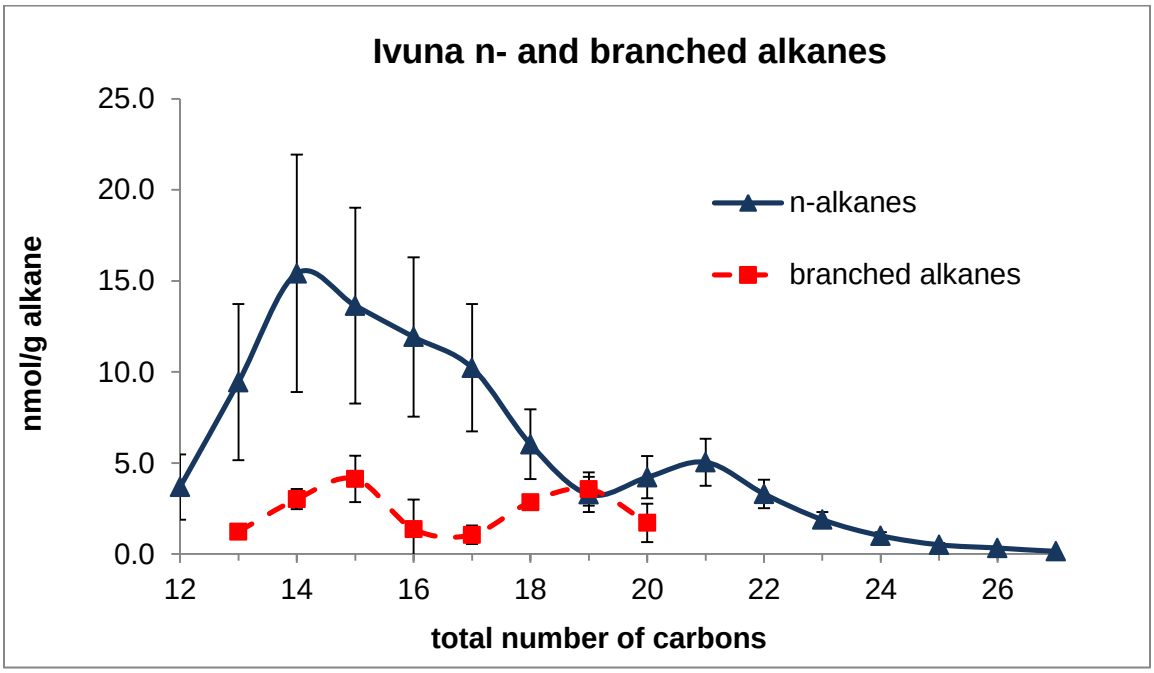

Figure 9. Alkane abundances in the Bells (top) and Ivuna (bottom) meteorites in nanomoles • g^{-1}. In Ivuna's abundances for species larger than 20 carbons, the lack of branched species and second n-alkane maximum raise the suspicion of contamination.

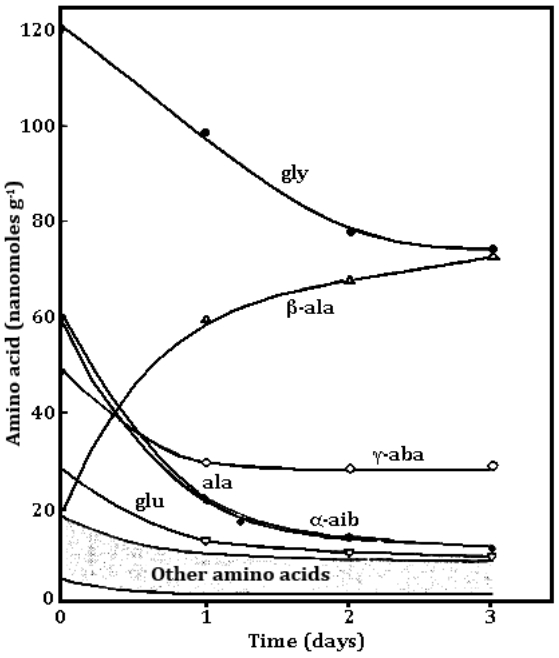

Figure 10. Amino acid concentrations in Murchison as a function of time at 186^{o}C (Cronin & Pizzarello, 1983). β-alanine is the only depicted amino acid that was synthesized during experimental heating.

III. ISOLEUCINE EPIMERIZATION IN THE STUDY OF CARBONACEOUS CHONDRITES

This chapter contains minor sections of text and figures already appearing in abstract form or presented at the 44th Lunar and Planetary Science Conference (Monroe & Pizzarello, 2013).

Modeling of isoleucine epimerization and considerations of stereoisomer abundances in MET 00426, a CR3 chondrite, validate the indigeneity of a reported 60% enantiomeric excess (*ee*) of D-*allo*-isoleucine (D-*a*Ile) (Pizzarello, Schrader, Monroe, & Lauretta, 2012) and exclude possible contamination of $ee_{\text{D}-a\text{Ile}}$ in MET 00426 by epimerization of terrestrial L-isoleucine (L-Ile) to D-*a*Ile (Elsila, Glavin, Dworkin, Martins, & Bada, 2012; Pizzarello & Monroe, 2012). This chapter contains a proof which illustrates that in the case of α-epimerization, $ee_{\text{D}-a\text{Ile}}$ can only be increased by $ee_{\text{L}-\text{ile}}$ if $ee_{\text{L}-\text{ile}} > ee_{\text{D}-allo}$. The opposite was true for MET 00426, and formal logic is applied to prove that contamination could not have contributed to $ee_{\text{D}-a\text{Ile}}$ in that meteorite. Another diagnostic inequality, $[\text{L}-allo][\text{L}-\text{ile}] > [\text{D}-allo][\text{D}-\text{ile}]$, is derived and shown to be true if α-epimerization is capable of raising $ee_{\text{D}-a\text{Ile}}$ for a given sample.

Other modeling of isoleucine epimerization and the measured disequilibria between the isoleucines and their α-epimers, the *allo*-isoleucines, in a suite of CR chondrites suggest that these amino acids' residence in the aqueous phase was short-lived ($< 10^5$ years at 25°C and $< 10^2$ years at 75°C). This finding complicates the history of meteoritic organics despite widespread, ~Myrs aqueous alteration and indicates that these organics may have been protected from sufficient conditions to fully α-epimerize.

Finally, the application of isoleucine stereoisomer relative abundances to describe alteration conditions is explored.

3.1 Introduction

3.1.1 Symmetry and Enantiomeric Excess (*ee*)

Natural symmetry has probably intrigued humans for thousands of years. Symmetry in marine, molluscan shells or the leaves of a maple tree can be appreciated with the unaided eye. A microscopic examination of snowflakes or diatomaceous silica reveals more examples of increasingly complex symmetry, and the discovery of the foundational symmetric or antisymmetric wavefunctions in quantum mechanics demonstrated that natural symmetry extends to the subatomic scale.

Symmetry in the scientific sense often applies to mineralogy and chemistry, and objects are shown to be symmetric due to planes of reflection or axes of proper and improper rotation. Some objects contain many planes and axes of symmetry. Set and group theory demonstrate that there are 17 unique groups of plane symmetry (sometimes called wallpaper groups) and even more groups in molecular symmetry: each group has a unique set of symmetry operations which define it. $B_{12}H_{12}^{2-}$, for example, is a member of I_h, the highly symmetric, icosahedral group, which is characterized by 120 symmetry operations in total. There are low symmetry groups as well, and the lowest of these is C_1. With no symmetry operations other than E, the identity operation, the constituents of group C_1 are asymmetric (Cotton, 1990; Miessler & Tarr, 2004).

At the molecular level, chirality is a term for asymmetry often used to describe tetrahedral carbon centers, and a chiral molecule has the property of being non-superimposable on its mirror image. These non-superimposable, mirror image pairs are

called enantiomers. Chirality does not necessarily imply asymmetry (*e.g.*, a 3-bladed propeller exhibits C_3 symmetry), but asymmetry implies chirality. When carbon is bound to four different constituents in a tetrahedral configuration, it lacks any planes of symmetry, has a non-superimposable mirror image, and is therefore chiral (Vollhardt & Schore, 2003; Miessler & Tarr, 2004; Cronin & Reisse, 2005).

The purity of a chiral substance can be measured in enantiomeric excess (*ee*): an *ee* of 100% indicates the maximum possible difference between abundances of two enantiomers. Other terms like 'chiral excess' and 'enantiomeric ratio' contain the same concept of measurable, molecular asymmetry in a mixture of enantiomers. Amino acids, many of which contain one or more chiral centers, appear in living systems with exclusively L enantiomers, and of the 21 amino acids coded for in DNA (protein amino acids), glycine is the only one which cannot exist as an L or D enantiomer. Sugars appear almost exclusively as D enantiomers. Life's preference for chiral asymmetry is due primarily to the efficiency of a homochiral framework: in terms of chemical energy, it is wasteful to produce a compound that one cannot use, and in terms of information storage, it is more costly to code for additional proteins to manipulate the other enantiomer (Bonner, 1991). The origin of homochirality on Earth remains a mystery, and whether homochirality was essential to the earliest is an ongoing field of research (Bonner, 1991; Cronin & Reisse, 2005) which includes the search for evidence of molecular symmetry breaking and amplification of asymmetry (Soai, Shibata, Morioka, & Choji, 1995). Though proteins are polymers of L amino acids, they just as easily could have been polymers of D amino acids if the first life had this configuration.

The notion that meteorites contributed large amounts of organic material to the early Earth (Chyba & Sagan, 1992) combined with the confirmation of L enantiomeric excesses in meteoritic amino acids (Cronin & Pizzarello, 1997) raises the question of whether meteoritic input might have given the proteins of earliest life a hand in the direction of left.

3.1.2 Molecular Asymmetry in Meteoritic Amino Acids

Though several investigations in the 1960s detected amino acids in Murray, Bruderheim, Orgueil, Karoonda, Abee, Hvittis, Norton County, and several other stones using ion exchange chromatography and spectrophotometry, they were complicated by contamination and could not confirm the indigeneity of amino acids with confidence. These studies are reviewed and referenced elsewhere (Hayes, 1967). The presence of meteoritic amino acids was unconfirmed until shortly after the fall of Murchison in 1969 (Kvenvolden, et al., 1970), and those analyses reported that all amino acids found in the meteorite were racemic mixtures. Equal amounts of L- and D- enantiomers were the expected result of a-biotic—and presumably achiral—syntheses. This expectation was repeated in many studies, including a later study of Murchison with another detection of racemic isovaline which specifically invoked isovaline's resistance to racemization as proof of the abiotic, extraterrestrial processes by which it was formed (Pollock, Cheng, Cronin, & Kvenvolden, 1975).

Isovaline (Fig. 3) cannot racemize *via* deprotonation-initiated reversal of a chiral carbon center (Fig. 11) due to the α-methyl group and absence of an α-H (Neuberger, 1948). Enantiomeric excesses of isovaline and other amino acids can be decreased photolytically or radiolytically (Garrison, 1972), and gamma radiation can cause

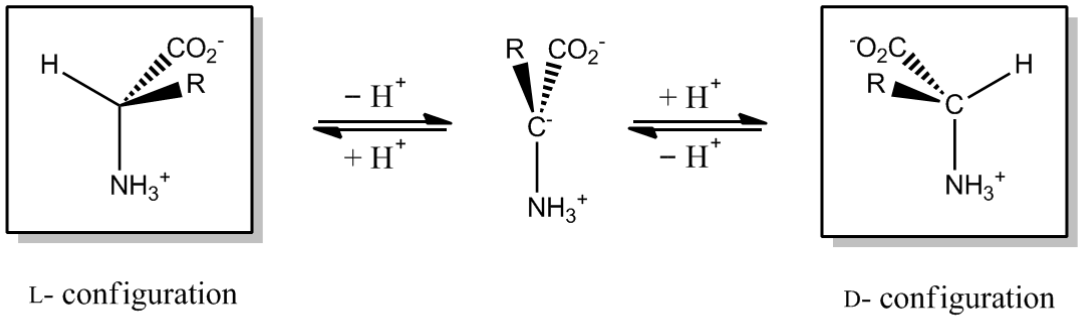

L- configuration

D- configuration

Figure 11. Proton loss and re-acquisition may result in chiral reversal. A chiral, α-H amino acid (L-amino acid zwitterion, left) may undergo reversible, symmetric reversal *via* carbanion intermediate (center). Chiral configuration is retained or reversed depending on whether proton reacquisition occurs on the side of the molecule from which the previous proton was removed. R- is an alkyl group.

destruction of amino acids and decrease *ee* by up to 5% (Bonner, Blair, & Lemmon, 1979). Though these alternate routes for reduction of *ee* may have acted on asteroidal parent body exteriors, they likely affected a minority of samples.

The first confirmed, indigenous enantiomeric excess in meteorites was 8.4 ± 6% of L-isovaline in Murchison (Cronin & Pizzarello, 1997), and several later studies of α-methyl amino acids have confirmed excesses of the same molecule in Murchison and other carbonaceous chondrites nearing 19% (Pizzarello & Cronin, 2000; Pizzarello, Zolensky, & Turk, 2003; Glavin, Callahan, Dworkin, & Elsila, 2011). L-isovaline is a non-protein amino acid, so it is unlikely to have been contaminated, and its resistance to racemization was used to argue that natal *ee* would be preserved as the reported enantiomeric excess. As analytical studies expand the findings of *ee* in meteorites, the source of *ee* remains a mystery. Circularly polarized light and chiral catalysis on

meteorite surfaces are intriguing, but no plausible source capable of producing the extent of observed asymmetry has emerged (Pizzarello & Groy, 2011).

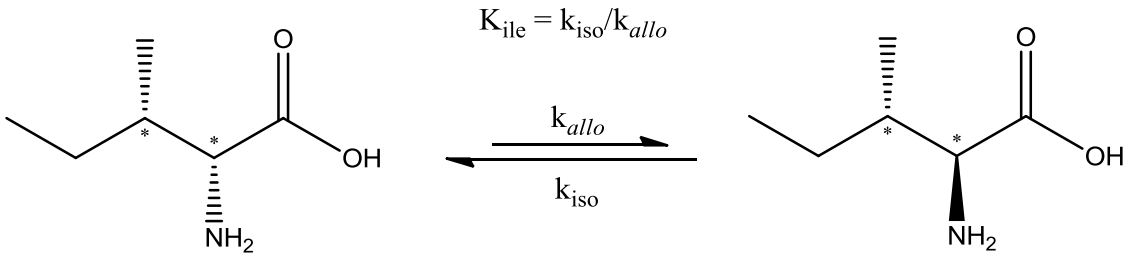

D-*allo*-isoleucine L-isoleucine

Figure 12. α-epimerization interconverts D-*allo*-isoleucine and L-isoleucine (also L-*allo*-isoleucine and D-isoleucine) with chiral reversal of the α-carbon by the process depicted in Fig. 10. *Indicates chiral carbon. Note that both molecules contain an (*S*) configuration at the β-carbon. β-epimerization is the much slower process involving chiral reversal of the β-carbon.

3.1.3 Enantiomeric Excesses and Molecular Abundances in Progressively Altered CR Chondrites

Analyses of a suite of 6 nitrogen- and amino-acid-rich CR chondrites spanning petrologic type 3 to 1 demonstrated a decreasing trend in the *ee* of L-Ile and D-*a*Ile with increasing aqueous alteration by petrologic type and carbonate abundance (Pizzarello, Schrader, Monroe, & Lauretta, 2012). In contrast to many CMs, L-isovaline contained a ~2% excess in only two of the meteorites and no excess in the others. Since any *ee* of a chiral aldehyde precursor produces the *ee* of the isoleucine stereoisomers after amino acid synthesis, any process decreasing precursor *ee* prior to synthesis would decrease the final *ee* of L-Ile and D-*a*Ile. In the case of L-Ile and D-*a*Ile, (*S*)-2-methyl-butanal is the common precursor because the chiral carbon of that aldehyde becomes the β-carbon of L-Ile and D-

*a*Ile. The paper also concluded that the presence of abundant amino acids and sugar alcohols in CR3s which experienced little to no aqueous alteration demonstrated that an extended aqueous alteration phase was not essential to the formation of at least some water-soluble, organic compounds. Lastly, the measured 60% *ee* of D-*allo*-isoleucine in MET 00426, a highly pristine CR3 chondrite (Abreu & Brearley, 2010), remains the largest reported *ee* of a non-protein amino acid.

The claims of 60% *ee* of D-*allo*isoleucine and the argument that aqueous alteration decreased *ee*s overall by racemizing aldehyde precursors elicited concerns with (1) analytical separation, (2) terrestrial amino acid contamination, and (3) the scientific argument linking decreases in *ee* of L-Ile and D-*a*Ile to aqueous alteration (Elsila, Glavin, Dworkin, Martins, & Bada, 2012). The section of the original authors' reply (Pizzarello & Monroe, 2012) regarding the concern of separation is not relevant here, but concerns (2) and (3) are relevant to each other, and responding to these concerns has necessitated the work of sections 3.2.1 – 3.2.5.

Table 9. Enantiomeric excesses in CR chondrites (Pizzarello, Schrader, Monroe, & Lauretta, 2012). †Shows L-proteinogenic amino acid excesses; *allo*/Ile ratios were calculated exclusively from L-*a*Ile/D-Ile. (Pizzarello & Holmes, 2009)*

	LAP*	EET	MET	PCA	QUE	MIL	GRA1*
$ee_{\text{L-Ile}}$	3.6	26†	50	19	50†	46†	14.0
$ee_{\text{D-}a\text{Ile}}$	2.2	21	60	19	34.5	18	12.1
allo/Ile	1.4	1.8†	2.2	2.0	1.1†	1.4†	2.3

Terrestrial contamination by multiple amino acids is best addressed with compound-specific isotopic analyses (recall section 1.3), but isotope ratio analyses

require more sample extract than the standard GC-MS and were impossible with the amount of available samples. In response, a theoretical approach to assess special cases of contamination by terrestrial L-isoleucine is presented in subsections 3.2.1, 3.2.2, and 3.2.5.

The commenters' third concern disputes the explanation for the negative correlation of *ee* to aqueous alteration with two justifications: (1) the unobserved identical *ee*s in L-Ile and D-*a*Ile (Table 9) which should have resulted from the chiral aldehyde precursor and (2) the impossibility of reducing both $ee_{\text{L}-\text{Ile}}$ and $ee_{\text{D}-a\text{Ile}}$ without β-epimerization, a process too slow to be reasonably applied to the asteroidal parent body or ice fields of Antarctica.

3.2 Results and Discussion

Modeling and consideration of isoleucine epimerization have several novel applications to the study of meteorites, including assessing special cases of possible meteorite contamination and providing an indicator of total duration of aqueous alteration in the presence of the isoleucine stereoisomers. The following section contains general examples of epimerization with models, elaborates on the conditions required to increase an enantiomeric excess of D-*a*Ile by contaminating a meteorite with terrestrial L-Ile, and includes models of epimerization backwards in time to constrain durations of aqueous alteration. All reversible, first order kinetic calculations were performed using Microsoft Excel or LabView software written for the project. The finite difference approximation was used to estimate amino acid concentration changes during up to 10,000 calculated reaction steps for each reaction.

3.2.1 Conditions for Increasing $ee_{\text{D}-a\text{Ile}}$

L-Ile is abundant in the biosphere, and large enantiomeric excesses of L-Ile can signal terrestrial contamination of a meteorite. Given the proper conditions (ample time, liquid water, certain pH ranges, ideal range of warm temperatures, etc.) some of this L-Ile will α-epimerize to D-*a*Ile, allowing the proposition that contaminant L-Ile may be a source of reported enantiomeric excess in D-*a*Ile. Given that interconversion of the isoleucine stereoisomers is governed by the kinetics of α- and β- epimerization, measurable conditions related to the *ee* increase of D-*a*Ile will be derived.

The proof begins with the establishment of the following inequality and the inclusion of the definition of *ee* to find other inequalities which must be true when $ee_{\text{D}-a\text{Ile}}$ is increasing:

$$\frac{d}{dt}(ee_{\text{D}-a\text{Ile}}) > 0 \qquad \textbf{(1)}$$

$$ee_{\text{D}-a\text{Ile}} = \frac{[\text{D}-a\text{Ile}]-[\text{L}-a\text{Ile}]}{[\text{D}-a\text{Ile}]+[\text{L}-a\text{Ile}]}\cdot 100\%$$

The following substitutions will be used for convenience and clarity:

$$[\text{D}-a\text{Ile}] = A;\ [\text{L}-a\text{Ile}] = B;\ [\text{L}-\text{Ile}] = C;\ [\text{D}-\text{Ile}] = D$$

The definition of *ee* is substituted into inequality **(1)** and differentiated with respect to time:

$$\frac{d}{dt}\left(\frac{A-B}{A+B}\right) > 0$$

$$\frac{d}{dt}\left(\frac{A}{A+B}\right) - \frac{d}{dt}\left(\frac{B}{A+B}\right) > 0$$

or

$$\frac{d}{dt}A(A+B)^{-1} > \frac{d}{dt}B(A+B)^{-1} \quad \textbf{(2)}$$

Let $\frac{d}{dt}A = A'$ and $\frac{d}{dt}B = B'$ so that **(2)** becomes:

$$A'(A+B)^{-1} - A(A'+B')(A+B)^{-2} > B'(A+B)^{-1} - B(A'+B')(A+B)^{-2}$$

Simplify by multiplying by $(A+B)^2$ and rearranging:

$$A'(A+B) - A(A'+B') > B'(A+B) - B(A'+B')$$
$$AA' + BA' - AB' - AA' > AB' + BB' - BA' - BB'$$
$$2BA' > 2AB'$$
$$BA' > AB'$$
$$\frac{A'}{A} > \frac{B'}{B}$$

or

$$\frac{\frac{d}{dt}[\text{D} - a\text{Ile}]}{[\text{D} - a\text{Ile}]} > \frac{\frac{d}{dt}[\text{L} - a\text{Ile}]}{[\text{L} - a\text{Ile}]} \quad \textbf{(3)}$$

If denominators in **(3)** seem conceptually unnecessary for increasing $ee_{\text{D}-a\text{Ile}}$, please see appendix B for an example and short justification of the inequality normalized to concentration.

Inequality **(3)** includes the isoleucines as well since their abundances affect the creation or consumption of the *allo*isoleucines, and the derivative of *ee* with respect to

time has been converted into standard derivatives of *allo*isoleucine concentrations with respect to time.

Here the derivation splits with the inclusion of β-epimerization. If β-epimerization is dramatically slower than α-epimerization (as suggested by the experiments in literature and our lab and the significantly decreased acidity of the β-C proton versus the α-C proton), its effects can be excluded for modeling at lower temperature or short time. The derivation with α-epimerization will be addressed first and followed by the derivation including both α- and β-epimerization.

α-epimerization only:

The following first-order rate equations include only α-epimerization:

$$\frac{d[\text{D} - a\text{Ile}]}{dt} = A' = -k_2 A + k_1 C$$

$$\frac{d[\text{L} - a\text{Ile}]}{dt} = B' = -k_2 B + k_1 D$$

Both are substituted into **(3)**:

$$B(-k_2 A + k_1 C) > A(-k_2 B + k_1 D)$$

$$-k_2 AB + k_1 BC > -k_2 AB + k_1 AD$$

$$BC > AD \qquad \textbf{(4a)}$$

or

$$[\text{L} - a\text{Ile}][\text{L} - \text{Ile}] > [\text{D} - a\text{Ile}][\text{D} - \text{Ile}]$$

This inequality is usable simply with measured isoleucine abundances. As long as **(4a)** is satisfied, $ee_{\text{D}-a\text{Ile}}$ continues to rise.

Note that the left side of the inequality is the product of the concentrations of the two L-amino acids and that the right side is the same but for the two D-amino acids. This is similar to a two-component, racemizing system, wherein the D-enantiomer's *ee* will be increase if its concentration is lower than the L-enantiomer's (in this case, the *ee* of D- would be increasing from a negative number until reaching equilibrium at zero).

Once the sides of the inequality become equal and make it false, the system has reached chiral equilibrium, and $ee_{\text{D}-a\text{Ile}}$ is no longer rising. Inequality **(4a)** can be manipulated to reveal an alternate indicator of chiral equilibrium:

$$2BC > 2AD$$

$$2BC + AC - BD > 2AD + AC - BD$$

$$AC + BC - AD - BD > AC + AD - BC - BD$$

$$(C - D)(A + B) > (A - B)(C + D)$$

$$\frac{C - D}{C + D} > \frac{A - B}{A + B}$$

This contains the definition of *ee*; therefore if $ee_{\text{D}-a\text{Ile}}$ is increasing with time at a given time, then **(5a)** is also true at that time:

$$ee_{\text{L}-\text{Ile}} > ee_{\text{D}-a\text{Ile}} \qquad \textbf{(5a)}$$

If only α-epimerization is considered, the *ee* value of equilibrium is reached when $ee_{\text{L}-\text{Ile}} = ee_{\text{D}-a\text{Ile}}$, and $ee_{\text{L}-\text{Ile}}$ and $ee_{\text{D}-a\text{Ile}}$ no longer change with time.

The mathematical derivation of **(5a)** from **(1)** allows their logical connection in a conditional statement. The antecedent **(1)** begins the conditional, and if **(1)** is true, then any mathematical consequence (called the logical consequent) must be true as well. The conditional is commonly illustrated with antecedent P, consequent Q, and a right arrow:

$P \rightarrow Q$. The above derivation could be written $(\mathbf{1}) \rightarrow (\mathbf{5}\boldsymbol{a})$ and read "if $\frac{d}{dt}(ee_{\text{D}-a\text{Ile}}) > 0$, then $ee_{\text{L}-\text{Ile}} > ee_{\text{D}-a\text{Ile}}$". Other changing *ee* may be similarly derived, and the results are included in Table 10.

Table 10. Conditional statements defining differences between $ee_{\text{L}-\text{Ile}}$ and $ee_{\text{D}-a\text{Ile}}$ during increase or decrease of *ee* by α-epimerization. The previously derived $(\mathbf{1}) \rightarrow (\mathbf{5}\boldsymbol{a})$ appears first in this table and is followed by the three other related, derivable conditionals.

P	→	**Q**
$\frac{d}{dt}(ee_{\text{D}-a\text{Ile}}) > 0$	→	$ee_{\text{L}-\text{Ile}} > ee_{\text{D}-a\text{Ile}}$
$\frac{d}{dt}(ee_{\text{L}-\text{Ile}}) < 0$	→	$ee_{\text{L}-\text{Ile}} > ee_{\text{D}-a\text{Ile}}$
$\frac{d}{dt}(ee_{\text{D}-a\text{Ile}}) < 0$	→	$ee_{\text{L}-\text{Ile}} < ee_{\text{D}-a\text{Ile}}$
$\frac{d}{dt}(ee_{\text{L}-\text{Ile}}) > 0$	→	$ee_{\text{L}-\text{Ile}} < ee_{\text{D}-a\text{Ile}}$

Equilibrium behavior will be explored and illustrated further in 3.2.3.

α- and β- epimerization:

The following first-order rate equations include both α- and β-epimerization:

$$\frac{d[\text{D} - a\text{Ile}]}{dt} = A' = -(k_2 + k_4)A + k_1C + k_3D$$

$$\frac{d[\text{L} - a\text{Ile}]}{dt} = B' = -(k_2 + k_4)B + k_3C + k_1D$$

Both are substituted into **(3)**:

$$B[-(k_2 + k_4)A + k_1C + k_3D] > A[-(k_2 + k_4)B + k_3C + k_1D]$$

$$B[k_1C + k_3D] > A[k_3C + k_1D]$$

$$k_3(BD - AC) > k_1(AD - BC)$$

$K_\beta = k_1/k_3$, the factor by which α-epimerization is faster than β-epimerization.

$$BD - AC > K_\beta(AD - BC) \quad \textbf{(4b)}$$

$ee_{\text{D}-a\text{Ile}}$ increases in time while inequality **(4b)** is true. Although this equation is less straightforward to use than **(4a)** or **(5a)** for the same result, it is still possible to quantitatively assess the direction of equilibrium without performing any modeling.

In cases of suspected contamination by terrestrial L-isoleucine and isoleucine epimerization alone, it has been shown that $ee_{\text{L}-\text{Ile}} > ee_{\text{D}-a\text{Ile}}$ if $ee_{\text{D}-a\text{Ile}}$ is increasing (as it must be if $ee_{\text{D}-a\text{Ile}}$ is in the process of being raised by contamination).

The inequalities derived in this section are descriptive only at the time of measurement, *i.e.,* anything derived so far can only describe whether $ee_{\text{D}-a\text{Ile}}$ was increasing, however slowly, at the time of that measurement. This may prove in certain cases that contamination is not occurring and, due to the direction of equilibrium, was not occurring before the diagnostic measurement. If $ee_{\text{D}-a\text{Ile}}$ is <u>decreasing</u> when a measurement is made, then before the measurement, $ee_{\text{D}-a\text{Ile}}$ was larger and still not subject to increase by α-epimerization. If $ee_{\text{D}-a\text{Ile}}$ is <u>increasing</u> when a measurement of a contaminated sample is made, at least some of the increase is due to the contaminant. Before contamination, if it was already true that $ee_{\text{L}-\text{Ile}} > ee_{\text{D}-a\text{Ile}}$, then $ee_{\text{D}-a\text{Ile}}$ was already increasing, and the increase is accelerated by addition of contaminant L-Ile. Lastly, if $ee_{\text{L}-\text{Ile}} \leq ee_{\text{D}-a\text{Ile}}$ and addition of contaminant makes true $ee_{\text{L}-\text{Ile}} > ee_{\text{D}-a\text{Ile}}$, that contaminant caused the system to change to be suitable to increases in $ee_{\text{D}-a\text{Ile}}$. The

following sections will calculate values for equilibrium and explore the behavior of the system in time in greater detail.

3.2.2 Exclusion of $ee_{\text{D}-a\text{Ile}}$ Contamination with Proof by Contrapositive

It has been shown that (**5a**) logically follows from (**1**), meaning that if $\frac{d}{dt}(ee_{\text{D}-a\text{Ile}}) > 0$, then $ee_{\text{L}-\text{Ile}} > ee_{\text{D}-a\text{Ile}}$.

Whether $ee_{\text{D}-a\text{Ile}}$ is rising in a given moment cannot be known from the previously derived section (statement is not bi-conditional), but *modus tollens* can be used to assess whether contaminant L-Ile can increase $ee_{\text{D}-a\text{Ile}}$ in cases where $ee_{\text{L}-\text{Ile}} \leq ee_{\text{D}-a\text{Ile}}$:

$$\frac{P \rightarrow Q, \neg Q}{\therefore\ \neg P}$$

Let the inequality $\frac{d}{dt}(ee_{\text{D}-a\text{Ile}}) > 0$ be antecedent P and $ee_{\text{L}-\text{Ile}} > ee_{\text{D}-a\text{Ile}}$ be consequent Q. $\neg Q$ therefore is $ee_{\text{L}-\text{Ile}} \leq ee_{\text{D}-a\text{Ile}}$, and in cases where $\neg Q$ is true, $\neg P$, $\frac{d}{dt}(ee_{\text{D}-a\text{Ile}}) \leq 0$, is also true.

Excluding consumption or creation of the isoleucine stereoisomers by processes other than α-epimerization, $ee_{\text{D}-a\text{Ile}}$ will not be increased by L-Ile if $ee_{\text{L}-\text{Ile}} \leq ee_{\text{D}-a\text{Ile}}$.

Certainly this specific argument cannot rule out terrestrial contamination of other compounds or determine for samples in which $ee_{\text{L}-\text{Ile}} > ee_{\text{D}-a\text{Ile}}$ whether any terrestrial L-Ile has epimerized to D-*a*Ile. A simpler but similar argument would defend the indigeneity of a meteoritic D-excess in an enantiomer of a protein amino acid. Given time to racemize, the concentrations of the enantiomers will become equal ($ee_{\text{D}} = ee_{\text{L}} = 0\%$),

but if the only available contaminant is the L-enantiomer, L- cannot increase the excess of D- unless the concentration of L- exceeds the concentration of D- in the system (which means $ee_D < 0$ and is rising to 0). During racemization and, in this example, reduction of the ee_D to 0%, some terrestrial amino acid converts into the D-enantiomer (as progressive isotopic 'lightening' of the D-enantiomer would show), but that conversion does not necessarily contaminate the calculated *ee* of the D-enantiomer.

3.2.3 Equilibrium Values for Enantiomeric Excess

Identification of equilibrium is essential to assess whether a system has reached equilibrium, and in the study of aqueous alteration of meteorites, allows the use of isoleucine stereoisomer ratios to determine whether amino acids have reached chiral equilibrium. In the case of amino acids with only two chiral configurations, chiral equilibrium is 0% *ee*. Because isoleucine and its stereoisomers have four chiral configurations which are subject to α- and β- epimerization, the behavior of the system as it approaches chiral equilibrium is more complicated.

In situations with insufficient time or heat to produce detectable results of β-epimerization (column 2 in Table 11 is labeled "α-epimerization only"), chiral equilibrium has been reached when both *ee*s equal their weighted average. Given enough time, β-epimerization (column 3) will reduce both *ee* to zero. The equilibrium constant K_{Ile} is the equilibrium value for $allo/$Ile in either case. In an α-only epimerization model (Fig. 13), disparate *ee*s gradually reach the equilibrium excess in **(6a)**. The lower *ee* will increase, the higher *ee* decrease, until both reach this equilibrium value. Another feature of the α-only epimerization model is that if the *ee*s do not equal each other, then equilibrium has not been reached, and the meteorite was sampled before α-epimerization

Table 11. Equilibrium values of enantiomeric excess and *allo*/Ile.

EQ value	α-epimerization only	α- and β- epimerization
ee	$\frac{[\mathrm{D}-a\mathrm{Ile}]-[\mathrm{L}-a\mathrm{Ile}]+[\mathrm{L}-\mathrm{Ile}]-[\mathrm{D}-\mathrm{Ile}]}{[\mathrm{D}-a\mathrm{Ile}]+[\mathrm{L}-a\mathrm{Ile}]+[\mathrm{L}-\mathrm{Ile}]+[\mathrm{D}-\mathrm{Ile}]}\cdot 100\%$	0%
$allo/\mathrm{Ile}$	$\mathrm{K_{ile}}$	$\mathrm{K_{ile}}$
	The equilibrium value of enantiomeric excess is the following weighted average: $ee_{EQ}=\frac{(A+B)*ee_{\mathrm{D}-a\mathrm{Ile}}+(C+D)*ee_{\mathrm{L}-\mathrm{Ile}}}{A+B+C+D}$ This reduces to **(6a)** by substituting the definition of *ee*. $\boldsymbol{ee_{EQ}=\frac{A-B+C-D}{A+B+C+D}\cdot 100\%}$ **(6a)**	Even when **(4b)** becomes false, both *ee*s decrease to zero. In this case the system has not reached equilibrium until both *ee*s equal 0.

$$[\mathrm{D}-a\mathrm{Ile}]=A;\ [\mathrm{L}-a\mathrm{Ile}]=B;\ [\mathrm{L}-\mathrm{Ile}]=C;\ [\mathrm{D}-\mathrm{Ile}]=D$$

reached its conclusion. The curves resemble curves for equilibration of a two-component system with $K_{eq}=1$, and the latter is probably a more intuitive framework for imagining *ee* behavior in time. Since *ee*s are arithmetic combinations of concentrations, it is unsurprising that *ee* resemble a concentration when plotted *versus* time.

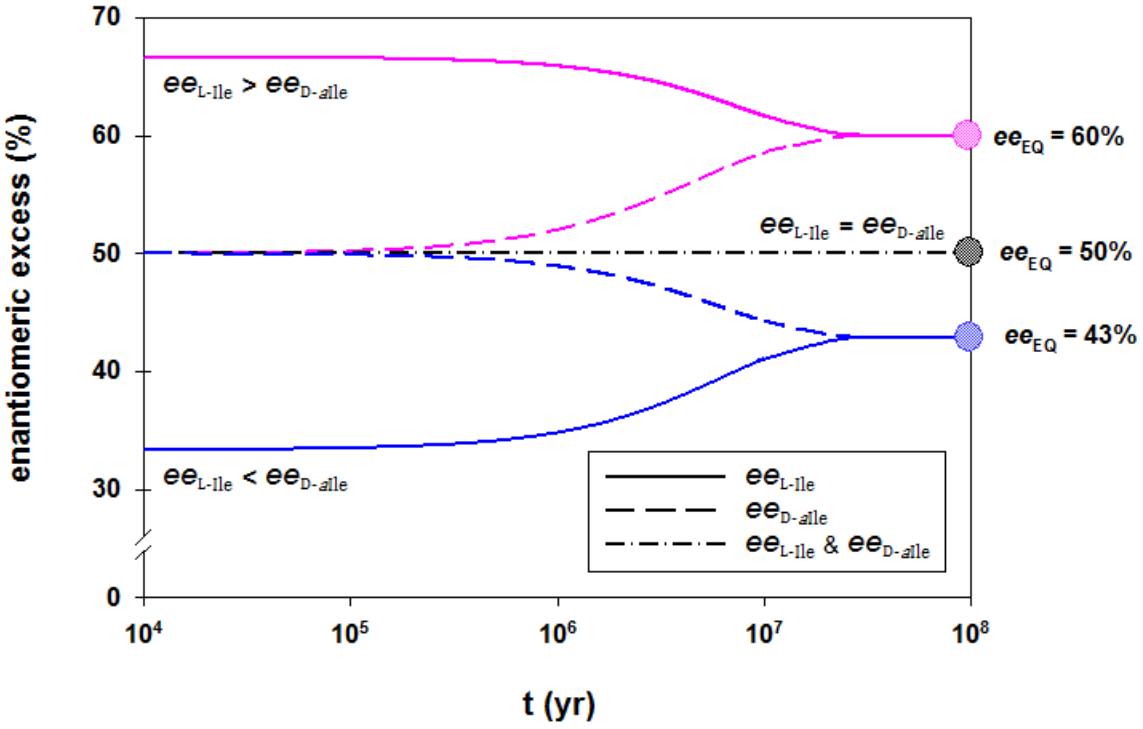

Figure 13. Three example α-epimerization scenarios with initial $ee_{D-a\text{Ile}}$ = 50% but different initial $ee_{L-\text{Ile}}$. General behavior is apparent as the unequal values approach equilibrium, and whichever *ee* is greater never becomes the lesser (only equal) in the same simulation. The initial values themselves were chosen only to illustrate that their relative values reflect the direction of equilibrium. The value of shared, final *ee* is determined by equilibrium (Table 11).

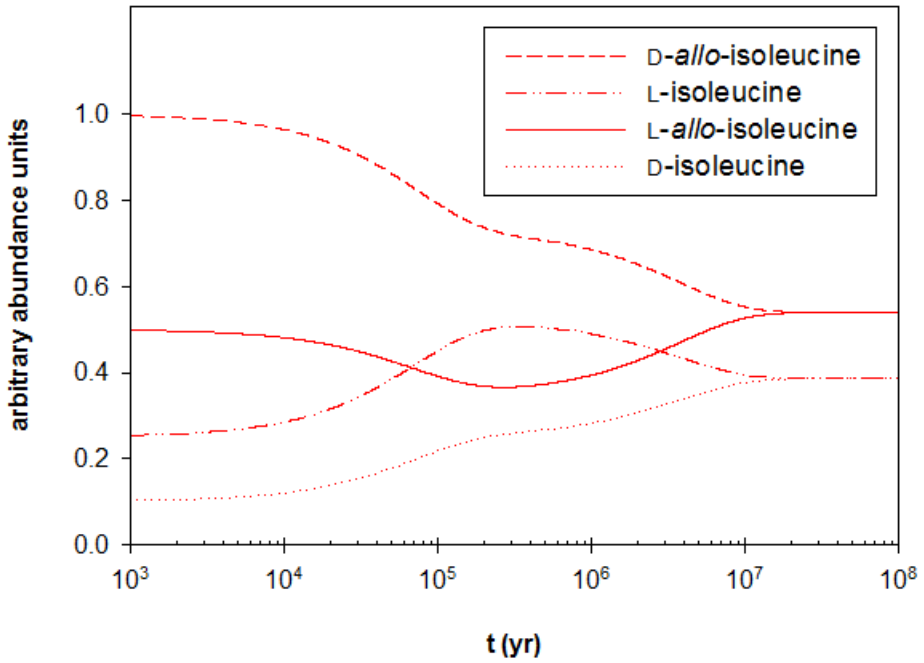

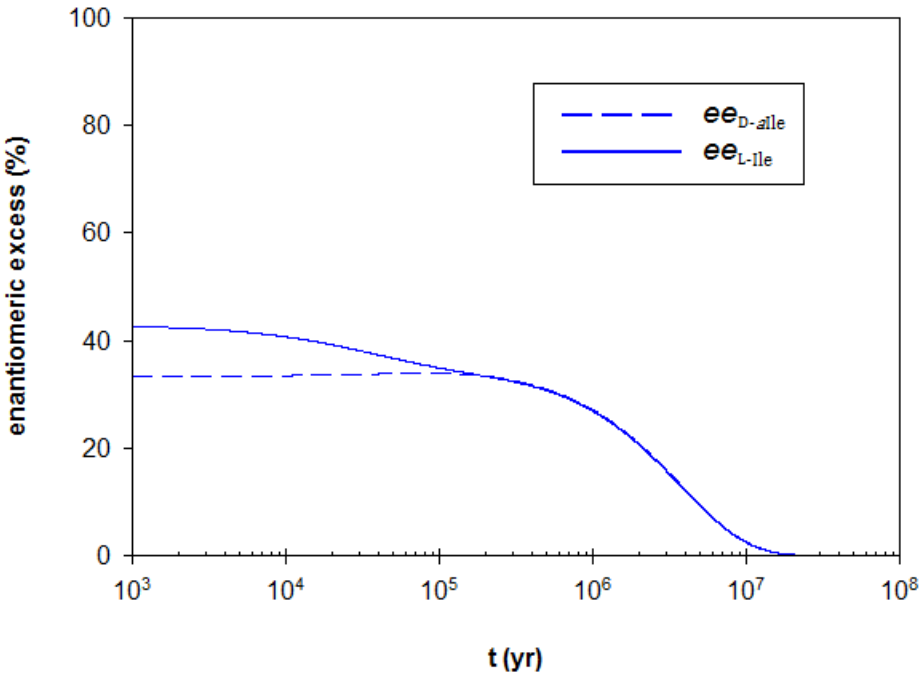

Figures 14 (top) and 15 (bottom). Individual amino acid concentrations and their calculated *ee*s during α- and β-epimerization at 298K (see following Fig. 16). Effects of α-epimerization are no longer visible after ~$5x10^5$ yr. Before ~10^5 yr, equilibration of *ee* resembles α-epimerization-only (Fig. 13) before *ee*s decrease together to 0.

3.2.4 Modeling of Isoleucine Epimerization and Contamination by Terrestrial L-Ile

Model behavior illustrates two central principles to the argument for assessing potential contamination: (1) the slope of each curve is either positive and eventually zero or negative and eventually zero, and (2) the system has reached equilibrium when the *ee* become equal.

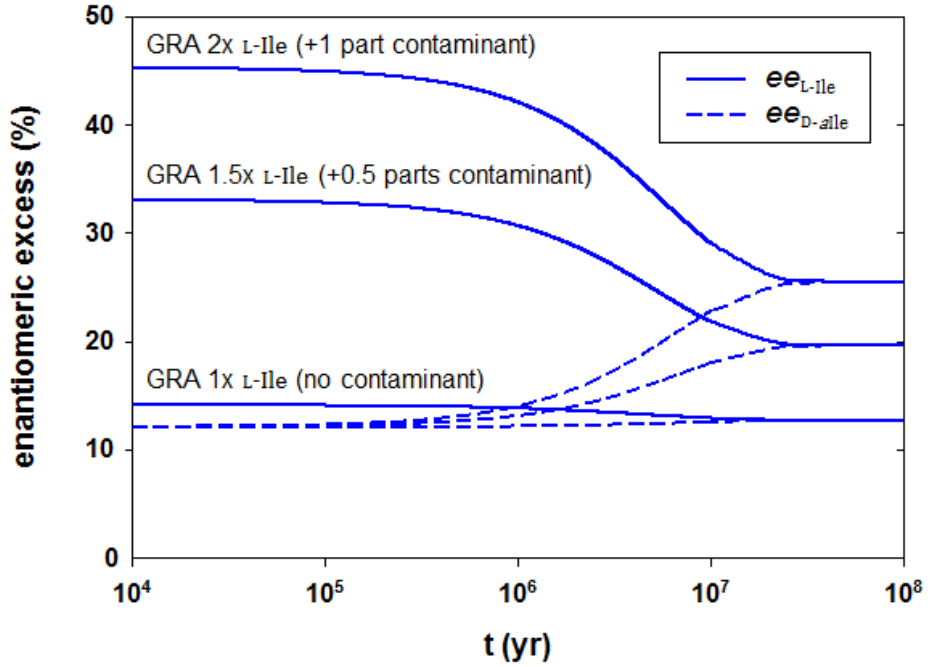

Figure 16. Equilibration of enantiomeric excesses during modeled α-epimerization of CR2 GRA 95229 with varying amounts of contaminant L-Ile added. Solid lines represent $ee_{\text{L-Ile}}$, dashed lines $ee_{\text{D-}a\text{Ile}}$. These dates are not meant to be absolute and result from the use of rate constants determined by Arrhenius plot extrapolation of epimerization studies of bovine bone fragments to 3°C (Bada J. L., 1972). Equilibrium *ee*s at 10^8 yr are 12.7%, 19.6%, and 25.5% for the (no contaminant), (+0.5 parts contaminant), and (+1 part contaminant) curves, respectively.

The first distinction is important from the standpoint of contamination because a measurement of unequal *ee* today, if modeled backwards in time, will only show historically larger differences between the *ee* (*i.e.*, greater disequilibrium). In other words, if conditions are insufficient to contaminate $ee_{\text{D}-a\text{Ile}}$ at the time of measurement, conditions were even less favorable for that contamination in the past if α-epimerization has been occurring.

3.2.5 Impossibility of Terrestrial L-Ile Contamination of $ee_{\text{D}-a\text{Ile}}$ in MET 00426

Section 3.2.1 proved that if $ee_{\text{D}-a\text{Ile}}$ is being increased by α-epimerization, then $ee_{\text{L}-\text{Ile}} > ee_{\text{D}-a\text{Ile}}$, and section 3.2.2 expanded the logic to opposite cases where $ee_{\text{L}-\text{Ile}} \leq ee_{\text{D}-a\text{Ile}}$ and $ee_{\text{D}-a\text{Ile}}$ is unchanging or decreasing. The latter was the case for MET 00426 ($ee_{\text{L}-\text{Ile}} = 50,\ ee_{\text{D}-a\text{Ile}} = 60$), so its $ee_{\text{D}-a\text{Ile}}$ was either unchanging or decreasing at the time of measurement. Generally speaking, a line of argument might well finish here because an excess which is either stagnant or decreasing during a continuous (albeit rate-varied) process is not being increased by contamination or anything else.

Since $ee_{\text{L}-\text{Ile}} \neq ee_{\text{D}-a\text{Ile}}$ in MET 00426, α-epimerization has not reached equilibrium (section 3.2.3), and in the proper conditions, $ee_{\text{D}-a\text{Ile}}$ would decrease further until $ee_{\text{L}-\text{Ile}} = ee_{\text{D}-a\text{Ile}}$ at their α-epimerization equilibrium value of approximately 57%. These statements strictly describe only the time of measurement, so the argument beginning this section is presented below using the results of modeling which α- and β-epimerize MET 00426's amino acid abundances. The rate constants used in these calculations almost certainly reflect conditions more suitable for α-epimerization

(buffered, mildly basic solution at 298K) than the sub-freezing desiccation MET 00426 and the other Antarctic meteorites likely experienced in the ice fields.

The following model includes β-epimerization, though it is so slow compared to α-epimerization ($10 < \alpha/\beta < 10^4$) that its effects can be virtually negligible for shorter timescales and cooler temperatures.

Fig. 17 illustrates that $ee_{\text{D}-a\text{lle}}$ was declining when it was measured. A historical theoretical maximum of 62.7% remains theoretical in the absence of isoleucine stereoisomer isotopic measurements to quantify contaminant L-Ile or precise constraints

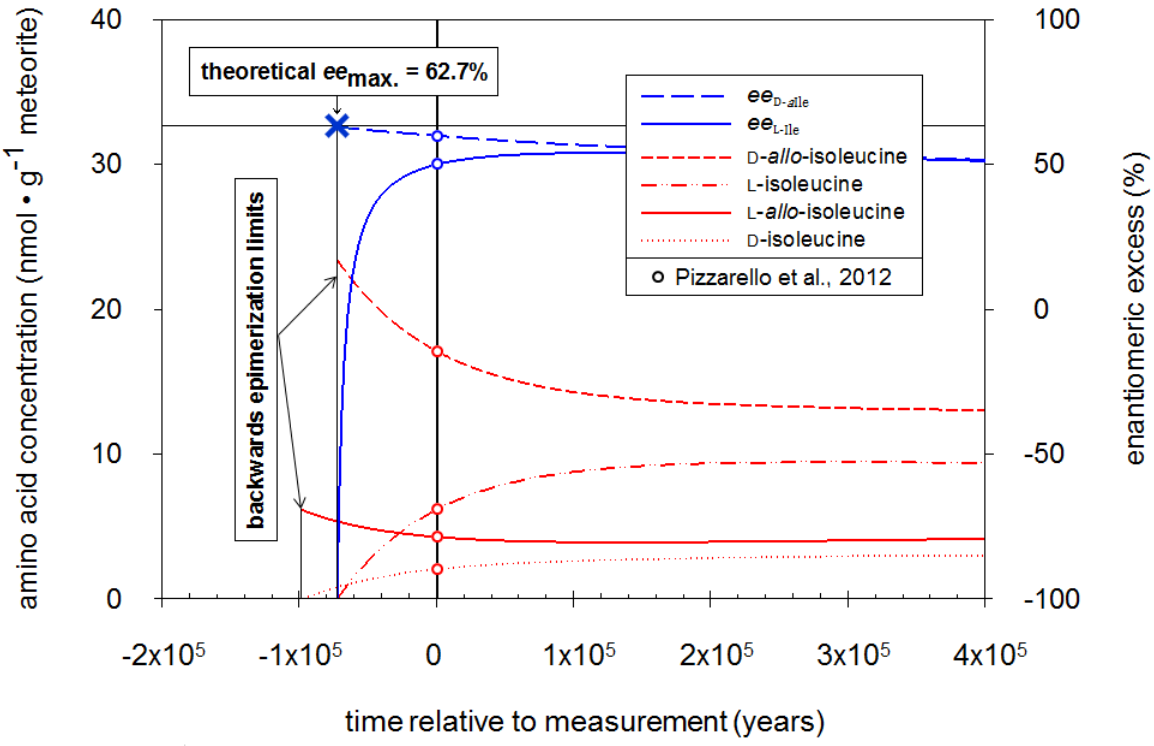

Figure 17. Modeled Epimerization of Isoleucine Stereoisomers in MET 00426. Reported amino acid concentrations and their calculated *ee* (Pizzarello, Schrader, Monroe, & Lauretta, 2012) are plotted on the $t = 0$ line, and the results of reversible, first-order kinetic modeling applied forwards and backwards in time define the lines which extend from -1x10^5 to +4x10^5 yr.

on aqueous alteration conditions. Contaminant L-Ile in this case would result in overestimation of the theoretical $ee_{\max}$. MET 00426 is reportedly one of the least aqueously altered meteorites in Earth collections (Abreu & Brearley, 2010), so the reported 60% may be the true maximum value for $ee_{\text{D}-a\text{Ile}}$.

Any contaminant L-Ile was not enough to raise $ee_{\text{L}-\text{Ile}}$ to exceed $ee_{\text{D}-a\text{Ile}}$ and change the direction of equilibrium so $ee_{\text{D}-a\text{Ile}}$ would be rising after arriving at Earth. This finding validates the reported enantiomeric excess of indigenous $\text{D}-a\text{Ile}$ in Pizzarello et al., 2012.

3.2.6 Constraining Durations of Aqueous Alteration of Amino Acids on Asteroidal Parent Bodies

Isoleucine epimerization can be useful for describing aqueous alteration in (1) relative degrees and for (2) constraining the duration of the aqueous phase in which the isoleucine stereoisomers were dissolved. This approach differs in several ways from existing application of isotopic and mineralogical analyses (see 1.1, 1.2) or relative abundances of amino acids (Glavin, Callahan, Dworkin, & Elsila, 2011) to gauge the degree of aqueous or thermal alteration. Individual amino acids do not contain long-lived radionuclides, so temperatures, absolute dates, and durations of hypothesized formation are transferred from petrology rather than concluded by measurement of the organics themselves. MicroRaman spectroscopy of meteoritic insoluble organic material (IOM) has positively correlated 1s-σ* exciton intensity with the degree of parent body metamorphism (Cody, et al., 2008), but the IOM is an abundant bulk solid and suitable for spectroscopic analyses in ways that individual amino acids cannot be. Abundances of

the isoleucine stereoisomers and knowledge of equilibrium conditions could be applied to gauge extent of aqueous alteration.

The second point of attaining equilibrium when *ee* become equal is useful for discussion about aqueous alteration and whether at least one indicator of aqueous alteration is present. In an environment without confounding chiral influences, if $ee_{\text{L}-\text{Ile}} \neq ee_{\text{D}-a\text{Ile}}$, disequilibrium exists. In a continuum of samples with similar starting materials but varying levels of alteration and detected *ee*, samples with the most disparate *ee* have experienced the least aqueous alteration, ones whose *ee* have become equal have experienced the most, and varying differences of *ee* in between would allow ordering by alteration. Though these amino acids are less abundant than others whose relative ratios have been used to gauge extents of aqueous alteration (glycine, β-alanine, and α-aminoisobutyric acid), if they are present in quantifiable abundances, use of the D-Ile and L-*a*Ile diastereomers may be advantageous due to the fact that the relative calculation is based on abundances of nearly identical, non-protein amino acids. These stereoisomers will have identical aqueous solubilities and extraction efficiencies independent of investigator, curatorial environment, and extraction procedure. The point of identical solubilities addresses an issue raised on account of the relative solubilities of amino acids and extraction bias (Shock & Schulte, 1990). Another advantage is based on amino acid ion yields by compound which may change relative to each other based on normal instrument variation or choice of reagents for amino acid derivatization in various labs. The sensitivity issue is resolved by analyzing diastereomers which typically elute within 30 seconds of each other and behave identically during derivatization and fragmentation upon analysis. The major disadvantage of using the isoleucine stereoisomers to assess the

extent of aqueous alteration is due to their lower overall abundances by comparison to the shorter amino acids like glycine, β-alanine, and α-aminoisobutyric acid.

The other application related to aqueous alteration uses rates of epimerization and measured disequilibria in meteorite amino acids. Reversible, first-order kinetics can be assumed to model α-epimerization backwards in time, and eventually the α-epimer pairs D-*a*Ile & L-Ile and L-*a*Ile & D-Ile will reach times where the concentration of one amino equals zero and the other equals the sum of their present concentrations. The path each species follows is determined by their relative concentrations and the value of the epimerization constant, K_{ile}.

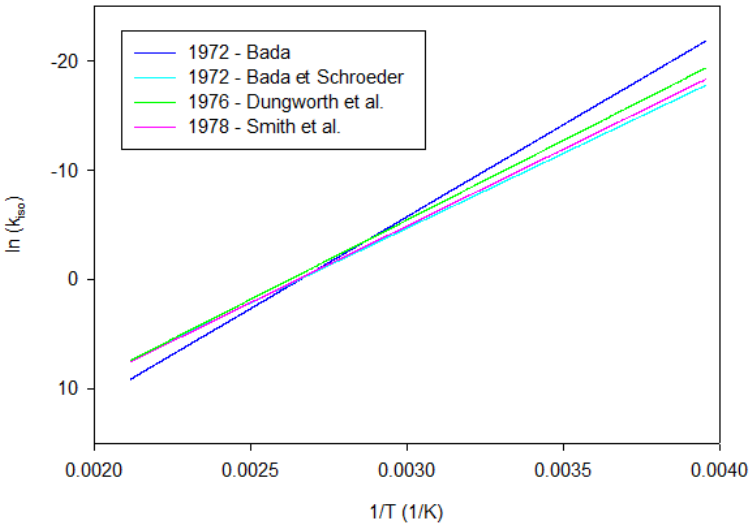

Figure 18. Arrhenius plot of 4 isoleucine epimerization studies. The 1972 Bada plot was extrapolated to the lower temperatures required for considering meteorites (-20°C to 75°C for this study) because it yields the smallest rate constants in that temperature range.

In order to calculate the most conservative estimate (the largest maximum) for total duration of aqueous alteration, the slowest rate constant is used for the modeling (Fig. 18). The temperature range of interest for this study was -20°C to 75°C, and the

smallest rate constant results from an Arrhenius plot generated by an isoleucine epimerization experiment at 5 temperatures between 101 and 148°C (Bada J. L., 1972).

$$log\ k_{iso}[yr^{-1}] = 19.41 - 7304.0 * T^{-1}$$

Rate constants were calculated for -20, -10, 0, 25, 50, and 75°C and combined with amino acid abundances of 7 CR chondrites (Pizzarello, Schrader, Monroe, & Lauretta, 2012) in these α-epimerization models to search backwards in time for the maximum possible duration of aqueous alteration.

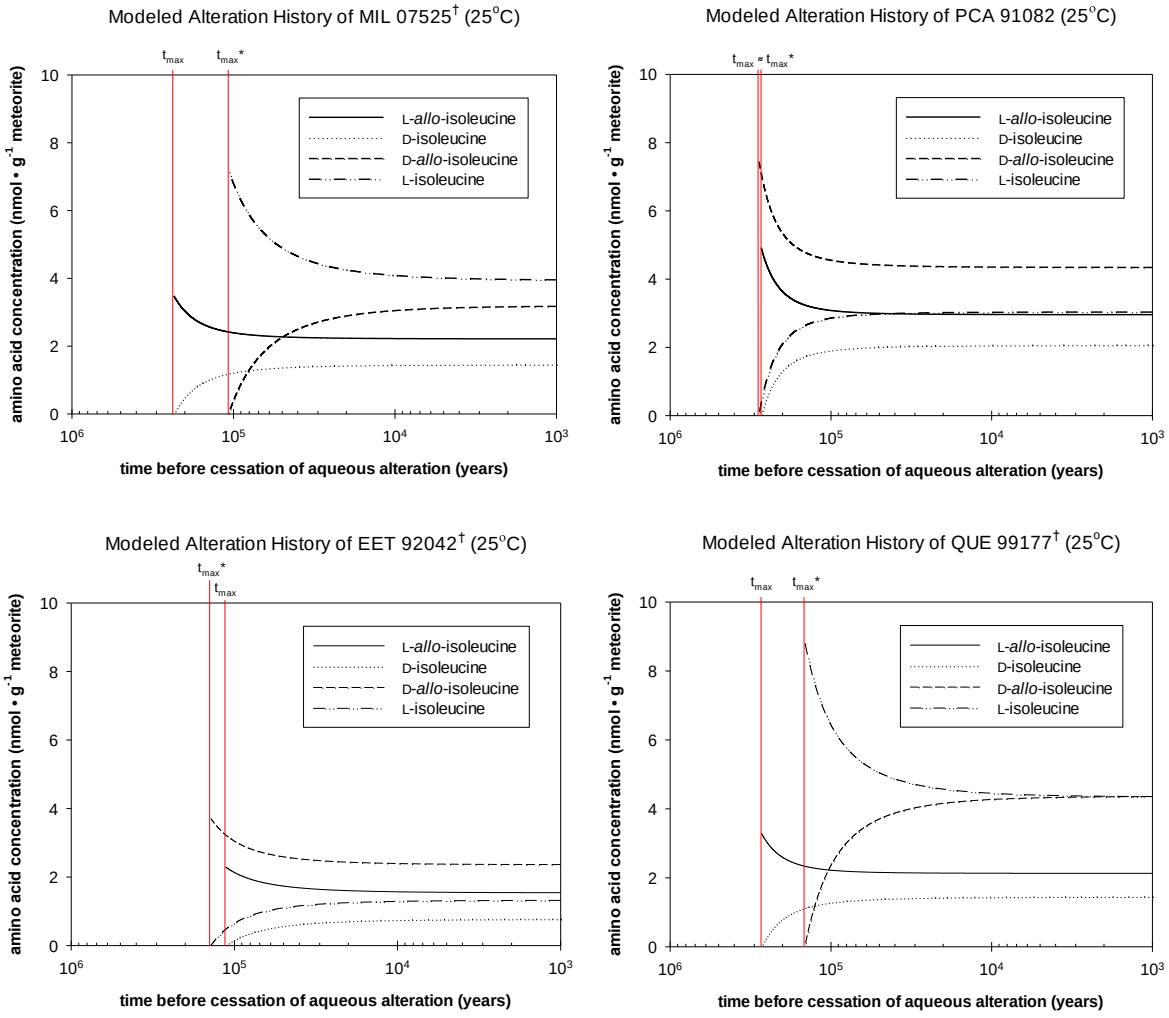

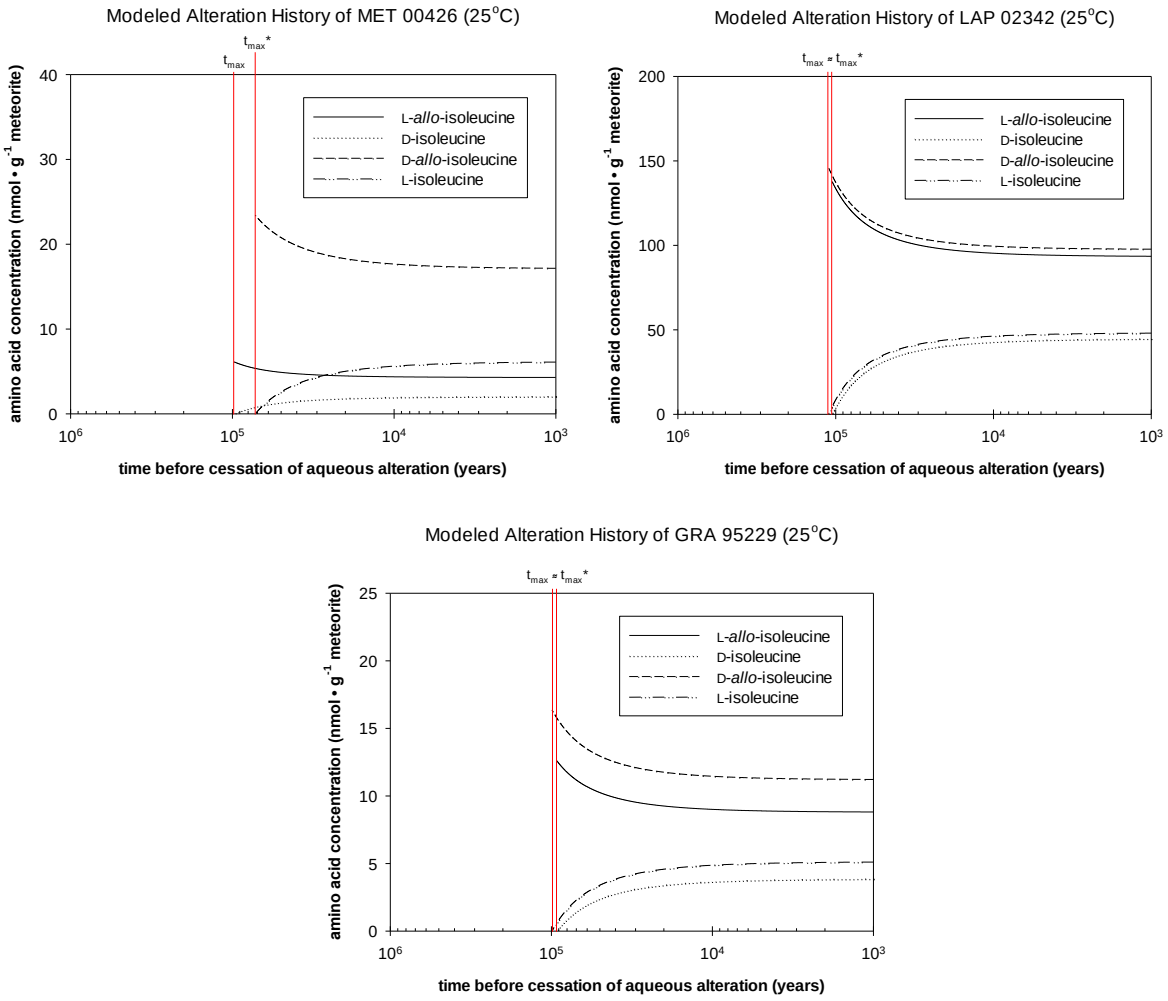

Figure 19. Red lines indicate the time at which an amino acid abundance reaches zero, indicating that aqueous alteration could not have continued further back in time. These ages use an extrapolated rate constant for 25°C (Bada J. L., 1972) and the reported isoleucine and *allo*isoleucine concentrations from 7 CR chondrites (Pizzarello, Schrader, Monroe, & Lauretta, 2012). †Denotes contamination.

Individual amino acid curves for the 25°C models are plotted (Fig. 19), and two maximum times are shown. Each time is calculated from a different α-epimer pair. Because L-isoleucine is the only protein amino acid, durations determined using it and D-*a*Ile, its α-epimer, are labeled $t_{max}{}^{*}$ to indicate the potential for contamination. The t_{max} without an asterisk is calculated from the other pair of α-epimers and is free from the

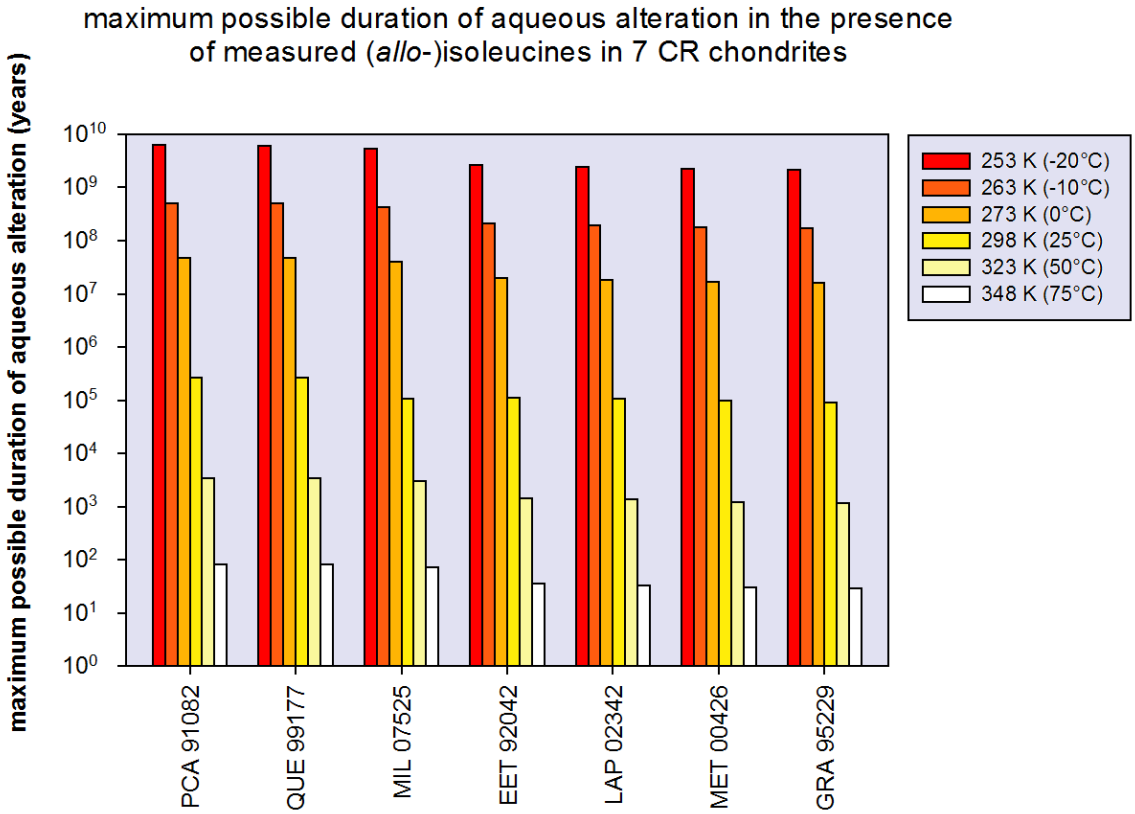

Figure 20. t_{max} values calculated using L-allo ↔ D-ile α-epimer pairs (see Figure 18 for a more detailed illustration of modeling at 25°C) from reported values in 7 CR chondrites (Pizzarello, Schrader, Monroe, & Lauretta, 2012) and extrapolated rate constants (Bada J. L., 1972) at temperatures -20, -10, 0, 25, 50, and 75°C.

possibility of contamination in any known way. This is the justification for exclusively plotting t_{max} in Fig. 20.

As summarized in Fig. 20, alteration conditions of 75°C allow < 10^2 yr of alteration in the presence of these amino acids. Though aqueous alteration of the parent body is said to have been episodic, the relatively short durations calculated in this study are difficult to reconcile with alteration durations of 10^6 - 10^7 yr (Zolensky, Krot, & Benedix, 2008), so some hypotheses are offered to explain the apparent contradiction between these timescales.

One possibility is the formation of amino acids in the last stages of freezing without sufficient time to epimerize. While this is additionally attractive because the final freezing of the liquid would increase precursor concentrations along with the "anti-freezes" such as ammonia and salts on the small scale, the solution temperatures would be very cold and perhaps unfavorable despite the high concentrations, and it is unclear how to prevent reaction or degradation of precursors during the warmer, aqueous episodes preceding the last one.

Another possibility is the early formation of amino acids and protection by encapsulation or adsorption to mineral grains or surfaces (*e.g.*, halite or phyllosilicates). This is compatible with the notion of an early, fast, and icy synthesis proposed in Pizzarello et al., 2012 as a way to preserve racemizable aldehyde precursors during amino acid synthesis.

Finally, the application of more complex parent body aqueous alteration models (multiple episodes, distinct fluid composition and conditions) to organic geochemical synthesis may be required to explain this apparently short timescale for the isoleucine stereoisomers. Perhaps these compounds were formed in the final episode of alteration or at greater, warmer depth before being transported by fluid to a colder, drier locale nearer to the parent body surface.

3.3 Conclusions

Consideration of isoleucine epimerization has several novel applications to the study of meteorites. Specific requirements to contaminate the other stereoisomers of L-isoleucine have been summarized, and a derivation newly presented here established that the enantiomeric excess of meteoritic D-*allo*-isoleucine is not increased by epimerizing

contaminant L-isoleucine so long as $ee_{\text{L}-\text{Ile}} \leq ee_{\text{D}-a\text{Ile}}$. Application of this approach to MET 00426 excluded contamination and confirmed the indigeneity of the largest enantiomeric excess of a non-protein amino acid ever reported. If contamination raises $ee_{\text{L}-\text{Ile}}$ without exceeding $ee_{\text{D}-a\text{Ile}}$, additional contaminant L-Ile actually slows the loss of indigenous $ee_{\text{D}-a\text{Ile}}$ due to the increased α-epimerization of L-Ile to D-*a*Ile.

Isoleucine epimerization modeling has also been applied to calculate maximum possible total durations of aqueous alteration. These durations were calculated using α-epimer abundances not able to be contaminated by any known means and were found to be relatively short (*e.g.*, ~10^2 yr at 75°C) compared to estimated durations of aqueous alteration on various asteroidal parent bodies (Zolensky, Krot, & Benedix, 2008) using the smallest extrapolated rate constants.

IV. EPIMERIZATION OF FREE D-*ALLO*-ISOLEUCINE AT 200°C

Flame-sealed, silica glass vials containing 1 mM D-*allo*-isoleucine dissolved in triple-distilled, degassed water were incubated at 200°C for anywhere between ~1 hour to ~3 months. Using GC-Mass Spectrometry (GC-MS) to analyze O-isopropyl, N-TFA derivatives of D-*allo*-isoleucine and its stereoisomers, we determined rate constants for the portion of the reaction in which the system follows reversible, first order kinetics (Ile/*allo* ≤ 0.5). At 200°C and assuming the epimerization constant $K_{ile} = 1.4$, the rate of conversion of D-*allo*-isoleucine to L-isoleucine was determined to be 470 ± 60 yr^{-1} and essentially reached equilibrium in 24 hours. β-epimerization products did not appear until samples had been incubated in excess of ~2 months.

4.1 Introduction

Studies of the destruction or racemization of amino acids for paleontological or geological purposes began shortly after the discovery of amino acids associated with fossils (Abelson, 1954). The first of these studies measured most of the protein amino acids' survival and racemization during heating and concluded that they might be useful for dating fossilized sediments aged ~10^5 yr (Hare & Abelson, 1967). The same study also identified L-isoleucine (hereafter L-Ile) and D-*allo*-isoleucine (hereafter D-*a*Ile) as an useful pair of amino acids due to the existence of two chiral centers (α- and β-carbons or C2 and C3, respectively), the comparatively slow reversal of the chiral center at the β-carbon, and the ease of separating the compounds analytically. The slow reversal of the chiral center at the β-carbon prolongs equilibration and presumably would allow dating of older sediments. With the exception of Threonine, all other protein amino acids contain a single chiral center at the α-carbon and become racemic by interconversion directly

between L and D enantiomers (e.g., L-aspartic acid ↔ D-aspartic acid). The conversion of L-Ile to D-Ile technically does not occur because it "would require simultaneous inversion at two chiral centers" (Bada J. L., 1986), though one of these inversions could happen on the same molecule after inversion of the other chiral center.

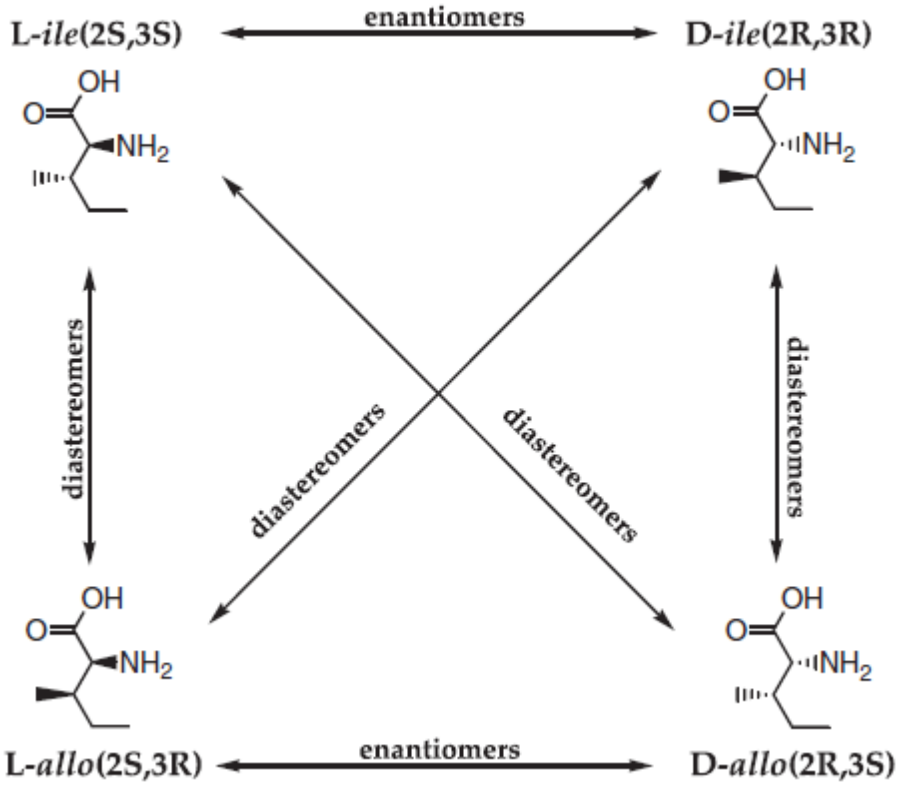

Figure 21. Reprinted schematic representation of Isoleucine diastereomeric and enantiomeric relationships (Chaban & Pizzarello, 2010). Note the difference in shorthand (L-ile is L-Ile and D-*allo* is D-*a*Ile).

L-Ile and D-*a*Ile convert into each other *via* a process called α-epimerization when the symmetry of the chiral center at is reversed following loss and acquisition of protons on opposite sides of the molecule. D-Ile and L-*a*Ile, the other two stereoisomers, undergo

α-epimerization in the same way. When the reversal of symmetry occurs at the β-C, L-Ile interconverts with L-*a*Ile and D-Ile with D-*a*Ile, and this process is called β-epimerization.

After the introduction of isoleucine epimerization to sediment dating, later studies expanded its usefulness by determining rate constants under different conditions (pH, Temperature, and various bound forms vs. "free" isoleucine to name a few) and measuring the extents of amino acid racemization in sediments which could be compared to precise isotope chronometers (Bada & Schroeder, 1972; Bada J. L., 1972; Dungworth, Schwartz, & Van De Leemput, 1976; Smith, Williams, & Wonnacott, 1978; Bada J. L., 1986; Wehmiller & Hare, 1971; Kriausakul & Mitterer, 1978).

The apparent scientific consensus for α-epimerization in solution and in the presence of natural carbonates is that the system kinetically follows one of two behaviors based on reaction progress. In a system beginning with L-Ile (recall that among the four possible stereoisomers, L-Ile is the only one found in proteins), reaction progress can be measured with the *allo*isoleucine/Isoleucine (*allo*/Ile) ratio which begins at zero and approaches equilibrium and the epimerization constant, K_{ile}. When *allo*/Ile ratio exceeds a certain value along the way to completion, the system adopts a slightly different kinetic behavior. Different values have been calculated for this kinetic change, and their range is 0.3 – 0.9 (Wehmiller & Hare, 1971; Bada & Schroeder, 1972; Mitterer, 1975; Kriausakul & Mitterer, 1978). When the *allo*/Ile is between zero and this value, the system follows reversible, first-order kinetics, and when *allo*/Ile is between this value and K_{ile}, the system follows apparent parabolic kinetics. Parabolic kinetics are typically used to describe oxidation of metallic surfaces which slow according to a parabolic law; the change in mass of the metal, Δm, can be described by $\Delta m^2 = k_p t$ (Pieraggi, 1987).

Combining plots of concentrations for one system following reversible, first order and another following apparent parabolic kinetics illustrates that they differ the most only when the system following apparent parabolic kinetics takes longer to reach equilibrium near the end of the reaction.

In a model experiment beginning with pure L-Ile, the ratio *allo*/Ile begins at 0 and increases in time until equilibrium is reached and *allo*/Ile = K_{ile} (recall subsection 3.2.3 and Table 11). Isoleucine stereoisomers have unique applications to meteorites (see chapter 3), and some meteorites contain *allo*/ile ratios in excess of K_{ile} (Pizzarello, Schrader, Monroe, & Lauretta, 2012). To our knowledge, epimerization of pure D-*allo*-isoleucine has never been measured or its kinetics explored from low Ile/*allo* (extremely high *allo*/Ile) ratios.

4.2 Materials and Methods

All water used in this study for glassware rinsing or solution preparation was triple-distilled, and all glassware was annealed at 550°C for at least 8 hours following rinsing. A 0.99 ± 0.02 mM stock of D-*allo*isoleucine was prepared and analyzed *via* GC-MS for contaminants (none found). Incubation vials were made from I.D. x O.D. 5 mm x 8 mm silica glass tubing which was sealed at one end, annealed, loaded with 250 uL of D-*allo*isoleucine stock, degassed until bumping with a KnF Neuberger [model UN726.3 FTP], and sealed with an oxygen/acetylene torch. The headspace to liquid ratio was approximately 4:1.

Sealed vials were individually wrapped in aluminum foil for easy handling and placed in a standalone GC oven set to maintain a temperature of 200°C. Temperature was monitored for the entire duration of the experiment by two K-type thermocouples and

loggers with downloadable storage. Vials were removed from the oven after anywhere from ~1.4 hours (1.6E-04 yr) to ~3 months (2.5E-01 yr), 20-40 µL of solution were removed for analysis, and the remaining solutions were frozen at -20°C in case of repeat analyses.

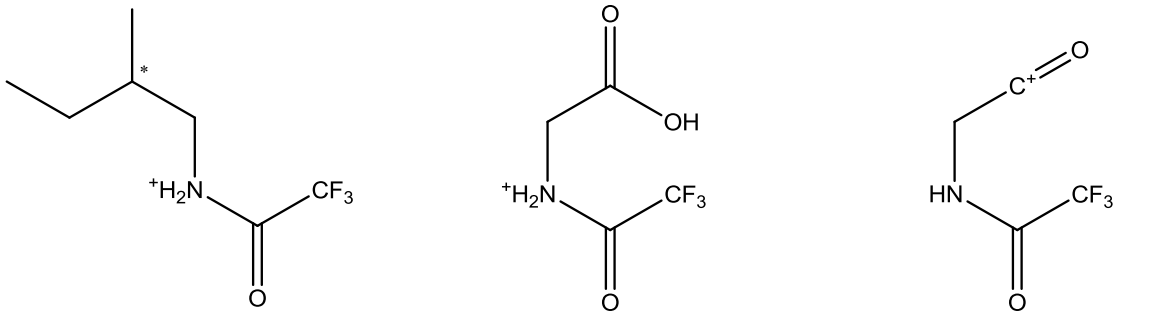

Molecular Weight: 182.16 Molecular Weight: 171.07 Molecular Weight: 153.06

Figure 22. Likely structures of major ionic species resulting from electron impact of O-isopropyl, N-TFA isoleucine derivatives during GC-MS.

Samples were dried in a rotary evaporator and derivatized with 25 µL isopropanol HCl (~3 N) at 100°C for one hour. These samples were allowed to cool for 10 minutes, then centrifuged at approximately 270 g (m/s^2) for 1 minute. Following evaporation of the alcohol, the isopropyl esters were reacted with 25 µL trifluoroacetic anhydride (TFAA) in 25 µL dichloromethane (DCM) at 100°C for 5 minutes. These samples were allowed to cool for 10 minutes, and then centrifuged for 1 minute. The resulting N-TFA-O-isopropyl amino acid derivatives were concentrated by evaporation under dry argon at room temperature and re-dissolved in DCM for concentration on a solids injector. GC–MS analyses employed a Chirasil-Dex-CB column of 25 m x 0.25 mm and 0.25 µm film thickness by Varian with a 99.999% helium flow of 0.6 mL min^{-1} and oven programmed for 65°C for 5 minutes, 2° min^{-1} until 85°C, then 4° min^{-1} to 200°C. Negative control

vials were filled with 250 µL of thrice distilled water and randomly analyzed according to the same methods. The sum of integrated ions 182, 171, and 153 (Fig. 22) was used to calculate relative abundances of the isoleucine stereoisomers in all samples.

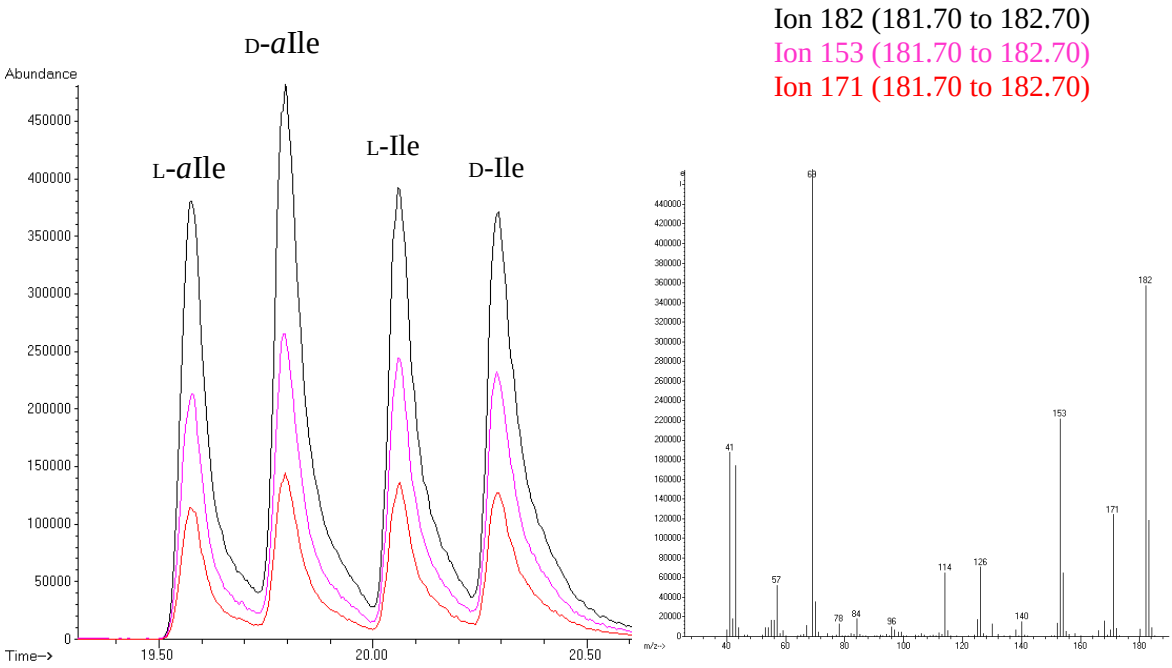

Figure 23 (left). Positive ions with m/z 182, 171, and 153 are colored and labeled (left). Elution order from a Chirasil-Dex column is L-*a*Ile, D-*a*Ile, L-Ile, and D-Ile. The separation of L-*a*Ile and D-*a*Ile over 24 samples was 0.29 ± 0.02 minutes. Figure 24 (right). Typical mass spectrum at the time of maximum peak height.

4.3 Results

A series of D-*a*Ile samples incubated at 200°C in a modified Gas Chromatography (GC) oven for up to two months illustrated the α-epimerization of D-*a*Ile to L-Ile with time. L-*a*Ile and D-Ile, the β-epimerization products had only begun to appear in traces after two months.

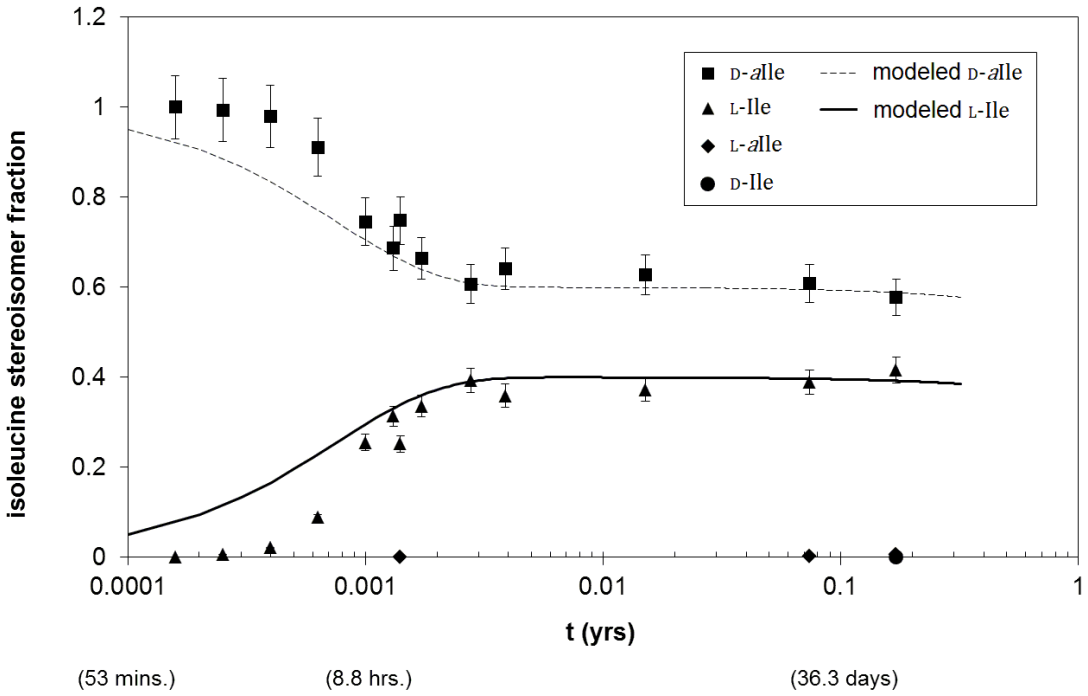

Figure 25. Epimerization of D-*allo*-isoleucine at 200°C. Other stereoisomers are created by α- and β- epimerization. The dotted and solid lines depict concentrations changing according to reversible, first-order kinetics and the rate constants determined by our experiments.

Rate constants were determined using previously established assumptions and calculations, and the approach and presentation in the following section are inspired by the appendix of a study beginning with L-Ile in calcareous marine sediments (Bada & Schroeder, 1972). For the purposes of evaluating a system beginning with D-*a*Ile, a few simple substitutions are made:

For α-epimerization as a reversible, first order reaction, the rate of disappearance of D-*a*Ile is given by:

$$-\frac{d[\mathrm{D}-a\mathrm{Ile}]}{dt} = k_{allo}[\mathrm{D}-a\mathrm{Ile}] - k_{iso}[\mathrm{L}-\mathrm{Ile}]$$

If L-Ile is initially present in trace amounts compared to D-*a*Ile,

$$[\text{D} - a\text{Ile}]_{initial} \cong [\text{D} - a\text{Ile}] + [\text{L} - \text{Ile}]$$

and

$$-\frac{d[\text{D} - a\text{Ile}]}{dt} = (k_{allo} + k_{iso})[\text{D} - a\text{Ile}] - k_{iso}[\text{D} - a\text{Ile}]_{initial}$$

Integration of this expression and substitution of the epimerization constant ($\text{K}_{\text{ile}} = \frac{k_{iso}}{k_{allo}}$) yields:

$$\text{Ln}\left[\frac{1 + (\text{Ile}/allo)}{1 - \text{K}_{\text{ile}}(\text{Ile}/allo)}\right] = (1 + \text{K}_{\text{ile}}) \cdot k_{allo} \cdot t + \text{constant}$$

This is plotted below, where the slope $= (1 + \text{K}_{\text{ile}}) \cdot k_{allo}$.

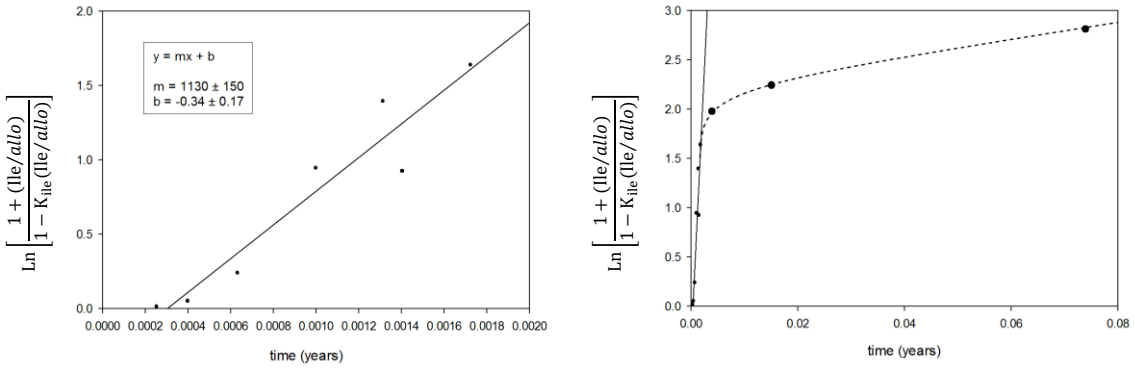

Figure 26. Plot of reversible, first-order kinetic regime (left) and expanded plot to include apparent parabolic regime (right).

The slope of the plot in Fig. 26 was used in to determine $k_{allo} = 470 \pm 60\ yr^{-1}$.

4.4 Discussion

The assumed $K_{ile} \approx 1.4$ is consistent with the literature, though reviews including references of the determination of the epimerization state that it has been measured between 1.25 and 1.4 in various studies (Smith, Williams, & Wonnacott, 1978). If extrapolated rate constants are calculated from published Arrhenius constants, by comparison this study measured the slowest rate for this process (Table 12). A previous review of isoleucine epimerization rates concluded that the two major factors affecting rate constant (other than temperature) were pH and ionic strength. The existence of a de-protonated reaction intermediate results in faster rates at higher pHs when de-protonation occurs more frequently (Smith, Williams, & Wonnacott, 1978).

Table 12. Comparison of experimentally determined rate constant to extrapolated rate constants at 200°C. Regression statistics were unavailable for the Arrhenius plots.

	this study	Bada (1972)	Bada and Schroeder (1972)	Dungworth et al. (1976)	Smith et al. (1978)
buffered pH	N/A	8.4	7.6	7.0	7.6
observed T (°C)	200	101 - 148	100 - 148	110 - 150	125 - 180
k_{iso}	660 ± 90 yr^{-1}	9300 yr^{-1}	1600 yr^{-1}	1700 yr^{-1}	1900 yr^{-1}

The small rate constant from our measurements results from the absence of buffer, the inevitable de-carboxylation of some amino acid resulting in some lower pH, and the use of triple-distilled (minimized ionic strength) water. Unbuffered solutions with minimized ionic strength enable measurement of the smallest possible rate constants for this reaction and expand the maximum known range for these rate constants while being the first experimental measurements in systems starting exclusively with D-*a*lle. Knowledge of the range of these constants and the environmental factors which affect

their values is essential to justify the choice of rate constants for use in modeling introduced in chapter three, subsection 3.2.6.

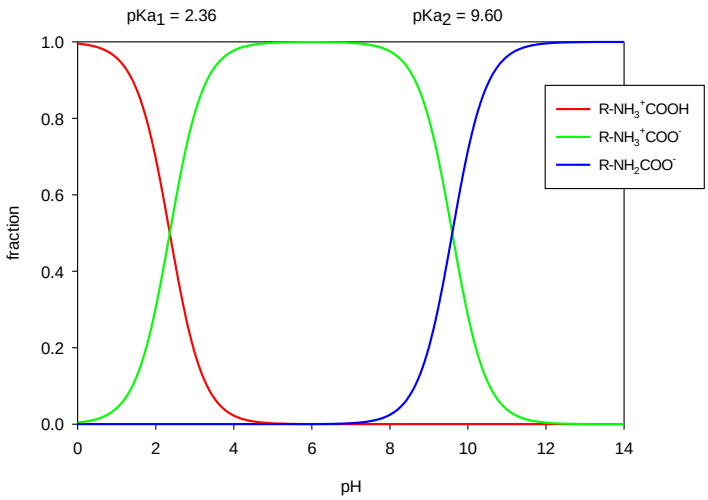

Figure 27. Isoleucine speciation plot. At least one atom of the molecule is ionized at the depicted pHs, decreasing the likelihood of the reaction's occurring in the gas phase.

4.5 Conclusion

The observed behaviors of epimerization and the existence of two kinetic regimes are maintained at low Ile/*allo* ratios as many experiments had demonstrated for low *allo*/Ile ratios. To our knowledge, isoleucine epimerization had never been measured in scenarios with *allo*/Ile > ~1.5, a range characteristic of meteoritic organic extracts that does not appear on Earth due to the abundance of protein L-isoleucine. We measured a value of 660 ± 90 yr^{-1} for k_{iso}, the rate constant determining the rate of conversion of L-isoleucine to D-*allo*-isoleucine. Our measured rate constant is a factor of 2.1-2.8 lower than the smallest extrapolated rate constant from previous studies. Reversible, first-order kinetic plots may be used to predict general behavior of an α-epimerizing system of isoleucine stereoisomers.

V. CONCLUSION

Meteorites are essential to understanding the Solar System because they uniquely bridge past and present, planetesimal and planet, and, now that life has taken root on Earth, represent the rare and sometimes violent contact between bodies now-inhabited and not-yet inhabited by life in the form of terrestrial contamination. The study of organic molecules in meteorites is interesting for the same reason that it is difficult: compounds such as amino acids, sugars, and nucleobases are present in meteorites and abundant in the biosphere. Terrestrial contamination is inevitable, and most of chapter 3 of this dissertation introduces an approach to exclude contamination by L-isoleucine.

Consideration of isoleucine epimerization excludes contamination by establishing logical requirements for changing enantiomeric excesses, and the enantiomeric excess of D-*allo*-isoleucine cannot be increased by epimerizing contaminant so long as $ee_{\text{L}-\text{Ile}} \leq ee_{\text{D}-a\text{Ile}}$. This work validates the indigeneity of the largest enantiomeric excess of a non-protein amino acid ever reported (60% $ee_{\text{D}-a\text{Ile}}$ in MET 00426) in response to suggestions that terrestrial L-isoleucine had contaminated this excess.

The other focus of this dissertation is the causal relationship between aqueous alteration of asteroidal parent bodies and the abundance of organic material in carbonaceous meteorites. Chapter 2 contains the first thorough organic analyses of a pristine fragment of Bells, an anomalous, petrologic type 2 carbonaceous chondrite, which illustrates a possible chemical result of aqueous geochemistry of nitrogen-poor parent bodies. Survival of aldehydes, ketones, and amino acids despite a mildly oxidizing, mildly basic alteration phase solicits hypotheses for protection of these

organics by mineral phases and introduces the possibility that the organics were not present for the entirety of the pervasive aqueous phase evidenced by petrology of Bells.

In addition to excluding terrestrial contamination by L-isoleucine, isoleucine epimerization in the rest of chapter 3 is capable of (1) gauging degree of aqueous alteration and (2) constraining the total, maximum duration of asteroidal parent body aqueous alteration in the presence of these amino acids. Calculations of short maximum durations (*e.g.*, ~10^2 yr at 75°C) for this aqueous phase also indicate that these organics were isolated or their epimerization otherwise slowed by mineral encasement, adsorption, fluid transport and deposition to drier and/or colder locales, or another process. Kinetic studies comprise chapter 4 with measurements at high *allo*/Ile ratios uniquely found in meteorites that combine with decades of literature regarding L-isoleucine epimerization to justify the use of reversible, first-order kinetics for the duration calculations presented here.

The terms ‘soluble’ and ‘insoluble’ describe meteoritic organic materials and the analytical ease of their extraction by water and organic solvents, but this same relative solubility would have existed for the parent body fluid as well. The insoluble materials, much like insoluble mineral phases, cannot be transported as the soluble materials can. During fluid convection or other transport, short-chain amino acids probably visited multiple, distinct physicochemical environments on the parent body during their solvation. The finding of abundant soluble organics in MET 00426, a CR3 chondrite regarded as one of the least aqueously altered stones, does not necessarily challenge the supposed role of water in forming the meteoritic organic suite because the soluble organics are mobile. Amino acids could have been deposited and dried in a matter of

minutes given the proper situation. The precise timing and setting of amino acid formation remains a mystery which calls for any isotope or other studies to determine whether the soluble organics detected on a meteorite were formed there.

REFERENCES

Abelson, P. H. (1954). Amino Acids in Fossils. *The National Academy of Sciences: Abstracts of Papers Presented at the Annual Meeting* (p. 576). Washington, D.C.: American Association for the Advancement of Science.

Abreu, N. M., & Brearley, A. J. (2010). Early solar system processes recorded in the matrices of two highly pristine CR3 carbonaceous chondrites, MET 00426 and QUE 99177. *Geochimica et Cosmochimica Acta*, 1146-1171.

Amelin, Y., Krot, A. N., Hutcheon, I. D., & Ulyanov, A. A. (2002). Lead Isotopic Ages of Chondrules and Calcium-Aluminum-Rich Inclusions. *Science*, 1678-1683.

Bada, J. L. (1972). The dating of fossil bones using the racemization of isoleucine. *Earth and Planetary Science Letters*, 223-231.

Bada, J. L. (1986). Isoleucine Stereoisomers on the Earth. *Nature*, 314-316.

Bada, J. L. (1991). Amino Acid Cosmogeochemistry. *Philosophical Transactions: Biological Sciences*, 349-358.

Bada, J., & Schroeder, R. (1972). Racemization of isoleucine in calcareous marine sediments: kinetics and mechanism. *Earth and Planetary Science Letters*, 223-231.

Başer, K. H., & Buchbauer, G. (2010). *Essential Oils: Science, Technology, and Applications.* Boca Raton, FL: CRC Press.

Blinova, A., Alexander, C. M., Wang, J., & Herd, C. D. (2011). Mineralogy and Mn-Cr Extinct Radionuclide Dating of a Dolomite from the Pristine Tagish Lake Meteorite. *Workshop on the Formation of the First Solids in the Solar System.* Tucson, AZ: Lunar and Planetary Institute.

Blinova, A., Alexander, C. M., Wang, J., & Herd, C. D. (2012). Mineralogy and Mn-Cr Extinct Radionuclide Dating of a Dolomite from the Pristine Tagish Lake Meteorite. *43rd Lunar and Planetary Science Conference.* Tucson, AZ: Lunar and Planetary Institute.

Bonner, W. A. (1991). The origin and amplification of biomolecular chirality. *Origins of life and evolution of biospheres*, 59-111.

Bonner, W. A., Blair, N. E., & Lemmon, R. M. (1979). Racemization of Isovaline by γ-Radiation, Cosmological Implications. *Journal of the American Chemical Society*, 1049-1050.

Botta, O., Glavin, D. P., Gerhard, K., & Bada, J. (2002). Relative Amino Acid Concentrations as a Signature for Parent Body Processes of Carbonaceous Chondrites. *Origins of Life and Evolution of the Biosphere*, 143-163.

Botta, O., Martins, Z., & Ehrenfreund, P. (2007). Amino acids in Antarctic CM1 meteorites and their relationship to other carbonaceous chondrites. *Meteoritics & Planetary Science*, 81-92.

Brearley, A. J. (1995). Aqueous alteration and brecciation in Bells, an unusual, saponite-bearing CM chondrite. *Geochimica et Cosmochimica Acta*, 2291-2317.

Brearley, A. J. (2005). Nebular versus Parent-Body Processing. In A. M. Davis, *Meteorites, Comets, and Planets: Treatise on Geochemistry* (pp. 247-268). Kidlington, Oxford: Elsevier Ltd.

Brearley, A. J., Hutcheon, I. D., & Browning, L. (2001). Compositional Zoning and Mn-Cr Systematics in Carbonates from the Y791198 CM2 Carbonaceous Chondrite. *32nd Lunar and Planetary Science Conference.* Tucson, AZ: Lunar and Planetary Institute.

Brennecka, G. A., Weyer, S., Wadhwa, M., Janney, P. E., Zipfel, J., & Anbar, A. D. (2010). 238U/235U Variations in Meteorites: Extant 247Cm and Implications for Pb-Pb Dating. *Science*, 449-451.

Brownlee, D. E. (1985). Cosmic Dust: Collection and Research. *Annual Reviews in Earth and Planetary Sciences*, 147-173.

Bullock, E. S., Gounelle, M., Grady, M. M., & Russell, S. S. (2003). Different Degrees of Aqueous Alteration in Sulphides within the CI1 Chondrites. *34th Lunar and Planetary Science Conference.* Tucson, AZ: Lunar and Planetary Institute.

Bunch, T. E., & Chang, S. (1980). Carbonaceous chondrites--II. Carbonaceous chondrite phyllosilicates and light element geochemistry as indicators of parent body processes and surface conditions. *Geochimica et Cosmochimica Acta*, 1543-1577.

Burbine, T. H., McCoy, T. J., Meibom, A., Gladman, B., & Keil, K. (2002). Meteoritie Parent Bodies: Their Number and Identification. In W. F. Bottke, A. Cellino, P. Paolicchi, & R. P. Binzel, *Asteroids III* (pp. 653-667). Tucson, AZ: University of Arizona Press.

Callahan, M. P., Martin, M. G., Burton, A. S., Glavin, D. P., & Dworkin, J. P. (2014). Amino acid analysis in micrograms of meteorite sample by nanoliquid

chromatography–high-resolution mass spectrometry. *Journal of Chromatography A*, 30-34.

Cassidy, W. A. (2012). *Meteorites, Ice, and Antarctica: A Personal Account.* Cambridge, UK: Cambridge University Press.

Chaban, G. M., & Pizzarello, S. (2010). Ab initio calculations of 6- and 7-carbon meteoritic amino acids and their diastereomers. *Meteoritics and Planetary Science*, 1053-1060.

Chamberlin, T. C., & Chamberlin, R. T. (1908). Early terrestrial conditions that may have favored organic synthesis. *Science*, 897-911.

Chyba, C., & Sagan, C. (1992). Endogenous production, exogenous delivery and impact-shock synthesis of organic molecules: an inventory for the origins of life. *Nature*, 125-132.

Clayton, R. N. (1993). Oxygen Isotopes in Meteorites. *Annual Review of Earth and Planetary Sciences*, 115-149.

Clemett, S., Maechling, C., Zare, R., Swan, P., & Walker, R. (1993). Identification of complex aromatic molecules in individual interplanetary dust particles. *Science*, 721.

Cody, G. D., Alexander, C. M., Yabuta, H., Kilcoyne, A. L., Araki, T., Ade, H., . . . Mysen, B. O. (2008). Organic thermometry for chondritic parent bodies. *Earth and Planetary Science Letters*, 446-455.

Cooper, G. W., & Cronin, J. R. (1995). Linear and cyclic aliphatic carboxamides of the Murchison meteorite: hydrolyzable derivaties of amino acids and other carboxylic acids. *Geochimica et Cosmochimica Acta*, 1003-1015.

Cooper, G. W., Reed, C., Nguyen, D., Carter, M., & Wang, Y. (2011). Detection and formation scenario of citric acid, pyruvic acid, and other possible metabolism precursors in carbonaceous meteorites. *Proceedings of the National Academy of Sciences*, 14015-14020.

Cotton, F. A. (1990). *Chemical Applications of Group Theory, 3rd ed.* New York, NY: Wiley-Interscience.

Cronin, J. R., & Pizzarello, S. (1990). Aliphatic hydrocarbons of the Murchison meteorite. *Geochimica et Cosmochimica Acta*, 2859-2868.

Cronin, J. R., Pizzarello, S., & Gandy, W. E. (1979). Amino Acid Analysis with o-Phthalaldehyde Detection: Effects of Reaction Temperature and Thiol on Fluorescence Yields. *Analytical Biochemistry*, 174-179.

Cronin, J., & Pizzarello, S. (1983). Amino acids in meteorites. *Advances in Space Research*, 5-18.

Cronin, J., & Pizzarello, S. (1997). Enantiomeric excesses in meteoritic amino acids. *Science*, 951-955.

Cronin, J., & Pizzarello, S. (1999). Amino Acid Enantiomer Excesses in Meteorites: Origin and Significance. *Advances in Space Research*, 293-299.

Cronin, J., & Reisse, J. (2005). Chirality and the Origin of Homochirality. In M. Gargaud, B. Barbier, H. Martin, & J. Reisse, *Lectures in Astrobiology, vol. 1* (pp. 473-508). Berlin & Heidelberg, Germany: Springer-Verlag Berlin Heidelberg.

de Leuw, S., Rubin, A. E., Schmitt, A. K., & T., W. J. (2009). 53Mn-53Cr systematics of carbonates in CM chondrites: Implications for the timing and duration of aqueous alteration. *Geochimica et Cosmochimica Acta*, 7433-7442.

Dungworth, G., Schwartz, A. W., & Van De Leemput, L. (1976). Composition and Racemization of Amino Acids in Mammoth Collagen Determined by Gas and Liquid Chromatography. *Comparative Biochemistry and Physiology*, 473-480.

Dyl, K. A., Bischoff, A., Ziegler, K., Young, E. D., Wimmer, K., & Bland, P. A. (2012). Early Solar System hydrothermal activity in chondritic asteroids on 1-10-year timescales. *Proceedings of the National Academy of Sciences*, 18306-18311.

Ehrenfreund, P., Glavin, D. P., Botta, O., Cooper, G. W., & Bada, J. L. (2001). Extraterrestrial amino acids in Orgueil and Ivuna: tracing the parent body of CI type carbonaceous chondrites. *Proceedings of the National Academy of Sciences*, 2138-2141.

Ehrenfreund, P., Rasmussen, S., Cleaves, J., & Chen, L. (2006). Experimentally Tracing the Key Steps in the Origin of Life: the Aromatic World. *Astrobiology*, 490-520.

Elsila, J. E., Charnley, S. B., Burton, A. S., Glavin, D. P., & Dworkin, J. P. (2012). Compound-specific carbon, nitrogen, and hydrogen isotopic ratios for amino acids in CM and CR chondrites and their use in evaluating potential formation pathways. *Meteoritics and Planetary Science*, 1517-1536.

Elsila, J. E., De Leon, N. P., Buseck, P. R., & Zare, R. N. (2005). Alkylation of polycyclic aromatic hydrocarbons in carbonaceous chondrites. *Geochimica et Cosmochimica Acta,* 1349-1357.

Elsila, J. E., Glavin, D. P., Dworkin, J. P., Martins, Z., & Bada, J. L. (2012). Inconclusive evidence for nonterrestrial isoleucine enantiomeric excesses in primitive meteorites. *Proceedings of the National Academy of Sciences,* E3288.

Endreβ, M., & Bischoff, A. (1996). Carbonates in CI chondrites: Clues to parent body alteration. *Geochimica et Cosmochimica Acta*, 489-507.

Engel, M. H., & Nagy, B. (1982). distribution and enantiomeric composition of amino acids in the Murchison meteorite. *Nature,* 837-840.

Engel, M., & Macko, S. (1997). Isotopic evidence for extraterrestrial non-racemic amino acids in the Murchison meteorite. *Nature, 389,* 265-268.

Epstein, S., Krishnamurthy, R. V., Cronin, J. R., Pizzarello, S., & Yuen, G. U. (1987). Unusual stable isotope ratios in amino acid and carboxylic acid extracts from the Murchison meteorite. *Nature,* 477-479.

Fieser, L. F., Tishler, M., & Sampson, W. L. (1941). Vitamin K Activity and Structure. *The Journal of Biological Chemistry,* 659-692.

Flynn, G., Keller, L., Jacobsen, C., & Wirick, S. (2004). An assessment of the amount and types of organic matter contributed to the Earth by interplanetary dust. *Advances in Space Research,* 57-66.

Garrison, W. M. (1972). Radiation-Induced Reactions of Amino-Acids and Peptides. *Radiation Research Reviews,* 305-326.

Gat, J. R. (1996). Oxygen and Hydrogen Isotopes in the Hydrologic Cycle. *Annual Review of Earth and Planetary Sciences,* 225-262.

Gilmour, I., & Pillinger, C. T. (1994). Isotopic Compositions of Individual Polycyclic Aromatic Hydrocarbons from the Murchison Meteorite. *RAS Monthly Notices,* 269.

Glavin, D. P., & Dworkin, J. P. (2009). Enrichment of the amino acid L-isovaline by aqueous alteration on CI and CM meteorite parent bodies. *Proceedings of the National Academy of Sciences,* 5487-5492.

Glavin, D. P., Callahan, M. P., Dworkin, J. P., & Elsila, J. E. (2011). The effects of parent body processes on amino acids in carbonaceous chondrites. *Meteoritics and Planetary Science,* 1948-1972.

Glavin, D. P., Elsila, J. E., Burton, A. S., Callahan, M. P., Dworkin, J. P., Hilts, R. W., & Herd, C. D. (2012). Unusual nonterrestrial L-proteinogenic amino acid excesses in the Tagish Lake meteorite. *Meteoritics & Planetary Science,* 1347-1364.

Grady, M. M. (2000). *Catalogue of Meteorites.* Cambridge, UK: Cambridge University Press.

Guo, W., & Eiler, J. M. (2007). Temperatures of aqueous alteration and evidence for methane generation on the parent bodies of CM chondrites. *Geochimica et Cosmochimica Acta,* 5565-5575.

Hamilton, P. B. (1965). Amino acids on hands. *Nature*, 284-285.

Hare, P. E., & Abelson, P. H. (1967). Racemization of amino acids in fossil shells. In *Carnegie Institution of Washington Year Book 66 (1966-1967)* (pp. 526-528).

Hayes, J. M. (1967). Organic constituents of meteorites--a review. *Geochimica et Cosmochimica Acta,* 1395-1440.

Herd, C. D., Blinova, A., Simkus, D. N., Huang, Y., Tarozo, R., Alexander, C. M., . . . Stroud, R. M. (2011). Origin and Evolution of Prebiotic Organic Matter as Inferred from the Tagish Lake Meteorite. *Science*, 1304-1307.

Hutcheon, I. D., Weisberg, M. K., Phinney, D. L., Zolensky, M. E., Prinz, M., & Ivanov, A. V. (1999). Radiogenic 53Cr in Kaidun Carbonates: Evidence for Very Early Aqueous Activity. *30th Lunar and Planetary Science Conference.* Tucson, AZ: Lunar and Planetary Institute.

Jilly, C. E., Huss, G. R., & Nagashima, K. (2013). Mn-Cr Dating of Secondary Carbonates in CR Chondrites. *44th Lunar and Planetary Science Conference.* Tucson, AZ: Lunar and Planetary Institute.

Kebukawa, Y., Nakashima, S., Ishikawa, M., Aizawa, K., Inoue, T., Nakamura-Messenger, K., & Zolensky, M. (2010). Spatial distribution of organic matter in the Bells CM2 chondrite using near-field infrared microspectroscopy. *Meteoritics & Planetary Science*, 394-405.

Kerridge, J. F. (1985). Carbon, hydrogen and nitrogen in carbonaceous chondrites: Abundances and isotopic compositions in bulk samples. *Geochimica et Cosmochimica Acta,* 1707-1714.

Kortenkamp, S., & Dermott, S. (1998). Accretion of Interplanetary Dust Particles by the Earth. *Icarus*, 469-495.

Kriausakul, N., & Mitterer, R. M. (1978). Isoleucine Epimerization in Peptides and Proteins: Kinetic Factors and Application to Fossil Proteins . *Science*, 1011-1014.

Krot, A. N., Hutcheon, I. D., Brearley, A. J., Pravdivtseva, O. V., Petaev, M. I., & Hohenberg, C. M. (2006). Timescales and Settings for Alteration of Chondritic Meteorites. In D. S. Lauretta, J. H. McSween, & R. P. Binzel, *Meteorites and the Early Solar System II* (pp. 525-553). Tucson, AZ: University of Arizona Press.

Krot, A. N., Petaev, M. I., Scott, E. R., Choi, B.-G., Zolensky, M. E., & Keil, K. (1998). Progressive alteration in CV3 chondrites: More evidence for asteroidal alteration. *Meteoritics & Planetary Science*, 1065-1085.

Kvenvolden, K., Lawless, J., Pering, K., Peterson, E., Flores, J., Ponnamperuma, C., . . . others. (1970). Evidence for extraterrestrial amino-acids and hydrocarbons in the Murchison meteorite. *Nature*, 923-926.

Lee, M. R., Lindgren, P., Sofe, M. R., Alexander, C. O., & Wang, J. (2012). Extended chronologies of aqueous alteration in the CM2 carbonacous chondrites: Evidence from carbonates in Queen Alexandra Range 93005. *Geochimica et Cosmochimica Acta*, 148-169.

Mangal, S. K. (2007). *Isoprenoid biosynthesis in higher plants.* New Delhi: Gene-Tech Books.

Martins, Z., Alexander, C. M., Orzechowska, G. E., Fogel, M. L., & Ehrenfreund, P. (2007). Indigenous amino acids in primitive CR meteorites. *Meteoritics & Planetary Science*, 2125-2136.

Matrajt, G., Brownlee, D. E., Sadilek, M., & Kruse, L. (2006). The fate of organic phases in porous IDPs and micrometeorites during atmospheric entry: a pulse-heating study. *37th Lunar and Planetary Science Conference Abstracts.* Tucson, AZ: Lunar and Planetary Institute.

May, K., Dapprich, S., Furche, F., Unterreiner, B., & Ahlrichs, R. (2000). Structures, C--H, and C--CH3 bond energies at borders of polycyclic aromatic hydrocarbons. *Physical Chemistry Chemical Physics, Royal Society of Chemistry*, 5084-5088.

McSween, H. Y., Ghosh, A., Grimm, R. E., Wilson, L., & Young, E. D. (2002). Thermal Evolution Models of Asteroids. In W. F. Bottke Jr., A. Cellino, P. Paolicchi, & R. P. Binzel, *Asteroids III* (pp. 559-571). Tucson, AZ: University of Arizona Press.

Miessler, G. L., & Tarr, D. A. (2004). *Inorganic Chemistry.* Upper Saddle River, NJ: Pearson Prentice Hall.

Mimura, K. (1995). Synthesis of polycyclic aromatic hydrocarbons from benzene by impact shock: Its reaction mechanism and cosmochemical significance. *Geochimica et Cosmochimica Acta*, 579-591.

Mitterer, R. M. (1975). Ages and Diagenetic Temperatures of Pleistocene Deposits of Florida Based on Isoleucine Epimerization in Mercenaria. *Earth and Planetary Science Letters*, 275-282.

Monroe, A. A., & Pizzarello, S. (2011). The soluble organic compounds of the Bells meteorite: Not a unique or unusual composition. *Geochimica et Cosmochimica Acta*, 7585-7595.

Monroe, A. A., & Pizzarello, S. (2013). Diastereomer amino acids and their significance for the prebiotic distribution of molecular asymmetry in the Solar System. *Lunar and Planetary Science Conference Abstracts.* Woodlands, TX: Lunar and Planetary Institute.

Muir, D. C., Norstrom, R. J., & Simon, M. (1988). Organochlorine Contaminants in Arctic Marine Food Chains: Accumulation of Specific Polychlorinated Biphenyls and Chlordane-Related Compounds. *Environmental Science Technology*, 1071-1079.

Neuberger, A. (1948). Stereochemistry of Amino Acids. *Advances in Protein Chemistry*, 297-383.

Palmer, E. E., & Lauretta, D. S. (2011). Aqueous alteration of kamacite in CM chondrites. *Meteoritics & Planetary Science*, 1587-1607.

Pearson, V. K., Kearsley, A. T., Sephton, M. A., & Gilmour, I. (2007). The labelling of meteoritic organic material using osmium tetroxide vapour impregnation. *Planetary and Space Science*, 1310-1318.

Peltzer, E. T., & Bada, J. L. (1978). alpha-Hydroxycarboxylic acids in the Murchison meteorite. *Nature*, 443-444.

Peltzer, E. T., Bada, J. L., Schlesinger, G., & Miller, S. L. (1984). The Chemical Conditions on the Parent Body of the Murchison Meteorite: Some Conclusions Based on Amino, Hydroxy, and Dicarboxylic Acids. *Advances in Space Rearch*, 69-74.

Petitat, M., Marrocchi, Y., McKeegan, K. D., Mostefaoui, S., Meibom, A., Zolensky, M. E., & Gounelle, M. (2011). 53Mn-53Cr ages of Kaidun carbonates. *Meteoritice & Planetary Science*, 275-283.

Pieraggi, B. (1987). Calculations of parabolic reaction rate constants. *Oxidation of Metals*, 177-185.

Pizzarello, S. (2003). The effect of meteorite powders in model amino acid syntheses and reactions. *Antarctic Meteorite Research* (p. 65). Tokyo, Japan: National Institute of Polar Research.

Pizzarello, S. (2006). The Chemistry of Life's Origin: A Carbonaceous Meteorite Perspective. *Accounts of Chemical Research*, 231-237.

Pizzarello, S. (2012). Catalytic syntheses of amino acids and their significance for nebular and planetary chemistry. *Meteoritics & Planetary Science*, 1291-1296.

Pizzarello, S., & Cooper, G. W. (2001). Molecular and chiral analyses of some protein amino acid derivatives in the Murchison and Murray meteorites. *Meteoritics & Planetary Science*, 897-909.

Pizzarello, S., & Cronin, J. R. (2000). Non-racemic amino acids in the Murray and Murchison meteorites. *Geochimica et Cosmochimica Acta*, 329-338.

Pizzarello, S., & Groy, T. (2011). Molecular asymmetry in extraterrestrial organic chemistry: An analytical perspective. *Geochimica et Cosmochimica Acta*, 645-656.

Pizzarello, S., & Holmes, W. (2009). Nitrogen-containing compounds in two CR2 meteorites: 15N composition, molecular distribution and precursor molecules. *Geochimica et Cosmochimica Acta*, 2150-2162.

Pizzarello, S., & Huang, Y. (2002). Molecular and isotopic analyses of Tagish Lake alkyl dicarboxylic acids. *Meteoritics & Planteray Science*, 687-696.

Pizzarello, S., & Huang, Y. (2005). The deuterium enrichment of individual amino acids in carbonaceous meteorites: A case for the presolar distribution of biomolecule precursors. *Geochimica et Cosmochimica Acta*, 599-605.

Pizzarello, S., & Monroe, A. A. (2012). Reply to Elsila et al.: Large enantiomeric excesses in primitive meteorites, an analytical and computational supplement. *Proceedings of the National Academy of Sciences*, E3289.

Pizzarello, S., & Williams, L. B. (2012). Ammonia in the Early Solar System: an Account from Carbonaceous Meteorites. *The Astrophysical Journal*, 161-166.

Pizzarello, S., Cooper, G. W., & Flynn, G. J. (2006). The Nature and Distribution of the Organic Material in Carbonaceous Chondrites and Interplanetary Dust Particles. In D. Lauretta, & H. Y. Mc Sween, Jr., *Meteorites and the Early Solar System II* (pp. 625-651). Tucson, AZ: University of Arizona Press.

Pizzarello, S., Feng, X., Epstein, S., & Cronin, J. R. (1994). Isotopic analyses of nitrogenous compounds from the Murchison meteorite: Ammonia, amines, amino acids, and polar hydrocarbons. *Geochimica et Cosmochimica Acta*, 5579-5587.

Pizzarello, S., Huang, Y., & Alexandre, M. R. (2008). Molecular asymmetry in extraterrestrial chemistry: Insights from a pristine meteorite. *Proceedings of the National Academy of Sciences (USA)*, 3700-3704.

Pizzarello, S., Huang, Y., Becker, L., J., P. R., Nieman, R. A., Cooper, G. W., & Williams, M. (2001). The Organic Content of the Tagish Lake Meteorite. *Science*, 2236-2239.

Pizzarello, S., Schrader, D., Monroe, A. A., & Lauretta, D. (2012). Large enantiomeric excesses in primitive meteorites and the diverse effects of water in cosmochemical evolution. *Proceedings of the National Academy of Sciences*, 11949–11954.

Pizzarello, S., Wang, Y., & Chaban, G. M. (2010). A comparative study of the hydroxy acids from the Murchison, GRA 95229 and LAP 02342 meteorites. *Geochimica et Cosmochimica Acta*, 6206-6217.

Pizzarello, S., Williams, L. B., Lehman, J., Holland, G. P., & Yarger, J. L. (2011). Abundant ammonia in primitive asteroids and the case for a possible exobiology. *Proceedings of the National Academy of Sciences (USA)*, 4303-4306.

Pizzarello, S., Zolensky, M., & Turk, K. A. (2003). Nonracemic isovaline in the Murchison meteorite: Chiral distribution and mineral association. *Geochimica et Cosmochimica Acta*, 1589-1595.

Platts, S. (2006). Contributions to chemical questions in origins of life (PhD thesis). Rensselear Polytechnic Institute.

Pollock, G. E., Cheng, C. N., Cronin, S. E., & Kvenvolden, K. A. (1975). Stereoisomers of isovaline in the Murchison meteorite. *Geochimica et Cosmochimica Acta*, 1571-1573.

Remusat, L., Guan, Y., Wang, Y., & Eiler, J. (2010). Accretion and Preservation of D-rich Organic Particles in Carbonaceous Chondrites: Evidence for Important Transport in the Early Solar System Nebula. *The Astrophysical Journal*, 1048-1058.

Sandford, S. A., Bernstein, M. P., & Dworkin, J. P. (2001). Assessment of the interstellar processes leading to deuterium enrichment in meteoritic organics. *Meteoritics and Planetary Science*, 1117-1133.

Schmitt-Kopplin, P., Gabelica, Z., Gougeon, R. D., Fekete, A., Kanawati, B., Harir, M., . . . Hertkorn, N. (2010). High molecular diversity of extraterrestrial organic matter in Murchison meteorite revealed 40 years after its fall. *Proceedings of the National Academy of Sciences (USA)*, 2763-2768.

Schrader, D. L., Franchi, I. A., Connolly, J. H., Greenwood, R. C., Lauretta, D. S., & Gibson, J. M. (2011). The formation and alteration of the Renazzo-like carbonaceous condrites I: Implications of bulk-oxygen isotopic composition. *Geochimica et Cosmochimica Acta*, 308-325.

Sephton, M. A., Pillinger, C. T., & Gilmour, I. (2001). Normal alkanes in meteorites: molecular d13C values indicate an origin by terrestrial contamination. *Precambrian Research*, 47-58.

Shaw, G. (2008). Earth's atmosphere - Hadean to early Proterozoic. *Chemie der Erde-Geochemistry*, 235-264.

Shock, E. L., & Schulte, M. D. (1990). Summary and implications of reported amino acid concentrations in the Murchison meteorite. *Geochimica et Cosmochimica Acta*, 3159-3173.

Simoneit, B. R. (2002). Biomass burning — a review of organic tracers for smoke from incomplete combustion. *Applied Geochemistry*, 129-162.

Smith, G. G., Williams, K. M., & Wonnacott, D. (1978). Factors Affecting the Rate of Racemization of Amino Acids and Their Significance to Geochronology. *The Journal of Organic Chemistry*, 1-5.

Soai, K., Shibata, T., Morioka, H., & Choji, K. (1995). Asymmetric autocatalysis and amplification of enantiomeric excess of a chiral molecule. *Nature*, 767-768.

Tyra, M. A., Brearley, A. J., Hutcheon, I. D., Ramon, E., Matzel, J., & Weber, P. (2009). Carbonate Formation Timescales Vary between CM1 Chondrites ALH84051 and

ALH84034. *40th Lunar and Planetary Science Conference.* Tucson, AZ: Lunar and Planetary Institute.

Tyra, M. A., Matzel, J., Brearley, A. J., & Hutcheon, I. D. (2010). Variability in Carbonate Petrography and NanoSIMS 53Mn/53Cr Systematics in Paired CM1 Chondrites ALH 84051, ALH 84049, and ALH 84034. *41st Lunar and Planetary Science Conference.* Tucson, AZ: Lunar and Planetary Institute.

Urey, H. (1955). The Cosmic Abundances of Potassium, Uranium, and Thorium and the Heat Balances of the Earth, the Moon, and Mars. *Proceedings of the National Academy of Sciences (USA)*, 127-144.

Vallentyne, J. R. (1964). Biogeochemistry of organic matter--II: Thermal reaction kinetics and transformation products of amino compounds. *Geochimica et Cosmochimica Acta*, 157-188.

Van Schmus, W. R., & Wood, J. A. (1967). A chemical-petrologic classification for the chondritic meteorites. *Geochimica et Cosmochimica Acta*, 747-765.

Vollhardt, K. P., & Schore, N. E. (2003). *Organic Chemistry: Structure and Function, 4th ed.* New York, NY: W. H. Freeman and Company.

Wadhwa, M., Srinivasan, G., & Carlson, R. W. (2006). Timescales of Planetesimal Differentiation in the Early Solar System. In D. S. Lauretta, J. H. McSween, & R. P. Binzel, *Meteorites and the Early Solar System II* (pp. 715-731). Tucson, AZ: University of Arizona Press.

Wan, P., Modro, T. A., & Yates, K. (1980). The kinetics and mechanism of acid catalysed hydrolysis of lactams. *Canadian Journal of Chemistry*, 2423-2432.

Wehmiller, J., & Hare, P. E. (1971). Racemization of Amino Acids in Marine Sediments. *Science*, 907-911.

Weisberg, M. K., McCoy, T. J., & Krot, A. N. (2006). Systematics and Evaluation of Meteorite Classification. In D. S. Lauretta, J. H. McSween, & R. P. Binzel, *Meteorites and the Early Solar System II* (pp. 19-52). Tucson, AZ: University of Arizona Press.

Yariv, S., & Cross, H. (2002). *Organo-Clay Complexes and Interactions.* New York, NY: Marcel Dekker, Inc.

Yokoyama, T., Alexander, C. M., & Walker, R. J. (2011). Assessment of nebular versus parent body processes on presolar components present in chondrites: Evidence from Osmium isotopes. *Earth and Planetary Science Letters*, 115-123.

Zolensky, M. E., Krot, A. N., & Benedix, G. (2008). Record of Low-Temperature Alteration in Asteroids. *Reviews in Mineralogy & Geochemistry*, 429-462.

Zolensky, M., Barrett, R., & Browning, L. (1993). Mineralogy and composition of matrix and chondrule rims in carbonaceous chondrites. *Geochimica et Cosmochimica Acta*, 3123-3148.

Zolensky, M., Bodnar, R., Tsuchiyama, A., Okudaira, K., Noguchi, T., Uesugi, K., & Nakano, T. (2004). Fluid inclusions in chondrites. *Abstracts of the Meteoritical Society* (pp. A118-A118). Fayetteville, AR: Department of Chemistry and Biochemistry, University of Arkansas.

APPENDIX A

CALCULATING INDIGENOUS ENANTIOMERIC EXCESS OF A CONTAMINATED METEORITE SAMPLE USING ISOTOPIC ENRICHMENT.

The following equation was developed to allow calculation of natal enantiomeric excess of a protein amino acid for which compound-specific isotopic measurements have been made. Terrestrial organics are isotopically 'light' in comparison to extraterrestrial organics, so contamination will decrease deuterium enrichment in a mixed sample. The following calculation requires an assumed δD (‰) for contaminant molecules. The basic principle is that of following the deuterons. Other isotopes could just as well be used but are not here.

Deuterium is a suitable stable isotope for measuring enrichments in meteoritic organics due to its large relative abundance in the molecule and low relative exchange/loss rates in solution. The enrichments of deuterium in meteoritic amino acids typically range from +450 to +7000‰ (Pizzarello & Huang, 2005; Elsila, Glavin, Dworkin, Martins, & Bada, 2012), and these enrichments are distinguishable from the terrestrial enrichments which typically fall within -300 to +300‰ for natural waters (Gat, 1996). Possible contamination would be isotopically distinct from indigenous molecules and, assuming contamination is not excessive, will not disguise all isotopic enrichments of the indigenous compounds. Racemization and the homochirality of the biosphere allow for another level of consideration of contamination (see chapter 1 of this dissertation for a summary), but that is not considered here.

Establish the following:

$n = \#$ of protons in molecule

$A =$ moles of indigenous L amino acid

$B =$ moles of contaminant L amino acid

$[\mathrm{L}] =$ measured abundance of L amino acid (includes contaminant)

$[\mathrm{D}] =$ measured abundance of D amino acid

$\left(\frac{D}{H}\right)_{\mathrm{L}} =$ measured isotope ratio of L amino acid

$\left(\frac{D}{H}\right)_{\mathrm{D}} =$ measured isotope ratio of D amino acid

$\left(\frac{D}{H}\right)_{*} =$ assumed isotope ratio of contaminant

$\left(\frac{D}{H}\right)_{\mathrm{VSMOW}} =$ isotope ratio of Vienna Standard Mean Ocean Water (VSMOW)

Three assumptions are made to continue: (1) no racemization has occurred after arrival at Earth, (2) the measured abundance and isotopic enrichment of the D amino acid have been unaffected by contamination, and (3) the D/H of the indigenous (non-contaminant) L amino acid is equivalent to the D/H of the D amino acid. The L amino acid abundance is $(A + B)$, though the relative contributions of indigenous and contaminant to the total are unknown at first, and, including Avogadro's number, the numbers of indigenous and contaminant deuterons are respectively given by $N_A * A * n * \left(\frac{D}{H}\right)_{\mathrm{D}}$ and $N_A * B * n * \left(\frac{D}{H}\right)_{*}$.

The measured D/H of the L amino acid is calculated by adding the indigenous and contaminant deuterons and dividing by the total number of protons of L:

$$\left(\frac{D}{H}\right)_{\mathrm{L}} = \frac{N_A * A * n * \left(\frac{D}{H}\right)_{\mathrm{D}} + N_A * B * n * \left(\frac{D}{H}\right)_{*}}{N_A * n * (A + B)}$$

This can be simplified and solved for B, the abundance of the contaminant:

$$(A + B)\left(\frac{D}{H}\right)_{\mathrm{L}} = A * \left(\frac{D}{H}\right)_{\mathrm{D}} + B * \left(\frac{D}{H}\right)_{*}$$

$$B = A * \frac{\left(\frac{D}{H}\right)_{\mathrm{D}} - \left(\frac{D}{H}\right)_{\mathrm{L}}}{\left(\frac{D}{H}\right)_{\mathrm{L}} - \left(\frac{D}{H}\right)_{*}}$$

This can be transformed to delta notation by multiplying by

$1 \Big/ \left(\frac{D}{H}\right)_{\mathrm{VSMOW}} \Big/ 1 \Big/ \left(\frac{D}{H}\right)_{\mathrm{VSMOW}}$, inserting $(1 - 1) = 0$, and rearranging:

$$B = A * \frac{\left(\frac{D}{H}\right)_{\mathrm{D}} \Big/ \left(\frac{D}{H}\right)_{\mathrm{VSMOW}} - \left(\frac{D}{H}\right)_{L} \Big/ \left(\frac{D}{H}\right)_{\mathrm{VSMOW}}}{\left(\frac{D}{H}\right)_{\mathrm{L}} \Big/ \left(\frac{D}{H}\right)_{\mathrm{VSMOW}} - \left(\frac{D}{H}\right)_{*} \Big/ \left(\frac{D}{H}\right)_{\mathrm{VSMOW}}}$$

$$B = A * \frac{\left[\left(\frac{D}{H}\right)_{D} \Big/ \left(\frac{D}{H}\right)_{\mathrm{VSMOW}} - 1\right] - \left[\left(\frac{D}{H}\right)_{L} \Big/ \left(\frac{D}{H}\right)_{\mathrm{VSMOW}} - 1\right]}{\left[\left(\frac{D}{H}\right)_{L} \Big/ \left(\frac{D}{H}\right)_{\mathrm{VSMOW}} - 1\right] - \left[\left(\frac{D}{H}\right)_{*} \Big/ \left(\frac{D}{H}\right)_{\mathrm{VSMOW}} - 1\right]}$$

$$B = A * \frac{\delta D_{\mathrm{D}} - \delta D_{\mathrm{L}}}{\delta D_{\mathrm{L}} - \delta D_{*}}$$

After combination with $A + B = [\mathrm{L}]$ from the initial measurement, this can be solved to yield the amount of contaminant:

$$B = ([\mathrm{L}] - B) * \frac{\delta D_{\mathrm{D}} - \delta D_{\mathrm{L}}}{\delta D_{\mathrm{L}} - \delta D_{*}}$$

$$B + B * \frac{\delta D_{\mathrm{D}} - \delta D_{\mathrm{L}}}{\delta D_{\mathrm{L}} - \delta D_{*}} = [\mathrm{L}] * \frac{\delta D_{\mathrm{D}} - \delta D_{\mathrm{L}}}{\delta D_{\mathrm{L}} - \delta D_{*}}$$

$$B = \frac{[\mathrm{L}] * \frac{\delta D_{\mathrm{D}} - \delta D_{\mathrm{L}}}{\delta D_{\mathrm{L}} - \delta D_{*}}}{1 + \frac{\delta D_{\mathrm{D}} - \delta D_{\mathrm{L}}}{\delta D_{\mathrm{L}} - \delta D_{*}}}$$

This amount of contaminant may then be subtracted from the total measured [L] to determine the abundance of the indigenous L-amino acid and allow calculation of indigenous enantiomeric excess.

APPENDIX B

EXAMPLE OF CONSTANT ENANTIOMERIC EXCESS DURING α-EPIMERIZATION DESPITE INCREASED CONVERSION TO D-*a*Ile VS. L-*a*Ile.

Equation **(3)** from section 3.2.1 seems needlessly complex if *ee* is mistakenly thought to increase so long as $\frac{d}{dt}[\text{D} - a\text{Ile}] > \frac{d}{dt}[\text{L} - a\text{Ile}]$. For application to *ee*, a change in concentration must be normalized by total concentration because the enantiomeric ratio [D/L] must change to shift *ee*. Changes in the difference between concentrations of enantiomers do not necessarily equate to changes in overall *ee.*

Examine a case in which $\frac{d}{dt}[\text{D} - a\text{Ile}] > \frac{d}{dt}[\text{L} - a\text{Ile}]$ but $\frac{d}{dt}(ee_{\text{D}-a\text{Ile}}) \leq 0$. Consider the following initial abundances of the isoleucines and *allo*isoleucines:

L-*a*Ile = 1.0 D-Ile = 2.0 D-*a*Ile = 2.0 L-Ile = 4.0

Both $ee_{\text{D}-a\text{Ile}}$ and $ee_{\text{L}-\text{Ile}}$ equal 33%. In an α-epimerization only model, no change in *ee* will occur even though more D-*a*Ile is being produced (by the greater L-Ile abundance) than L-*a*Ile until the reaction has reached equilibrium ($allo/\text{Ile} = \text{K}_{\text{ile}}$). At the start of this example, $allo/\text{Ile} = 0.5$. The proportional creation of L-*a*Ile and consumption of D-Ile prevents the increase of $ee_{\text{D}-a\text{Ile}}$ and decrease of $ee_{\text{L}-\text{Ile}}$, respectively.

APPENDIX C

PERMISSION TO REPRODUCE FIGURE 4 FROM GLAVIN, D. P., CALLAHAN, M. P., DWORKIN, J. P., & ELSILA, J. E. (2011). THE EFFECTS OF PARENT BODY PROCESSES ON AMINO ACIDS IN CARBONACEOUS CHONDRITES. *METEORITICS AND PLANETARY SCIENCE*, 1948-1972.

Copyright Clearance Center RightsLink®

Home | Account Info | Help

WILEY

Title: The effects of parent body processes on amino acids in carbonaceous chondrites
Author: Daniel P. GLAVIN,Michael P. CALLAHAN,Jason P. DWORKIN,Jamie E. ELSILA
Publication: Meteoritics & Planetary Science
Publisher: John Wiley and Sons
Date: Dec 22, 2010
© The Meteoritical Society, 2010

Logged in as:
Adam Monroe
Account #:
3000850756
LOGOUT

Order Completed

Thank you very much for your order.

This is a License Agreement between Adam A. Monroe ("You") and John Wiley and Sons ("John Wiley and Sons"). The license consists of your order details, the terms and conditions provided by John Wiley and Sons, and the payment terms and conditions.

Get the printable license.

License Number	3499580241281
License date	Oct 31, 2014
Licensed content publisher	John Wiley and Sons
Licensed content publication	Meteoritics & Planetary Science
Licensed content title	The effects of parent body processes on amino acids in carbonaceous chondrites
Licensed copyright line	© The Meteoritical Society, 2010
Licensed content author	Daniel P. GLAVIN,Michael P. CALLAHAN,Jason P. DWORKIN,Jamie E. ELSILA
Licensed content date	Dec 22, 2010
Start page	1948
End page	1972
Type of use	Dissertation/Thesis
Requestor type	University/Academic
Format	Electronic
Portion	Figure/table
Number of figures/tables	1
Original Wiley figure/table number(s)	Figure 4
Will you be translating?	No
Title of your thesis / dissertation	Application of Isoleucine Epimerization to Assess Terrestrial Contamination and Constrain the Duration and Effects of Aqueous Alteration of Carbonaceous Chondrite Meteorites
Expected completion date	Dec 2014
Expected size (number of pages)	100
Total	0.00 USD

ORDER MORE... CLOSE WINDOW

Copyright © 2014 Copyright Clearance Center, Inc. All Rights Reserved. Privacy statement.
Comments? We would like to hear from you. E-mail us at customercare@copyright.com

APPENDIX D

PERMISSION TO REPRODUCE MONROE, A. A. AND PIZZARELLO, S. (2011) THE SOLUBLE ORGANIC COMPOUNDS OF THE BELLS METEORITE: NOT A UNIQUE OR UNUSUAL COMPOSITION. GEOCHIMICA ET COSMOCHIMICA ACTA 75, 7585-7595.

Copyright Clearance Center RightsLink®

Home | Account Info | Help

Title: The soluble organic compounds of the Bells meteorite: Not a unique or unusual composition

Author: Adam A. Monroe,Sandra Pizzarello

Publication: Geochimica et Cosmochimica Acta

Publisher: Elsevier

Date: 1 December 2011

Copyright © 2011 Elsevier Ltd. All rights reserved.

Logged in as:
Adam Monroe

LOGOUT

Order Completed

Thank you very much for your order.

This is a License Agreement between Adam A. Monroe ("You") and Elsevier ("Elsevier"). The license consists of your order details, the terms and conditions provided by Elsevier, and the payment terms and conditions.

Get the printable license.

License Number	3496740009345
License date	Oct 26, 2014
Licensed content publisher	Elsevier
Licensed content publication	Geochimica et Cosmochimica Acta
Licensed content title	The soluble organic compounds of the Bells meteorite: Not a unique or unusual composition
Licensed content author	Adam A. Monroe,Sandra Pizzarello
Licensed content date	1 December 2011
Licensed content volume number	75
Licensed content issue number	23
Number of pages	11
Type of Use	reuse in a thesis/dissertation
Portion	full article
Format	both print and electronic
Are you the author of this Elsevier article?	Yes
Will you be translating?	No
Title of your thesis/dissertation	Application of Isoleucine Epimerization to Assess Terrestrial Contamination and Constrain the Duration and Effects of Aqueous Alteration of Carbonaceous Chondrite Meteorites
Expected completion date	Dec 2014
Estimated size (number of pages)	100
Elsevier VAT number	GB 494 6272 12
Permissions price	0.00 USD
VAT/Local Sales Tax	0.00 USD / 0.00 GBP
Total	0.00 USD

ORDER MORE... CLOSE WINDOW

Copyright © 2014 Copyright Clearance Center, Inc. All Rights Reserved. Privacy statement.
Comments? We would like to hear from you. E-mail us at customercare@copyright.com

APPENDIX E

PERMISSION TO REPRODUCE SCHEME 1 FROM CHABAN, G. M., & PIZZARELLO, S. (2010). AB INITIO CALCULATIONS OF 6- AND 7-CARBON METEORITIC AMINO ACIDS AND THEIR DIASTEREOMERS. *METEORITICS AND PLANETARY SCIENCE*, 1053-1060.

Copyright Clearance Center RightsLink®

Home | Account Info | Help

WILEY

Title: Ab initio calculations of 6- and 7-carbon meteoritic amino acids and their diastereomers
Author: Galina M. CHABAN,Sandra PIZZARELLO
Publication: Meteoritics & Planetary Science
Publisher: John Wiley and Sons
Date: Sep 22, 2010
© The Meteoritical Society, 2010

Logged in as:
Adam Monroe
Account #:
3000850756
LOGOUT

Order Completed

Thank you very much for your order.

This is a License Agreement between Adam A. Monroe ("You") and John Wiley and Sons ("John Wiley and Sons"). The license consists of your order details, the terms and conditions provided by John Wiley and Sons, and the payment terms and conditions.

Get the printable license.

License Number	3499590142519
License date	Oct 31, 2014
Licensed content publisher	John Wiley and Sons
Licensed content publication	Meteoritics & Planetary Science
Licensed content title	Ab initio calculations of 6- and 7-carbon meteoritic amino acids and their diastereomers
Licensed copyright line	© The Meteoritical Society, 2010
Licensed content author	Galina M. CHABAN,Sandra PIZZARELLO
Licensed content date	Sep 22, 2010
Start page	1053
End page	1060
Type of use	Dissertation/Thesis
Requestor type	University/Academic
Format	Electronic
Portion	Figure/table
Number of figures/tables	1
Original Wiley figure/table number(s)	Scheme 1
Will you be translating?	No
Title of your thesis / dissertation	Application of Isoleucine Epimerization to Assess Terrestrial Contamination and Constrain the Duration and Effects of Aqueous Alteration of Carbonaceous Chondrite Meteorites
Expected completion date	Dec 2014
Expected size (number of pages)	100
Total	0.00 USD

ORDER MORE... CLOSE WINDOW

Copyright © 2014 Copyright Clearance Center, Inc. All Rights Reserved. Privacy statement.
Comments? We would like to hear from you. E-mail us at customercare@copyright.com

APPENDIX F

DESIGN AND USE OF A 200 eV CO_2/CO_2^+ SOURCE FOR SIMULATED ATMOSPHERIC ENTRY OF METEORITIC MATERIAL IN THE HADEAN

Abstract

Interplanetary Dust Particles (IDPs) shower the modern Earth, producing organic carbon fluxes of ~$3.5x10^8$ g/yr, and geophysical modeling predicts that the same organic carbon fluxes to the early Earth (~4.4Ga) were approximately 10^{12} g/yr, decreasing by an order of magnitude every 300-400 Myr for Earth's first Gyr (Chyba & Sagan, 1992). The most common IDPs of diameter 10-50 μm and mass ~10 μg are decelerated by the atmosphere during entry, experiencing varying degrees of heating based on entry parameters (Kortenkamp & Dermott, 1998). The atmosphere at the time was also almost certainly anoxic, with abundances of CO_2 and H_2O and possible periods of trace H_2 (Shaw, 2008).

IDPs have been shown to contain a suite of organic volatile and non-volatile species including Polycyclic Aromatic Hydrocarbons (PAHs) (Clemett, Maechling, Zare, Swan, & Walker, 1993). Due to the IDPs' entry velocities from 10 - 50 km/s (Flynn, Keller, Jacobsen, & Wirick, 2004), PAHs traveling onboard that were volatilized during entry heating would be impacted by CO_2 and H_2O molecules at velocities corresponding to energies ranging from 30-500 eV—energies sufficient to induce reactions. After designing and characterizing performance of a 50-300 eV CO_2^+ source for attachment to a ^{69}Ga Time of Flight Secondary Ion Mass Spectrometer (ToF-SIMS), the PAH Benzo[a]pyrene was bombarded with 200 eV CO_2^+ for periods up to 100 hrs. ToF-SIMS was used to search for any signs of PAH carboxylation or heteroatom substitution. Though these products, if present, were absent to our detection, several questions were raised regarding the volatility of any potential products, the utility of a cold-stage reaction platform, and the potential for retooling of the CO_2^+ source for other gases.

Introduction

It has long been suspected that meteors and comets ferried or shock-synthesized organic compounds of prebiotic relevance to the early Earth: in 1908 it was noted that impactors "contained carbon, sulphur, phosphorus, and all other elements found in organic matter; and as they impinged more or less violently upon the surface formed of previous accessions of similar matter, there should have been generated various compounds of these elements" (Chamberlin & Chamberlin, 1908). Meteorites offer a unique platform from which to constrain the chemical starting conditions of Earth, for in the cases of observed falls, they have remained relatively undisturbed since the formation of the Solar System, and their present contents likely resemble the contents of similar stones falling to Earth shortly after accretion. In addition to indigenous organic content of meteorites, there is also interest in products of shock synthesis during meteors or airbursts, post impact vapor plumes, or post-impact recombination (Mimura, 1995). Though it has been noted that the kinetic energy of infalling particles must be damped by the surrounding atmosphere, experiments specifically designed to simulate organic synthesis resulting from such conditions are scarce. Since the Hadean (4.6 - 3.8 Ga) atmosphere was dominated by CO_2, collisions between CO_2 molecules and a falling body had to have taken place. Present day IDP observed entry velocities range from the escape velocity of Earth (11.2 km/s) to 72.8 km/s (Brownlee, 1985), and these relative velocities convert to CO_2 collision energies from 28.6 eV (2,760 kJ/mol) to 1.21 keV (117,000 kJ/mol)—energies sufficient to initiate reactions with molecules on the surfaces of incoming particles.

IDPs represent the majority of matter and the majority of organic carbon delivered to the Earth after 4.4 Ga, so it is likely that the particular suite of molecules onboard the IDPs may have majorly influenced prebiotic chemistry on Earth. We argue that the small size of IDPs (generally several μm in diameter) and their large surface area to volume ratio due to their 'fluffy' structure renders them not only highly effective deliverers of soluble organic material but also more efficient outgassers of volatile material during atmospheric entry heating. Pulse heating experiments of IDP analogues loaded with coronene, 2-pentadecanone, and lysine (all detected in IDPs) demonstrated that a microporous structure with a sublimable phase exhibited an ablative cooling or 'heatshield effect' that prevented complete sublimation of less volatile organic phases during simulated entry (Matrajt, Brownlee, Sadilek, & Kruse, 2006).

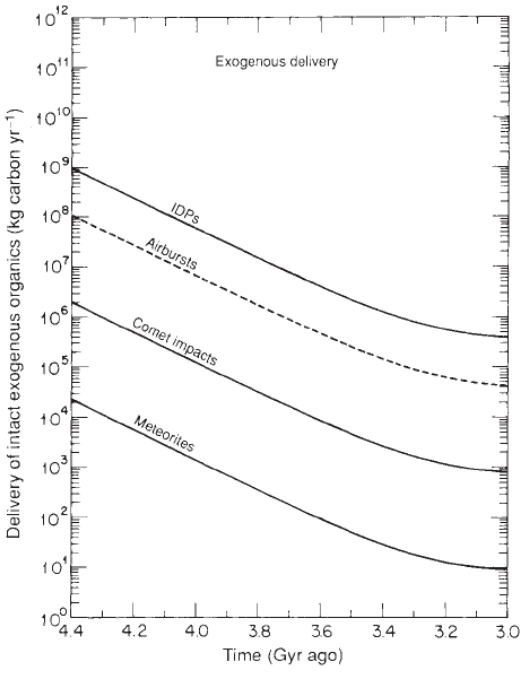

Figure 28. Estimated exogenous organics delivered between 4.4 and 3.0 Ga (Chyba & Sagan, 1992).

One class of organic compound found in high abundances in meteorites and IDPs is the Polycyclic Aromatic Hydrocarbon (PAH) (Clemett, Maechling, Zare, Swan, & Walker, 1993). Previously mentioned coronene is one of these, and other abundant PAHs in meteorites and IDPs include naphthalene, phenanthrene, fluoranthene, pyrene, chrysene, and benzopyrene (Gilmour & Pillinger, 1994; Elsila, De Leon, Buseck, & Zare,

2005). Oxygenated PAHs such as 1,4-naphthoquinone form the aromatic portion of vitamin K and other clotting co-factors (Fieser, Tishler, & Sampson, 1941), and hydroxylated or otherwise-functionalized PAHs have been offered as a potential coordination backbone for primordial RNA (Platts, 2006) as well as suitable amphiphiles for protocellular membranes (Ehrenfreund, Rasmussen, Cleaves, & Chen, 2006).

If a smaller PAH such as phenanthrene or benzopyrene sublimated from the surface of an infalling IDP and reacted with Hadean atmospheric CO_2 to produce a new, oxygenated PAH, the products of these reactions would be abundant. Our instrument modification enables simulation of atmospheric entry by producing a 200eV CO_2/CO_2^+ ion beam incident on a surface-adsorbed PAH.

ToF-SIMS offers mass resolutions on the order of 5 to 10 mamu, enough to distinguish the difference between O (15.995 amu) and CH_4 (16.031 amu). Heteroatom substitution is of key interest to this work, so SIMS measurements of irradiated products are ideal.

Methods

An ion source and its peripherals were constructed in the Cs source aperture of a Texas Instruments ^{69}Ga ToF-SIMS using the following: Tungsten nude Bayard-Alpert ionization gauge, Hewlett Packard 6209B DC power supply (0–350 V, 0–0.1 A), Lambda Instruments LK-352-FMOV DC power supply (0–60 V, 0–15 A), regulator, CO_2 tank, and voltmeter. The filament of the ion gauge was warmed sufficiently to emit electrons which ionized ambient CO_2, and the ionization gauge grid was charged to the desired ion energy, which in all of these experiments was 200 eV. Electron emission was calculated

using the voltage drop across a 10 Ω resistor in series with the grid, and the yield of the ion source was measured with a Keithley Instruments 602 solid state electrometer.

Behavior of the ion source was characterized at 6 ambient CO_2 pressures of 4.0, 5.0, 6.0, 7.0, and 8.0 x 10^{-7} and 1.0 x 10^{-6} Torr and electron emission currents ranging from 1-30 mA. Both electron and CO_2^+ beams were stable for at least 5 minutes before a performance point was recorded. A duct fan was installed to cool the housing nearest the filament.

PAHs phenanthrene, pyrene, chrysene, and benzo[a]pyrene were deposited separately by dissolution in acetone and dropwise concentration on Si wafers. Each wafer was inserted into the vacuum chamber (10^{-8} Torr) atop the ToF-SIMS sample platter. The survival times of phenanthrene, pyrene, and chrysene under high vacuum were between 5 and 60 minutes. These durations were too short to allow for bombardment with CO_2, preparation of the Ga-beam, and collection of spectra, but benzo[a]pyrene lasted upwards of 1 week with no noticeable sublimation under high vacuum. Blanks were taken of the bare Si wafer before deposition of control 7-D benzo[a]pyrene, and several spectra were taken following bombardment with 200 eV CO_2^+ for 0, 22, and 100 hours. Ion source performance was checked periodically every 2-8 hours to ensure consistent irradiation.

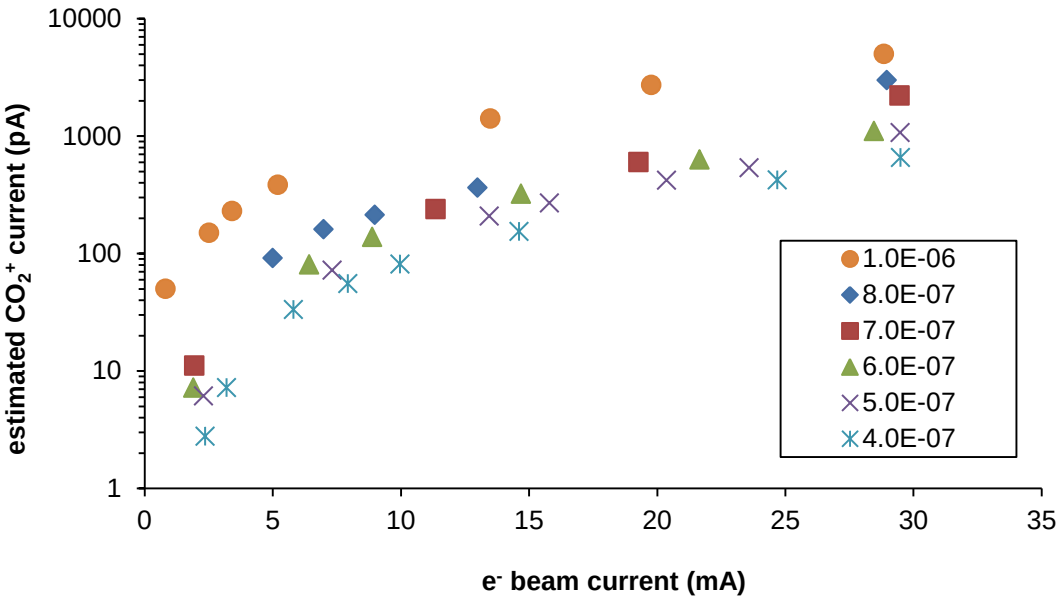

Figure 29. CO_2^+ current measured at the ToF-SIMS sample platter (target) vs. e^- emission current at various pressures CO_2 (Torr). These pressures were measured by the instrument vacuum chamber pressure gauge located several cm above the turbopump.

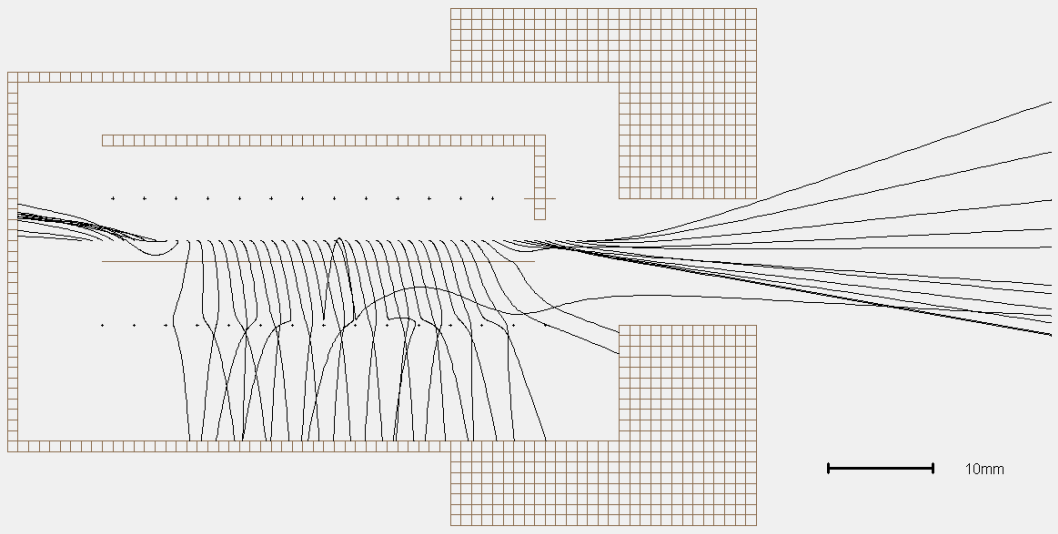

Figure 30. SIMION7®-generated trajectories of 44 amu singly-charged molecules in the ion source.

Results

Notable peaks include the parent (m/z 253), parent +/- CH (m/z 13), and the disappearance of impurities 207, 193, and 191. The target parent + COOH (m/z 298) peak was absent, and all mass calculations assuming oxygen heteroatom substitution produced average deviations between 12.5 and 20.3 mamu while structures containing only C, H, and D deviated within the allowed 3.9 and 7.4 mamu. Total ion yield was lower after the 100 hr. exposure, and parent +/- CH peaks seemed to be sustained despite exposure. During sample loading, it was noted that areas of the deposited PAH that appeared rough or inconsistently deposited before irradiation were transformed into smooth, more homogeneous deposits.

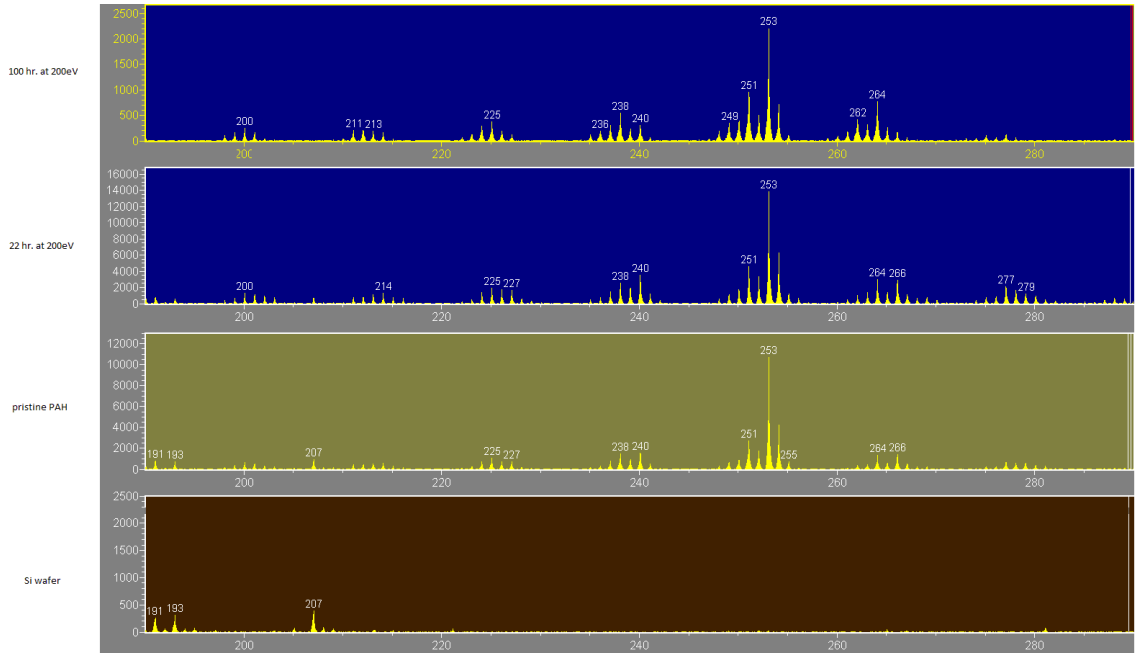

Figure 31. ToF-SIMS spectra of Si wafer, pristine PAH, and PAH after CO_2^+ bombardment of 22 and 100 hrs.

Discussion

The complete absence of peaks corresponding to PAH + COOH/COO^+ at m/z 298 or PAH + OH/O^+ at m/z 270 and apparent absence of any O heteroatom substitution raise one of at least four possibilities:

i. PAH + 200 eV CO_2 does not result in a carboxylated or hydroxylated PAH,
ii. the functionalized PAH is volatilized upon formation and lost to vacuum,
iii. the carboxylated PAH eventually decomposes into CO_2 (g) and PAH due to vacuum (as carboxylic acids are known to do during heating), or
iv. the functionalized PAH is destroyed during SIMS.

Explanation ii can be examined by the installation of a cold stage to trap any volatiles. The trapped materials can then be re-deposited onto the Si wafer for analysis via ToF-SIMS or analyzed *via* GC-MS since no other mass interferences at parent + COOH are likely.

Explanation iii can be ruled out with another control experiment beginning with a carboxylated PAH to see if the COOH survives impact; its survival could be verified by the mass difference due to the presence of two oxygens and lack of other interfering peaks in its mass range.

Explanation iv is least likely due to the facts that the parent m/z 253 remains and C-C, C-D, and C-H bonds on the perimeter of PAHs are approximately 500 kcal/mol (May, Dapprich, Furche, Unterreiner, & Ahlrichs, 2000), which indicates that the C-D bond survives desorption and ionization. In control experiments with non-deuterated PAHs, the parent with no proton loss remains as the primary ion, so deuterium's loss is

unlikely. If all m/z 253 ions are a hydrogenated (formerly deuterated), singly-charged benzo[a]pyrene, the mass difference of 2H (2.016 amu) versus D (2.014 amu) would be too narrow to differentiate with a mass resolution of 5-10 mamu. The C-C bond between PAH and COOH is also on the order of 500 kcal/mol, but steric bulk of the COOH may make it more susceptible to dissociation. Most molecules of interest, functionalized or not, would not survive a direct impact by a 7.2 keV ^{69}Ga ion, but other perimeter molecules ionized by the secondary smattering of electrons caused by the primary ion beam would be more gently desorbed, as the survival of the 253 peak and other PAH parents illustrate.

Conclusions

Though more experiments are required to exclude the possibility that PAH carboxylation cannot occur under the given conditions, the absence of indicative peaks tentatively indicates that it does not. The successful demonstration of the proposed atmospheric entry chemistry here would enable discussion about yet another opportunity for prebiotic organics to be synthesized. Additionally, if PAHs were key players in prebiotic organic aqueous chemistry, they must have been functionalized at some point or points; in the meteorite and IDP record, nonpolar aromatic hydrocarbons outweigh polar ones, so any potential conditions for conversion are important to investigate.

In future embodiments the same ion source can be tested and used with an N_2 or H_2O atmosphere to bombard PAHs or other molecules that can survive vacuum for long enough to be irradiated and observed. Although the meteorite record contains many amino acids, it is imaginable that hydrocarbons could have been aminated and carboxylated during entry to produce amino acids or aromatic hydrocarbons that could

have been N-heteroatom-substituted and/or aminated to produce the precursors of RNA. Each nucleobase contains one or 2 aromatic rings at most, and the aromatic hydrocarbon precursors benzene and naphthalene are extremely volatile under vacuum, so an alternate experimental setup design would have to accommodate this.